SAND2024-12338R

U.S. DEPARTMENT OF ENERGY | Office of NUCLEAR ENERGY | SPENT FUEL & HIGH-LEVEL WASTE DISPOSITION

Brine Availability Test in Salt (BATS) FY24 Update

Spent Fuel and High-Level Waste Disposition

Prepared for

U.S. Department of Energy

Office of Nuclear Energy

By Sandia National Laboratories

Kristopher Kuhlman[1], Melissa Mills[1], Richard Jayne[1], Edward Matteo[1], Courtney Herrick[1], Charles Choens[1], Matthew Paul[1], Philip Stauffer[2], Eric Guiltinan[2], Thom Rahn[2], Shawn Otto[2], Jon Davis[2], Daniel Eldridge[2], Jonny Rutqvist[3], Yuxin Wu[3], Mengsu Hu[3], Hang Chen[3], Jiannan Wang[3]

August 30, 2024

M2SF-24SN010303052

[1] Sandia National Laboratories
[2] Los Alamos National Laboratory
[3] Lawrence Berkeley National Laboratory

Sandia National Laboratories is a multimission laboratory managed and operated by National Technology & Engineering Solutions of Sandia, LLC, a wholly owned subsidiary of Honeywell International Inc., for the U.S. Department of Energy's National Nuclear Security Administration under contract DE-NA0003525.

DISCLAIMER

This is a technical document that does not take into account contractual limitations or obligations under the Standard Contract for Disposal of Spent Nuclear Fuel and/or High-Level Radioactive Waste (Standard Contract) (10 CFR Part 961).

To the extent discussions or recommendations in this document conflict with the provisions of the Standard Contract, the Standard Contract governs the obligations of the parties, and this presentation in no manner supersedes, overrides, or amends the Standard Contract.

This document reflects technical work that could support future decision making by the U.S. Department of Energy (DOE or Department). No inferences should be drawn from this document regarding future actions by DOE, which are limited both by the terms of the Standard Contract and Congressional appropriations for the Department to fulfill its obligations under the Nuclear Waste Policy Act including licensing and construction of a spent nuclear fuel repository.

U.S. DEPARTMENT OF ENERGY

National Nuclear Security Administration

Sandia National Laboratories

Los Alamos NATIONAL LABORATORY

WASTE ISOLATION PILOT PLANT WIPP NWP • DOE • LANL • ETAL • SNL

BERKELEY LAB

NFCSC DOCUMENT COVER SHEET[1]

Name/Title of Deliverable/Milestone/Revision No.	Brine Availability Test in Salt (BATS) FY24 Update
Work Package Title and Number	Salt Disposal R&D – SNL; SF-24SN01030305
Work Package WBS Number	1.08.01.03.03
Responsible Work Package Manager	Kristopher L. Kuhlman (Name/Signature)
Date Submitted	8/30/2024

Quality Rigor Level for Deliverable/Milestone[2]	☐ QRL-1 ☐ Nuclear Data	☐ QRL-2	☒ QRL-3	☐ QRL-4 Lab QA Program[3]

This deliverable was prepared in accordance with Sandia National Laboratories QA program, which meets the requirements of:

☒ DOE Order 414.1 ☐ NQA-1 ☐ Other

This deliverable was subjected to:

☒ Technical Review (TR) ☐ Peer Review (PR)

TR Documentation Provided
☐ Signed TR Report, or
☐ Signed TR Concurrence Sheet, or
☒ Signature of TR Reviewer(s) below

PR Documentation Provided
☐ Signed PR Report, or
☐ Signed PR Concurrence Sheet, or
☐ Signature of PR Reviewers below

Name and Signature of Reviewers

Jason Heath 8/27/24

NOTE 1: *This form should be filled out and submitted with the deliverable. Or, if the PICS:NE system permits, completely enter all applicable information in the PICS:NE Deliverable Form. The requirement is to ensure that all applicable information is entered either in the PICS:NE system or by using the NFCSC Document Cover Sheet.*

- *In some cases, there may be a milestone where an item is being fabricated, maintenance is being performed on a facility, or a document is being issued through a formal document control process where it specifically calls out a formal review of the document. In these cases, documentation (e.g., inspection report, maintenance request, work planning package documentation or the documented review of the issued document through the document control process) of the completion of the activity, along with the Document Cover Sheet, is sufficient to demonstrate achieving the milestone.*

NOTE 2: *If QRL 1, 2, or 3 is not assigned, then the QRL 4 box must be checked, and the work is understood to be performed using laboratory QA requirements. This includes any deliverable developed in conformance with the respective National Laboratory / Participant, DOE or NNSA-approved QA Program.*

NOTE 3: *If the lab has an NQA-1 program and the work to be conducted requires an NQA-1 program, then the QRL-1 box must be checked in the work Package and on the Appendix E cover sheet and the work must be performed in accordance with the Lab's NQA-1 program. The QRL-4 box should not be checked.*

EXECUTIVE SUMMARY

This report summarizes fiscal year 2024 (FY24) activities centered around a series of field tests in bedded salt at the Waste Isolation Pilot Plant (WIPP) funded by the Office of Spent Fuel and Waste Science and Technology in the Spent Fuel and Waste Disposition (SFWD) program of the US Department of Energy's Office of Nuclear Energy (DOE-NE).

High-level Purpose of Experiments: The Brine Availability Test in Salt (BATS) field tests are revealing both *brine occurrence* (i.e., where, and how much) and *brine migration* (i.e., how easily it moves) in the excavation damaged zone (EDZ). This understanding is foundational to develop a safety case for a future heat-generating waste repository in salt, and to starting up a generic repository program in salt to buy down risk.

BATS seeks to predict how much brine can flow into both ambient and heated excavations (e.g., boreholes or rooms) in salt. This work is educating and empowering new repository scientists on two fronts: "design and execution of field tests" and "prediction and modeling of coupled processes." DOE-NE capabilities in salt have grown and been tested through international modeling and benchmarking exercises (e.g., DECOVALEX, RANGERS, KOMPASS, and MEASURES; see Mills et al., 2024). The hands-on expertise we are building is a necessary step towards large-scale disposal demonstrations and eventual implementation.

Brine availability (i.e., brine occurrence and migration) is critical in salt repositories because:

1. water is needed to corrode waste forms and waste packages;
2. water is required for dissolution and transport of aqueous radionuclides off-site;
3. water is essential to gas generation (e.g., steel corrosion, microbial, or water radiolysis), which increases gas pressure—a potential driving force for migration out of a repository;
4. chloride in natural brines absorbs neutrons, thereby eliminating in-package nuclear criticality hazards; and
5. final creep closure of openings will be slowed by any brine backpressure at low porosity.

By investigating brine availability, the DOE-NE disposal research program can develop a repository conceptual model for disposal of heat-generating waste in salt that incorporates realistic and complex processes. The improved conceptual model is a key part in the transition from generic R&D to a future repository program.

Hot Salt Repository Conceptual Model: Generically, in a salt repository with hot radioactive waste surrounded by reconsolidating granular salt backfill, we expect the following nominal behavior:

1. decay heat from radioactive waste will dry out the backfill in the short term (weeks to months);
2. accelerated reconsolidation of hot granular salt backfill will eliminate porosity and permeability near the waste (decades to hundreds of years). This is the primary focus of the KOMPASS and MEASURES ongoing international collaborative efforts (Mills et al., 2024) and LBNL's modeling efforts with TOUGH-FLAC (Rutqvist et al., 2024);
3. after peak decay heat from the waste has passed (~1,000 years), the near-waste area will be dry, low-porosity, and impervious, slowing down future resaturation of the waste packages (this approach has been the focus of the RANGERS international collaborative effort); and
4. dry waste packages do not corrode, there are few mobile radionuclides in a dry system, and there will be little gas generation.

In salt, the hotter the waste, the more robust the disposal system due to heat-accelerated consolidation of backfill and closure of salt openings. A salt repository could accommodate the hottest expected waste packages (as high as 10 or 11 kW per package), with no thermal or criticality issues. A repository in salt would require less waste storage time, a smaller footprint, and no mitigative measures for in-package criticality, compared to argillite or crystalline repositories for the same inventory. These factors could significantly reduce the overall cost liability of a future repository.

<u>Key BATS 2 Achievements in FY24:</u> We highlight the following processes and outcomes

- Repeatable opening/closing of fractures due to cooling/heating cycles, as illustrated by argon breakthrough between the D and HP boreholes (Section 4.1.4).

This demonstrates the extreme sensitivity of the gas and brine flow system to small mechanical changes.

Fractures around hot waste will close.

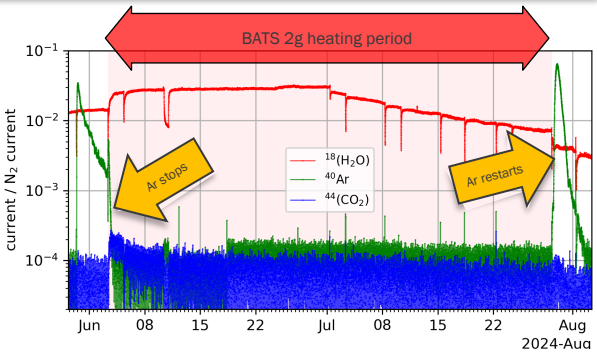

- Drying out of the BATS 2 array over ~2 years, as illustrated by water vapor production in the N_2 circulation system (HP borehole) and the reduced brine samples in the SM borehole (Section 4.1.2).

Since September 2023, the heated array produces similar amounts of brine as the unheated array, despite repeated heating (colored stripes).

Transient brine perturbation due to heating dies out as small amount of brine from clay in salt is exhausted.

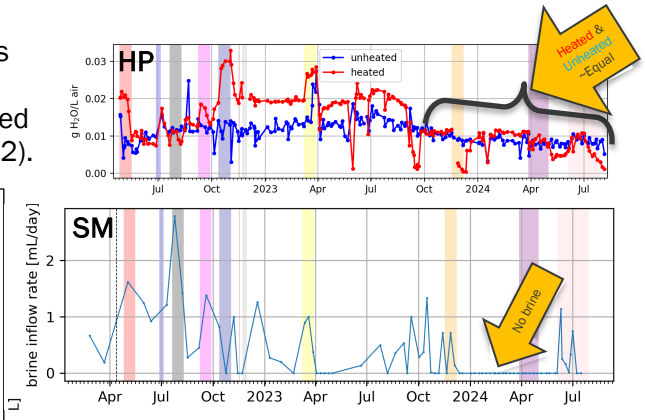

- Isotopic signature of fluid inclusions is different from brine samples collected during BATS 2 (Section 4.1.3).

The oxygen and hydrogen isotopes from laboratory analyses of WIPP fluid inclusions are different from BATS 2a condensed cold trap samples and liquid samples vacuumed from SM borehole.

Water isotopes show the contribution from fluid inclusions to BATS inflow is likely small (<30%).

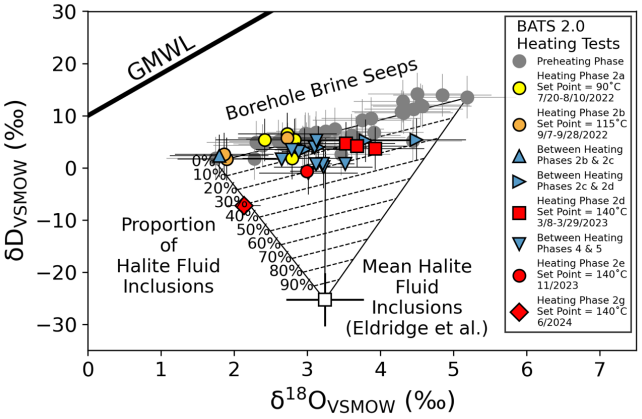

- Two changes are observed in brine composition, showing contributions from different salt layers (Section 4.7.2).

SM brine samples (red circles & lines) show brine from BATS 1 may have flow down through fractures (1) induced by heating. Brine now (2) looks more like historical observations in the same layer (MU-0, pink triangles).

Brine types associated with layers in the salt can be distinguished based on chemistry.

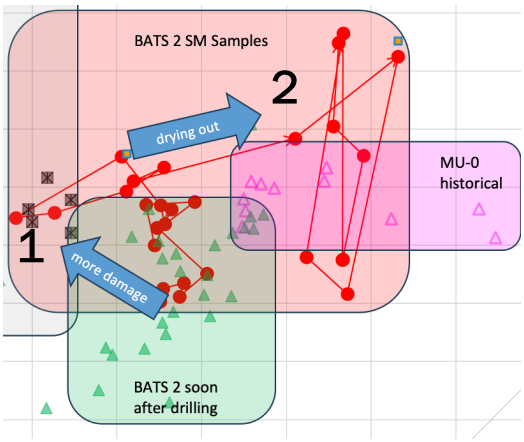

- Differences in acoustic emissions (AE) are consistently observed between the beginning and end of heating (Section 4.3).

Cooling produces many AE hits (3× to 4× heating). Beginning of heating (red arrow) has fewer *louder* events while beginning of cooling (blue arrow) has more *quieter* events. Quieter events may be located further from the sensors.

AE data reveal the asymmetry between heating and cooling in salt; fracture opening and closing are likely not 100% reversible (i.e., the same fractures repeatedly opening and closing reversibly).

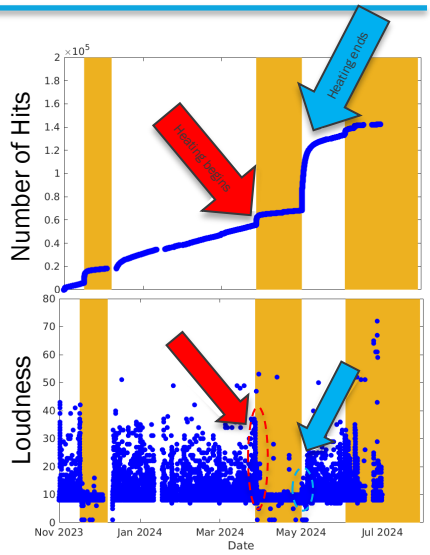

- Electrical Resistivity Tomography (ERT) observations were interpreted with a new clustering algorithm, which delineated the EDZ surrounding the BATS 2 array (Section 4.5).

Advanced interpretation methods explain responses to heating and cooling observed by differences around heater.

ERT can infer presence of conductive brine and fractures between boreholes.

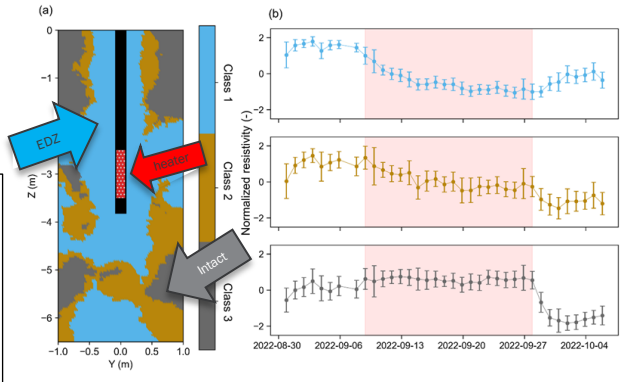

Next Steps (BATS 3) and Expected Outcome: Building on the successes of BATS 1 and BATS 2, BATS 3 will be extended to larger scales, longer periods, hotter temperatures, and more realistic conditions to better recreate conditions expected for high-level waste and spent fuel disposal in salt.

The specific short-term BATS 3 goals and corresponding problems being solved are listed below (Kuhlman et al., 2024a). We also indicate how we close out issues, moving on to the next phase:

- **Conduct heater tests for longer periods** (months to years) **under more representative conditions** (sealed borehole, not removing inflowing water). Longer tests with different boundary conditions will explore how long elevated brine production will be maintained from a newly drilled borehole. These intermediate scale tests will bridge the gap between the smaller and shorter-term BATS 1 and 2 tests (which we are closing out), with the expected disposal scale and conditions.
- **Optimize efficacy of modern sealings in presence of stress, brine, and heat**. Because the salt geologic barrier is so effective, drift and shaft seals of man-made openings are the focus of repository design optimization efforts. Salt repositories have unique engineered barriers (i.e., crushed salt, salt cements, *no bentonite*), and should leverage improvements in man-made materials from the last 30 years. Optimizing the engineered barrier system is a critical next step that bridges between science and application, bringing DOE-NE closer to the readiness level needed for implementation. This closes out aspects of the pure science investigation of EBS in salt, moving on to the optimization stage.
- **Create easy-to-understand visualizations of processes in salt repositories.** Time-lapse or stop-motion videos of brine seeps, creep closure, and EDZ development. These processes are too slow to see clearly without being sped up, but creating these types of visualizations of field observations is now well within our capabilities. These efforts will help more people (i.e., new staff, regulators, and stakeholders) understand the unique processes ongoing in a salt repository. Creating more outreach-ready materials can be used to build confidence in the overall program, as we close out purely theoretical generic investigations and move on to demonstrations and communicating our position.

International collaboration in model validation and benchmarking exercises (e.g., DECOVALEX-2027) will continue to build on the incredibly useful feedback we have received between experimentalists and modeling teams to date (Kuhlman et al., 2024b). BATS and DECOVALEX have also facilitated knowledge transfer between radioactive waste disposal programs in different countries and training the next generations of experimentalists and numerical modelers.

The DOE-NE team comprised of staff from WIPP, SNL, LANL, and LBNL will strive to continue our fruitful collaborative teamwork that has made BATS 1 and 2 possible. We continue to leverage the capabilities of team members and their organizations, producing results that are useful for both DOE-NE and DOE-EM missions.

ACKNOWLEDGMENTS

The project is financially supported by the Disposal Research program of DOE-NE's SFWST office. We acknowledge critical in-kind assistance from: Salado Isolation Mining Contractors (SIMCO) underground facilities personnel, who provide underground access, power infrastructure, and drilling support; and the DOE Office of Environmental Management (DOE-EM) Carlsbad Field Office (CBFO) chief scientist, George Basabilvazo, who directs Shawn Otto and Jon Davis of the WIPP Test Coordination Office (TCO). The authors additionally thank Jason Heath of Sandia National Laboratories (SNL) for technically reviewing this report.

CONTENTS

LIST OF FIGURES

LIST OF TABLES

REVISION HISTORY

This report is a FY24 update of a series of BATS experiment status reports.

The FY20 BATS report details construction of the BATS 1 arrays and the first round of heating (SAND2020–9034R). The FY21 report details further data collection during periods without active heating and results of gas tracer tests conducted between boreholes (SAND2021–10962R). The FY22 report detailed decommissioning of the BATS 1 heated array and construction of the BATS 2 heated array (SAND2022–12142R). The FY23 report described the data collection in the new BATS 2 heated array and the original unheated array from BATS 1. This report describes continued data collection, planning for subsequent BATS testing, and higher-level discussion of a future salt repository conceptual model.

Date	Version	Identifier
Aug 30, 2024	DOE-NE review	SNL sensitivity review: 1755097
Sept 18, 2024	Final version approved for unlimited release	

ACRONYMS

AC	alternating current
AE	acoustic emissions (also BATS boreholes)
BATS	Brine Availability Test in Salt
CBFO	Carlsbad Field Office
CRDS	cavity ring-down spectrometer
DC	direct current
DECOVALEX	DEvelopment of COupled models and their VALidation against EXperiments
DOE	Department of Energy
DOE-EM	DOE Office of Environmental Management
DOE-NE	DOE Office of Nuclear Energy
DSS	distributed strain sensing
DTS	distributed temperature sensing
EDZ	excavation damaged zone
EdZ	excavation disturbed zone
ERT	electrical resistivity tomography
FY	fiscal year (October-September)
GMWL	global meteoric water line
HFI	halite fluid inclusions
HP	BATS central heater/packer borehole
IPI	Inflatable Packers International
LANL	Los Alamos National Laboratory
LBNL	Lawrence Berkeley National Laboratory
LVDT	linear variable differential transformer
MB-139	marker bed 139 (also MB-140)
MPFM	multiparameter flowmeter
MU-0	map unit 0 (also MU-3)
PA	performance assessment
PVC	polyvinyl chloride
R&D	research and development
RH	relative humidity
RTD	resistance temperature detector
SDI	Salt Disposal Investigations
SFWD	Spent Fuel & Waste Disposition
SFWST	Spent Fuel & Waste Science and Technology
SIMCO	Salado Isolation Mining Contractors
SL	BATS seal borehole
SN	serial number
SNL	Sandia National Laboratories
SRS	Stanford Research Systems
TC	thermocouple
TCO	WIPP Test Coordination Office
THMC	thermal-hydrological-mechanical-chemical
TRH	temperature and relative humidity
UHP	ultra-high purity (99.999%)
US	United States
VSMOW	Vienna standard mean ocean water
VPG	Vishay Precision Group
WIPP	Waste Isolation Pilot Plant (DOE-EM facility)

SPENT FUEL AND HIGH-LEVEL WASTE DISPOSITION/SALT RESEARCH AND DEVELOPMENT

This fiscal year 2024 (FY24) report summarizes experiments conducted and data collected in phase 2 of the Brine Availability Test in Salt (BATS 2). The design and interpretation of the test is funded by the US Department of Energy's Office of Nuclear Energy (DOE-NE) Spent Fuel and Waste Disposition Program, under the Disposal Research and Development (R&D) program of the Office of Spent Fuel & Waste Science and Technology (SFWST). The experiment is located underground at the Waste Isolation Pilot Plant (WIPP), southeastern New Mexico, which is a DOE Office of Environmental Management (DOE-EM) site managed by the Carlsbad Field Office (CBFO). DOE-EM funds the WIPP Test Coordination Office (TCO), which provides critical implementation support for the continued execution of BATS.

A high-level test plan by Stauffer et al. (2015) places BATS in the context of a multi-year testing strategy, which involves examining a range of processes at multiple scales, culminating in drift-scale disposal demonstrations. The organization of the current phases of the BATS field test is outlined in "*Project Plan: Salt In-Situ Heater Test*" (SNL et al., 2020), and an updated five-year plan is given in "*Brine Availability Test in Salt (BATS) Extended Plan for Experiments at the Waste Isolation Pilot Plant (WIPP)*" (Kuhlman et al., 2024a).

An initial design of the BATS field test was laid out in Kuhlman et al. (2017), with context, historical comparisons, and motivation for the individual test components of BATS phase 1 (BATS 1). This milestone report presents data collected with a set of boreholes drilled in FY22, which constitutes the BATS 2 heated array. More details on the as-built state of the BATS 1 experiment can be found in the FY20 milestone report "*FY20 Update on Brine Availability Test in Salt*" (Kuhlman et al., 2020). An unheated array of boreholes, which has been monitored during both BATS 1 and 2, is described in several annual update reports from FY20 through this current FY24 report. The FY21 milestone report "Brine Availability Test in Salt (BATS) FY21 Update" (Kuhlman et al., 2021b) presented a summary of 2020–2021 data, including several gas tracer tests conducted between boreholes. The FY22 milestone report "*Brine Availability Test in Salt (BATS) FY22 Update*" (Kuhlman et al., 2022) presented a description of the decommissioning activities for the BATS 1 heated array and a description of the construction of the new BATS 2 heated array. The FY23 report "*Brine Availability Test in Salt (BATS) FY23 Update*" (Kuhlman et al., 2023) presented data collected during the first four heating phases in BATS 2 (a through d). This FY24 report presents approximately 2 years of ongoing BATS 2 data across three heating phases (BATS 2, e through g), as well as plans for next year and high-level strategy for how this testing fits into our short- and long-term goals.

This level 2 milestone report (M2) incorporates input from level 3 milestone reports (M3) recently completed as part of Salt Disposal Research R&D by Los Alamos National Laboratory (LANL; Guiltinan et al., 2024) and Lawrence Berkeley National Laboratory (LBNL; Rutqvist et al., 2024). The team preparing, designing, implementing, debugging, and interpreting the BATS results includes members from multiple DOE national laboratories, led by Sandia National Laboratories (SNL), including LANL and LBNL. The tight integration of our DOE-NE Salt R&D team over the last ten years has helped make the ongoing field experiment possible. The work presented here would not be possible without the DOE-EM WIPP Test Coordination Office (TCO), who is onsite and underground at WIPP every week.

1 BACKGROUND AND TEST OVERVIEW

1.1 MOTIVATION FOR BATS

The focus of the BATS field test campaign is brine availability in geologic salt. These field tests are the first part of a wider systematic multi-year field investigation campaign to bolster the existing long-term repository safety case for disposal of heat-generating radioactive waste in a salt repository. BATS seeks to improve current understanding for predictions of how much brine can flow into both ambient and heated excavations (e.g., boreholes or rooms) in salt. Brine availability is important to the long-term repository safety case for radioactive waste disposal in salt (Kuhlman & Sevougian, 2013) because:

1. water is needed to corrode waste forms and waste packages;
2. water is required for dissolution and transport of aqueous radionuclides off-site (gaseous radionuclides are typically not significant);
3. water is essential to gas generation (e.g., steel corrosion, microbial, or water radiolysis), which increases gas pressure—a potential driving force for migration out of a repository;
4. chloride in natural brines absorbs neutrons, thereby eliminating in-package nuclear criticality hazards; and
5. final creep closure of openings will be slowed by any brine backpressure, for low porosity.

Field tests under the larger field campaign will explore other performance aspects of the long-term repository safety case that are separate from the brine availability focus of the current BATS field test.

In a generic salt repository for “hot” radioactive waste (i.e., above brine boiling temperature at the waste package surface), the region around the waste packages will dry out. While drying out, additional water associated with clay in the salt and water bound up in hydrous evaporite minerals may also become mobile and evaporate. Thermal expansion in the host rock leads to a thermal pressurization “dam” or “divide,” driving some near-field brine towards lower pressure excavations, while simultaneously driving far-field brine away from the excavation (Tounsi et al., 2023). Boiling and evaporation of brine with salt mineral precipitation near the waste package will reduce porosity, while condensation of water away from the heat source will increase porosity due to dissolution of salt. This process was recently implemented in PFLOTRAN (Park et al., 2024). Creep closure will reconsolidate granular salt backfill to low porosity and permeability, which acts to heal the Excavation Damaged Zone (EDZ) or Excavated disturbed Zone (EdZ; both EDZ and EdZ are introduced below) associated with mined openings. The combination of heat and creep closure will create a relatively dry, low-porosity, low-permeability zone around the waste packages (e.g., Blanco-Martín et al., 2018).

Generically, in a salt repository with hot radioactive waste surrounded by reconsolidating granular salt backfill, we expect the following nominal behavior or base scenario:

1. decay heat from radioactive waste will dry out the backfill in the short term (weeks to months);
2. accelerated reconsolidation of hot granular salt backfill will eliminate porosity and permeability near the waste (decades to hundreds of years—this is the primary focus of the KOMPASS and MEASURES ongoing international collaborative efforts (Mills et al., 2024) and LBNL’s modeling efforts with TOUGH-FLAC (Rutqvist et al., 2024);

3. after peak decay heat from the waste has passed (~1,000 years), the near-waste area will be dry, low porosity, and impervious, slowing down future resaturation of the waste packages (this has been found in the RANGERS international collaborative effort); and
4. dry waste packages do not corrode, there are few mobile radionuclides in a dry system, and there will be little gas generation.

Variant scenarios (i.e., off normal) in a safety assessment might include deviations from these expected behaviors (Kuhlman et al., 2024c). For example, some of the waste packages may be much cooler, and the system might not fully eliminate pore space around them, there may be some residual permeability near the cooler waste in the system after the peak decay heat has passed, and therefore there may be enough moisture to drive corrosion and gas generation.

It is possible to develop a salt safety case that relies solely upon the ability of the geologic salt formation to provide complete containment of the waste in the far field, without taking credit for the complex processes near the waste, including rapid closure of porosity, the drying out of the salt, or the expected low levels of gas generation in a hypersaline system. This would be a conservative approach, using a simpler bounding analysis to avoid the need for complex predictions associated with some more complex processes. But instead, by investigating and striving to understand and predict these complex processes, the safety case for a repository in salt can be more physically realistic and have a larger safety margin than a safety case built upon many conservatisms.

Understanding the processes that make up the base and variant scenarios is a key step towards making a defendable safety case for a future repository in salt.

In undisturbed geologic salt systems, the ultra-low permeability and porosity of salt (Beauheim & Roberts, 2002) provides the natural barrier to contain radioactive waste over performance assessment (PA) relevant time scales (10^4 to 10^6 years). However, near-field conditions (e.g., fluid pressures, liquid saturation, and chemical composition) and processes (e.g., brine and gas flow, waste package corrosion, precipitation and dissolution of salt, thermal expansion and contraction of salt and brine, and salt creep) are more complex to account for in disturbed scenarios (i.e., off-normal scenarios like early waste package failure or inadvertent human intrusion). The current state of the salt, both damaged and far-field intact salt are the initial conditions for long-term performance assessment (PA) simulations. BATS is focused on understanding processes necessary to quantify inflow rates and brine composition in the near field (i.e., at scales of cm to m from the heat source) for normal scenarios with the aim to improve:

1. our understanding of coupled THMC processes affecting prediction of near field conditions;
2. conceptual models of near-field behavior that inform the safety case; and
3. the numerical models, constitutive relationships, and parameterizations that are implemented in process models and PA models.

Brine availability in a salt repository depends on both the distribution of water in the host salt geologic formation and the flow and transport properties of the EDZ or EdZ surrounding an excavation (Kuhlman & Malama, 2013; Kuhlman, 2019).

The EDZ is a region surrounding excavations where the salt is damaged, and both its material properties (i.e., porosity and permeability) and state (i.e., pressure, stress, or temperature) have changed—the EDZ is often equivalently called the “disturbed rock zone”. The EdZ is a larger region surrounding the EDZ, where only the variables are disturbed from their far-field values, while rock material properties are unchanged (Davies & Bernier, 2005). The primary EDZ property of interest for the BATS field test is the distribution and evolution of mechanical damage and subsequent changes to hydrologic properties (i.e., porosity, permeability, and the nature of induced fractures) around the

access drift and test boreholes, which provides the primary path for flow around the access drifts and test boreholes.

1.2 BATS PHASES

The initial BATS "shakedown" test location was in WIPP drift E-140 (Figure 1), utilizing existing boreholes. Referred to as BATS 1s or simply "the shakedown test," it was performed June 2018 through April 2019 (Boukhalfa et al., 2019; Guiltinan et al., 2020).

BATS phase 1 began with two nearly identical new horizontal borehole arrays (heated and unheated) drilled in the Salt Disposal Investigation (SDI on map) area of WIPP (on the south side of N-940 west of E-540; Figure 1 and Figure 2). BATS phase 1a refers specifically to testing that occurred from January to March 2020 and involved data collection from both the heated and unheated arrays during the first heating phase. BATS phase 1b was conducted from January to June 2021 and involved addition of gas tracers to the D boreholes in both the heated and unheated arrays. BATS phase 1c was conducted July to August 2021 and involved adding liquid tracers in the same heated and unheated D boreholes (Kuhlman et al., 2021b). Here, the references to the "BATS 1" boreholes mean the boreholes used in phases 1a through 1c in the N-940 drift, not the 1s shakedown test boreholes in drift E-140.

BATS 2 heated array boreholes were drilled October 2021 and January through February 2022 in the N-940 drift at WIPP, approximately 20 feet [6.1 m] west of the BATS 1 heated array. No new unheated array was drilled as part of this effort; the BATS 1 unheated array has been continuously monitored since 2020. Several heater testing events have occurred so far in BATS 2 (July 2022 through August 2024) named BATS 2a, 2b, 2c, 2d, 2e, and 2f, with possible follow-on testing to occur in these boreholes, depending on their availability and condition. The BATS 2 heater tests are being conducted in the most recently constructed (October 2021 through February 2022) heated borehole array.

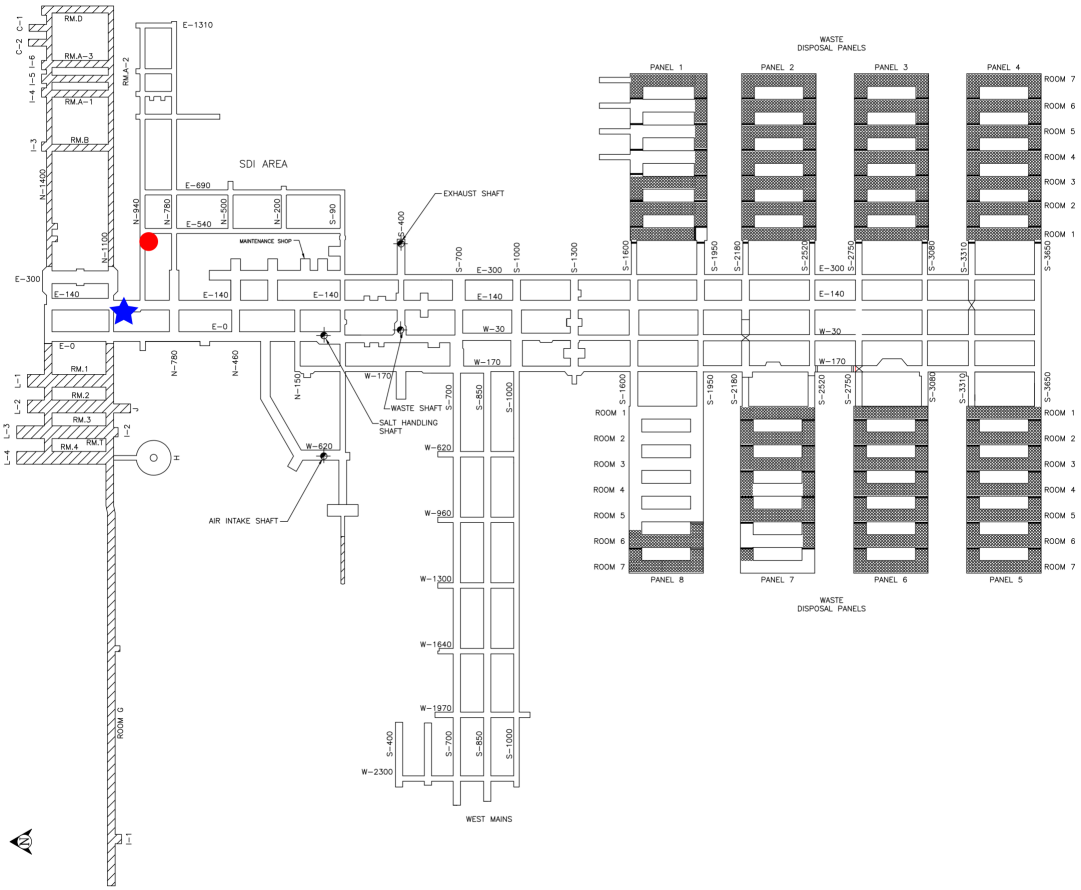

Figure 1. Updated (2024) WIPP underground map. Location of BATS phases 1 and 2 indicated with red circle. BATS 1s shakedown test location indicated with blue star.

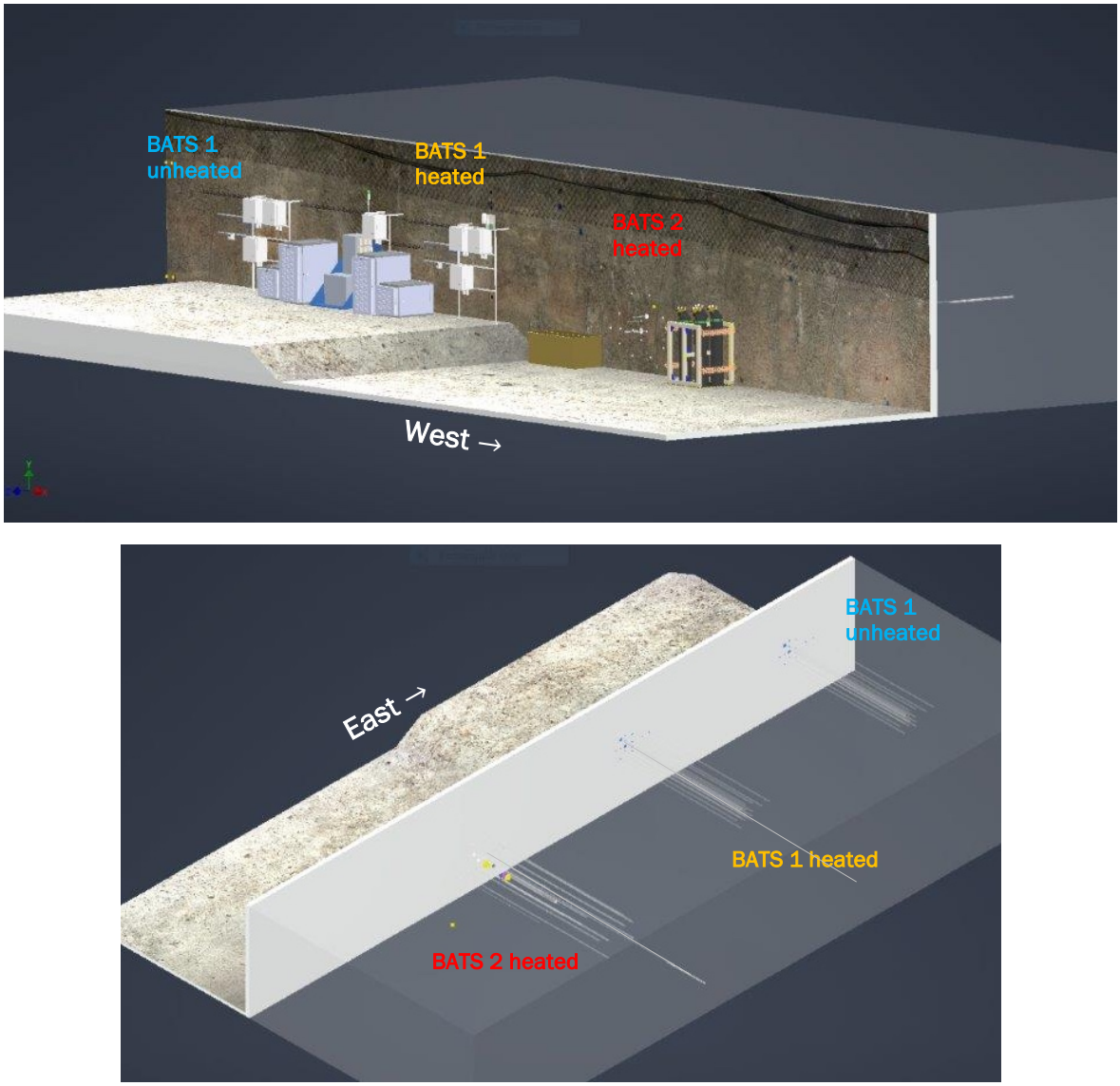

Figure 2. Layout of borehole arrays and in-drift equipment in N-940 showing relative positions of BATS 1 and BATS 2 arrays. Boreholes are completed in the south side of drift; the unheated array is east of the heated arrays. Bottom subplot shows orientation of boreholes into the salt (salt is not shown).

1.3 BATS FIELD TEST COMPONENTS

The western test array of BATS 2 is heated by the heater in the central HP borehole, and the eastern array is the unheated array from BATS 1 (see Kuhlman et al., 2020, for detailed info on the unheated array). Figure 2 shows the location of the adjacent BATS 1 and BATS 2 arrays in the N-940 drift. More detailed information on the location and drilling sequence of the BATS 2 array, and the location of sensors, can be found in tables given in the appendices of Kuhlman et al. (2023).

The HP boreholes in the two BATS 1 arrays were 6.9 m apart horizontally and at the same level vertically, while the BATS 2 heated array is 13 m west and 1 m lower vertically than the unheated array (distance between HP boreholes).

The heated BATS 2 array is configured with several types of instruments in the central HP borehole and surrounding satellite boreholes. See Table 1 for a listing of information on the various boreholes, and Figure 3 for views of the boreholes and temperature sensor locations from three different viewpoints.

Compared to BATS 1 (including the unheated array, which is still partially monitored), there are additional AE and E boreholes (four per sensor type in BATS 2 heated array compared to three per sensor in each array for BATS 1a), and the SL, AE, and E boreholes are all slightly longer. The narrowest boreholes in BATS 1 were 1.75 inches [4.4 cm] diameter, while the narrowest boreholes in BATS 2 are 2.1 inches [5.3 cm] diameter. Temperature distribution, strain, and brine movement are monitored with thermocouples, fiber-optic distributed strain sensing (DSS) and temperature sensing (DTS), acoustic emissions (AE) monitoring, and electrical resistivity tomography (ERT).

Table 1. Summary of BATS 2 heated array boreholes.

Type	Purpose	Boreholes per array	Diameter [cm]	Length [m]	Isolation Device
HP	Heater, packer, borehole closure, N_2 circulation, gas sampling	1	12.2	3.66	Inflatable packer
D	Tracer source, gas permeability testing	1	5.3	4.57	Inflatable packer
SM	Liquid sampling	1	5.3	4.57	Mechanical packer
F	Fiber-optic temperature and strain	2	5.3	5.49 & 9.14	Grouted
E	Electrical resistivity tomography (ERT) electrodes	4	5.3	5.79	Grouted
AE	Acoustic emissions (AE) and ultrasonic travel-time tomography sensors	4	5.3	3.35	Sensors on borehole wall with de-centralizer
T	Thermocouples	2	5.3	5.49	Grouted
SL	Cement seals behind mechanical packers with embedded sensors	1	12.2	3.51	Mechanical packer

Inflatable packers are used in the HP and D boreholes to isolate the region behind the packer from the drift air (Table 1). This is to prevent dry-out of the salt, loss of moisture, and contamination of samples. The rubber packer bladders are inflated to approximately 80 psi [5 bars] pressure above atmospheric pressure. The HP borehole packer has multiple pass-through tubes or pipes, to allow sensors and power to reach the isolated part of the borehole. These pass-throughs are sealed with wire compression nuts, made by Conax Technologies. The D borehole packer has a port for application of gas pressure behind the inflated packer but does not have wire pass-throughs.

Mechanical packers are also used in the SM and SL boreholes to isolate the rear part of the borehole from the drift environment. The mechanical packers use mechanical compression of a rubber sleeve by tightening nuts on a threaded rod to isolate the rear of the borehole. The wires to the sensors behind the packer are sealed against the inside of the threaded pipe with plumber's putty.

2 TEST DESIGN DETAILS

The following testing methods relate to the setup and initial monitoring of the BATS 2 heated array. For the as-built details of the BATS unheated array boreholes and more information on BATS 1 in general, see previous milestone reports by Kuhlman et al. (2020; 2021b).

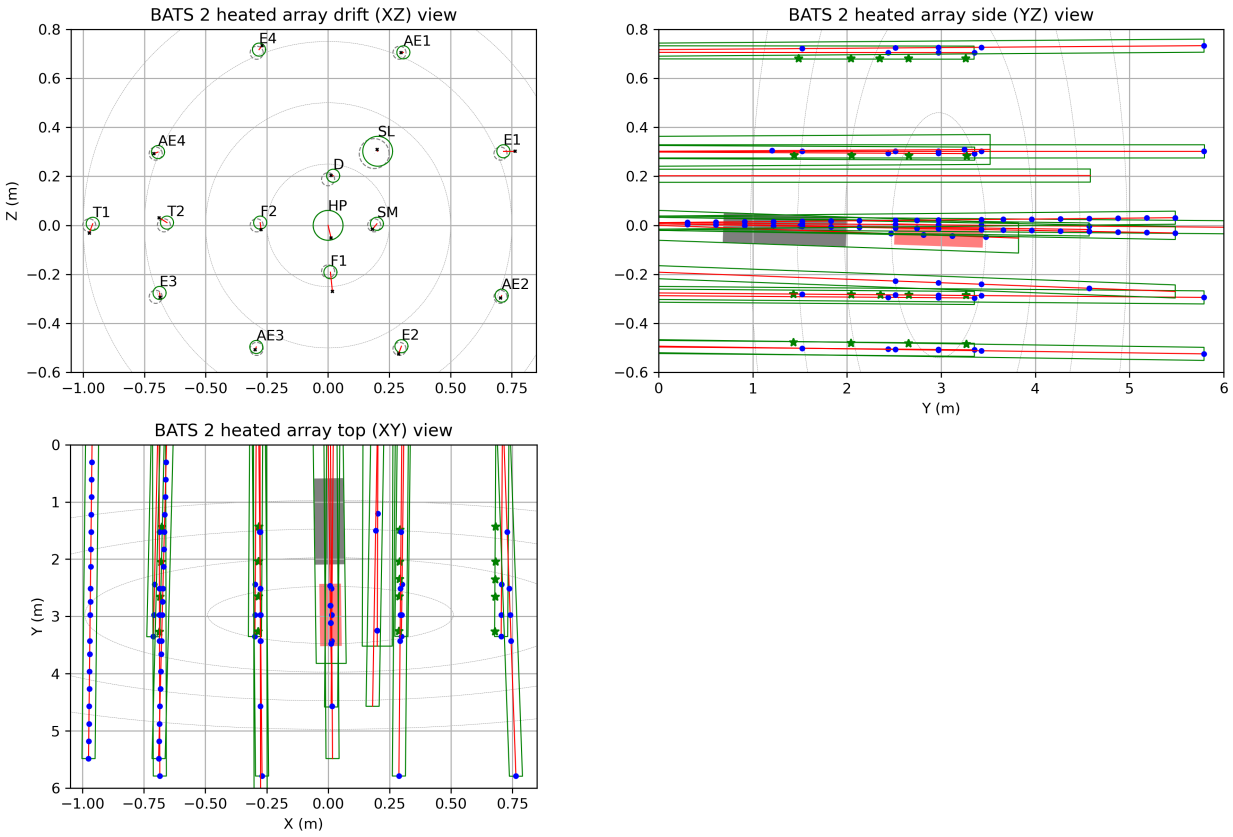

Figure 3. Drift, side, and top views of BATS 2 array. Drift view shows proposed (gray dashed) and as-built (green) borehole positions in drift; red line is axis of boreholes with "×" indicating ends of boreholes. Side and top views show thermocouple and resistance temperature detector (RTD) locations (blue dots), AE sensor locations (green stars), HP heater (red box), and HP packer (gray box). Gray contours indicate distance from center of the heated interval.

To date, seven heater tests have been conducted in BATS 2. BATS 2a, 2b, 2c, and 2d were in FY23, and BATS 2e, 2f, and 2g were in FY24. The first four tests consisted of a three-week heating phase, followed by at least two weeks of cool down phase. These heater tests are discussed in detail in Kuhlman et al. (2023). This report shows data from these tests, but mostly for comparison against the most recent three tests. BATS 2e conducted a similar test to BATS 2d, to confirm the repeatability of the response. The heater controller in BATS 2f and 2g was at a similar temperature setpoint, but longer in duration (5 weeks and 8 weeks of heating) to investigate the potential dry-out of the salt from repeated heating.

The full-length heater test periods are referred to as BATS 2a through BATS 2g. The setpoints, achieved power, and temperatures observed are discussed in detail in Section 4.1.6.

3 CONFIGURATIONS OF BATS 2 BOREHOLES AND MEASUREMENTS

The following subsections describe things that have changed in measurement equipment associated with the BATS 2 heated array. The boreholes in the unheated array were completed as part of BATS 1, and they are described in Kuhlman et al. (2020). The as-built configuration of the BATS 2 heated array boreholes is presented in Kuhlman et al. (2023).

This section follows the structure of previous reports, but most parts of the BATS 2 setup have not changed this year, so their subsections are short.

In FY24, a battery backup system (comprised of four 12 V 100 Ah lead acid batteries) was installed in the BATS array to improve the ability of system to survive short (hours) to medium (days) length power outages. The battery system can only power things that run on 12 V DC power. The battery cannot power the heater, the AE data acquisition, nor the gas analyzer—these components use 120 V AC power.

3.1 HP (HEATER AND PACKER) BOREHOLE

There is one central 12.54-ft [3.82 m] long and 4.8-inch [12.2 cm] diameter HP borehole. The 1250-watt quartz lamp heater (BATS 1 used a 750 W heater of the same physical size) and centralized borehole-closure gauge are mounted behind the 4.5-inch [11.4 cm] diameter 4.2-ft [1.3 m] long inflatable packer, which is built around a 0.5-inch [12.5 mm] stainless steel pipe.

The configuration of the HP borehole, the packer, heater, and in-borehole sensor configurations have not changed in FY24, but the plumbing and analysis of the gas flowing out of the HP borehole has changed and is described in the following subsubsection.

3.1.1 ROUTING AND ANALYSIS OF GAS STREAMS

Upstream of the HP borehole, a bottle of ultra-high purity (UHP) N_2 gas flows at a constant mass flowrate maintained via a programmable Omega flow controller (FMA-2605A-V2). During BATS 2 the heated array is mostly run at a constant flowrate, 100 std mL/min (i.e., mass flowrate at standard temperature and pressure), while the unheated array is maintained at 25 std mL/min.

Multiple N_2 bottles are now connected in parallel to address the previous choice between flowing gas at a high flowrate and running out of gas over a long weekend, or flowing gas at a low flowrate and having the system become overwhelmed with water vapor (i.e., condensation in the tubing and instrumentation, as happened during BATS 2d). A second N_2 regulator was added that allows multiple bottles of UHP N_2 gas to be connected to the inflow system in parallel, doubling the amount of N_2 available. This allowed higher flowrates of gas to be set at the beginning of a heated period, while minimizing the risk of running out of gas over a weekend. BATS 2e was run at a higher flowrate, but as the BATS 2 system has dried out over the course of two years, this has been less of a problem (this approach will be considered for new BATS 3 boreholes, where higher brine production rates are likely).

The plumbing of gas has simplified significantly since summer 2023, specifically:

- The Picarro CRDS failed. At first it was removed to debug and troubleshoot the instrument, but it was deemed unrepairable It was permanently removed from HP gas stream on July 31, 2023.
- The switching of solenoids between the heated and unheated arrays stopped. On September 5, 2023, the solenoids were fixed in one position permanently, so that the heated HP borehole gas stream flowed through the Stanford Research Systems (SRS) QMS-200 gas analyzer. The heated and unheated array gas streams are essentially fixed and no longer share any common tubing.

In July 2023, the Picarro CRDS was removed from the WIPP underground. Starting in November 2023, water samples were collected manually in the underground using a cold trap constructed with a slurry of crushed dry ice (i.e., solid CO_2 that sublimates at -78.5 ºC) and ethanol. At each sampling event, the heated array gas stream is diverted through two manual three-way values (Figure 4) and a cold trap for approximately one hour. Once sampling is complete, the liquid sample is then collected in a transportation container, which is sent to LANL for analysis using a Picarro CRDS in the lab.

Testing of the approach in the lab, it was found the approach to be approximately 97% efficient at removing water from a simulated gas stream. Guiltinan et al. (2024) includes more details on the design, testing, and implementation of the cold trap.

Figure 5 shows the previous gas plumbing (top is same figure as Kuhlman et al., 2023), and the simplified gas plumbing (bottom) after replacing the Picarro CRDS with the cold trap and fixing the switching solenoids. The cold trap was added to the heated array gas stream immediately after the heated borehole, before the multi-parameter flow meter (MPFM; Figure 5).

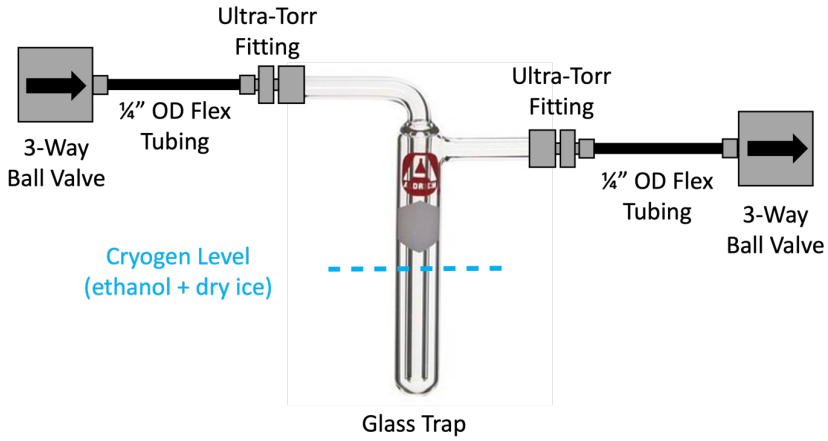

Figure 4. Cold trap used to collect water samples for isotopic analysis at LANL, replacing the inline Picarro CRDS system (Guiltinan et al., 2024).

The SRS QMS-200 gas analyzer is a quadrupole mass spectrometer operating in a vacuum chamber evacuated with a turbomolecular pump. The unit splits the sample, directing most of it to the backing vacuum pump, which permits the unit to directly sample gases at atmospheric pressure.

The output streams from the gas analyzers go through another pair of plumbing tees and three-way solenoid-actuated valves before passing through a pair of air temperature and relative humidity (RH) probes (labeled as TRH probes in Figure 5) and a pair of canisters of desiccant, with subsequent TRH probes at the outflow. The TRH probes before and after the desiccant are used to confirm the RH of the gas stream, and to confirm the desiccant is removing all the moisture from the gas stream. This final set of switching valves ensures that one set of desiccant canisters is associated with the heated array and the other associated with the unheated array, even though the intervening gas analyzers are switching between arrays.

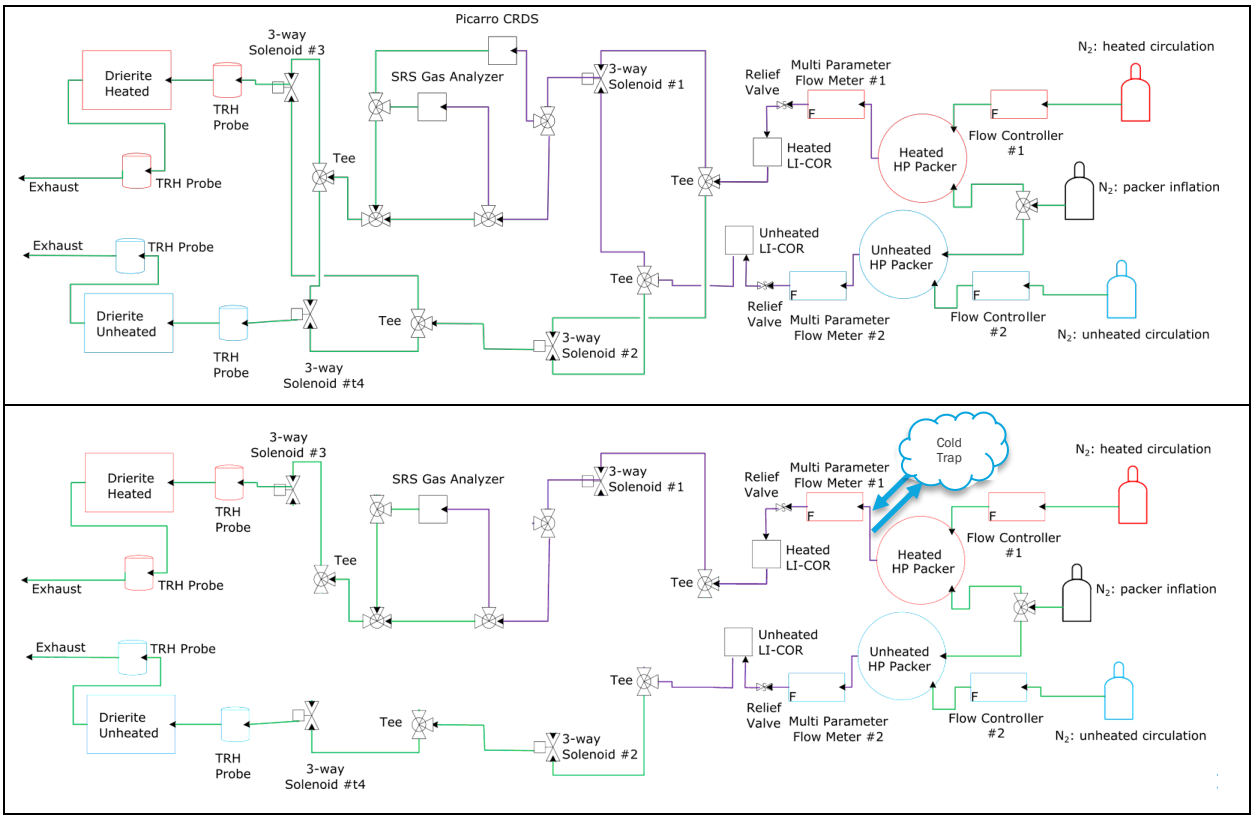

Figure 5. Plumbing schematic of BATS 2 from 2022 to July 2024 (top) and after September 2023 (bottom). Gas flow from HP boreholes (right) through Picarro, Stanford Research System (SRS), and LI-COR gas analyzers to exhaust (left). Green lines are 0.25-inch [6.4 mm] polyethylene tubing, purple lines are 0.25-inch stainless steel tubing, red items are only for the heated array, and blue items are only for the unheated array, gray items switch between the heated and unheated arrays. TRH measures temperature and relative humidity.

3.2 AE (ACOUSTIC EMISSION) BOREHOLES

There are four 11-ft [3.35 m] long (2.1-inch [5.3 cm] diameter) AE boreholes with multiple piezoelectric sensors, namely Physical Acoustics Nano30 AE sensors, in each borehole.

The configuration of the boreholes and in-borehole sensors of the AE system has not changed in FY24, but the processing and recording of AE has changed as described below.

To help deal with significant noise issues, data has been initially filtered multiple times throughout processing. Initially, data is bandpass filtered at 75 to 700 kHz, where hits with frequencies outside this range are discarded. Signals are amplified by 60 dB by inline preamplifiers before reaching the AE systems, where signals must cross a 28 dB threshold to be recorded. Additionally, signals must 10 msec long to be recorded. Post recording, data is further filtered by increasing the signal using a partial power frequency method, where the energy content in the 10 to 250 kHz frequency band must be greater than or equal to 50% of the total energy of a recorded waveform to be considered, otherwise data is removed.

The unheated array from BATS 1 was left in place and is still active for the current and future phases of testing. Eight sensors are installed into three unheated BATS 1 AE boreholes.

3.3 T (THERMOCOUPLE) BOREHOLES

There are two 19-ft [5.5 m] long (2.1-inch [5.3 cm] diameter) T boreholes with 18 thermocouples in each (grouted outside 0.75-inch [19.1 mm] polyvinyl chloride (PVC) conveyance pipe; Table A-3). One of the boreholes is at 2-ft [61 cm] radial distance away from the edge of the heated borehole (T2), and the other at 3-ft [91 cm] radial distance (T1). The configuration of the T boreholes and in-borehole sensors have not changed in FY24.

3.4 E (ELECTRICAL RESISTIVITY TOMOGRAPHY) BOREHOLES

There are four 18-ft [5.79 m] (2.1-inch [5.3 cm] diameter) E boreholes with 16 ERT electrodes on the outside of each 0.75-inch [19.1 mm] PVC conveyance pipe (12-inch [30 cm] spacing between adjacent electrodes, starting from the far end of the borehole), with grout installed in the space inside and outside the PVC.

The configuration of the E boreholes and in-borehole sensors have not changed in FY24.

3.5 F (FIBER OPTIC) BOREHOLES

There is one 18-ft [5.5 m] (2.1-inch [5.3 cm] diameter) F1 borehole and a second 30-ft [9.1 m] F2 borehole, both with grouted distributed fiber-optic sensors.

The configuration of the F boreholes and in-borehole sensors have not changed in FY24.

3.6 D (SOURCE) BOREHOLE

There is one 15-ft [4.6 m] (2.1-inch [5.3 cm] diameter) D borehole with a 2.1-foot [64 cm] long 1.9-inch [4.8 cm] diameter Inflatable Packers International (IPI) packer inflated in the borehole (with the back of the packer set at 1.53 m depth).

The configuration of the D borehole, packer, and in-borehole sensors have not changed in FY24.

3.7 SM (SAMPLE) BOREHOLE

A 15-ft [4.6 m] long and 2.1-inch [5.3 cm] diameter liquid sampling (SM) borehole is plugged with a mechanical packer beyond major fractures near the drift wall (the back of the packer is set at 1.35 m depth).

The configuration of the SM borehole, packer, and in-borehole sensors have not changed in FY24.

3.8 SL (SEAL) BOREHOLE

The 11.5-ft [3.5 m] deep SL borehole has a pair of composite lab-constructed cement seals emplaced and sealed behind a mechanical packer (the back of the packer is set at 1.05 m depth).

The configuration of the SL borehole, packer, and in-borehole sensors have not changed in FY24.

3.9 IN-DRIFT OBSERVATIONS

Ambient drift air pressure, air temperature, ventilation (i.e., “wind”) speed, RH, and barometric pressure are monitored in the drift between the BATS 1 unheated and BATS 2 heated arrays.

The configuration of these sensors has not changed in FY24.

4 BATS 2 BOREHOLE OBSERVATIONS

Previous BATS 1 reports (Kuhlman et al., 2020; 2021b) presented data collected January 2020 to August 2021 in BATS phase 1, which included several heater and tracer tests. This report presents

BATS 2 data from the BATS 2a heating period (starting July 2022) through BATS 2g (ending July 2024). Data from 2022 and 2023 are repeated from Kuhlman et al. (2023), along with new data. Discussion is centered around new data (since summer 2023) or comparison between new data and previous data.

4.1 DATA FROM HP BOREHOLES

Dry UHP N_2 gas is circulated through the interval isolated behind the HP packer. The gas inflow location is at the back of the borehole (i.e., the inlet gas is directed to the area behind both heater reflectors through a 0.25-inch [6.4 mm] stainless steel tube), and the gas outflow location is on the back of the packer. The mass flowrate of N_2 gas into the interval behind the packer is controlled by an Omega flow controller between the N_2 gas bottle regulator (set to approximately 20 psi [1,379 mbar] gauge pressure) and the packer. The flowrate of gas out of the packer-isolated interval is measured immediately downstream of the packer with an Omega multi-parameter flowmeter (MPFM), which measures mass flowrate, temperature, and pressure.

4.1.1 HP: GAS STREAM PRESSURE AND FLOWRATE TIME SERIES

Figure 6 shows the time series of gas stream mass flowrate (i.e., the active flow controller between the gas source and the HP packer, and the passive mass flowmeter downstream of the packer) averaged every 10 minutes by Campbell CR1000X dataloggers.

The legends and titles in Figure 6 and subsequent figures use the naming convention of variables in the data spreadsheets produced by the WIPP TCO. In these variables, the BATS 2 heated or BATS 1 unheated arrays are indicated by a starting letter “H” or “U”. The next letters relate to the BATS 2 borehole (in this case “HP”). Finally, “GQUp” and “GQDown” refer to gas “G” flowrate “Q” up and downstream of the packers in the heated and unheated arrays (see Figure 6).

In most time series plots, the minor tick-marks indicate weeks (each Monday). The colored dots indicate individual 10-minute average values, while lines of the same color are used to connect dots but may not be representative of the value between averages.

The colored vertical stripes are common across all time-series figures and are associated with key testing events listed in

Table 2. The fifth through seventh heating events, BATS 2e through BATS 2g, occurred in FY24; they are new since the last annual data report (i.e., below dashed line in table). The heater events are labeled with letters above the top edge of Figure 6 for clarity of explanation but are not labeled with letters on every subsequent figure.

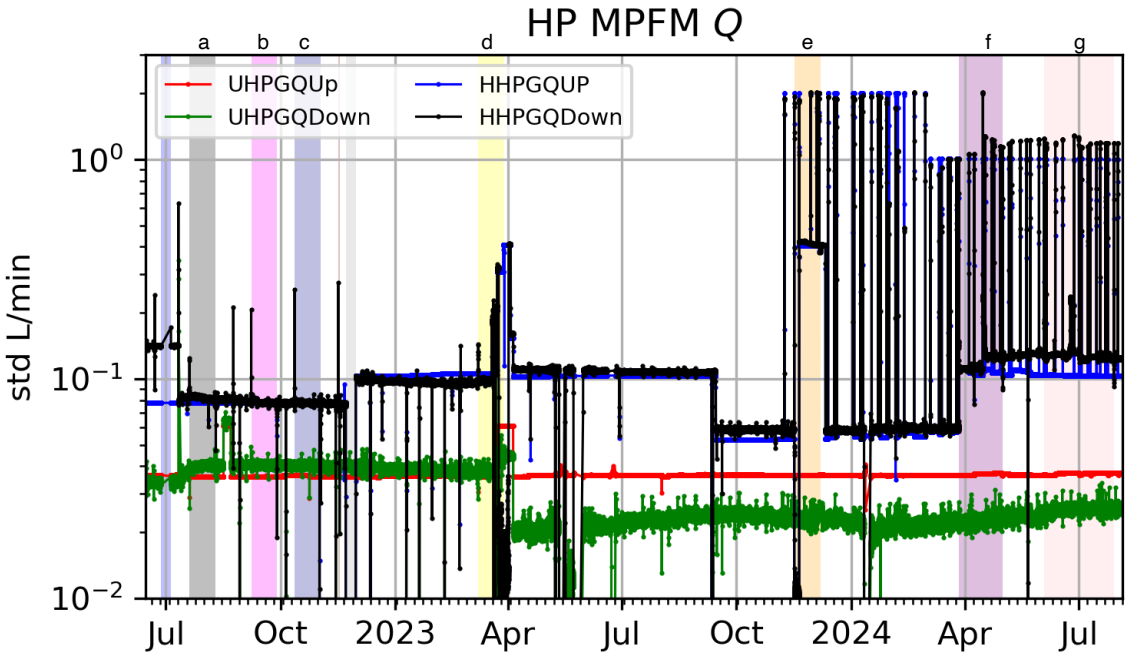

Figure 6. Gas stream mass flowrates (GQ) up- and down-stream of HP packer for heated (H) and unheated (U) arrays.

In Figure 6, the mass flowrates of gas upstream and downstream of the packers are close to the same (i.e., red vs. green for unheated; and black vs. blue for heated) during most of the data record. Since the BATS 2d test, the downstream flowrate in the unheated array (green) is slightly lower than the upstream flowrate in the unheated array, which is not as expected (the unheated array should not be impacted by the heater test in the adjacent array), but this difference is small and is accentuated because of the logarithmic y-axis scale.

In preparation for the BATS 2e heating test, the gas flowrate was increased to 400 std mL/min, considering that the last heater test, under similar conditions (BATS 2d) produced large amounts of water, which led to condensation in the circulation tubing. The flowrate was then reduced back down to "background" of 75 std mL/min after BATS 2e. At the beginning of BATS 2f, the gas flowrate was increased to 100 std mL/min and has remained there.

Starting in late 2023 (near BATS 2e), the short jumps in heated array gas flowrates to 1 to 2 std L/min are times when the active sampling was being conducted in the underground using the cold trap (most of the sampling periods are 1 hour long). The cold trap sampling event details are listed in Table A-6.

Table 2. BATS 2 events associated with colored bars in timeseries figures.

Event	Color	Begin	End
Higher gas flowrate to initially dry out HP boreholes	Pink	25 Apr 2022 12:30	16 May 2022 09:00
WIPP power maintenance	Blue	27 Jun 2022 08:30	05 Jul 2022 10:15
BATS 2a heater test (90 °C setpoint – 3 weeks)	Black	20 Jul 2022 08:29	10 Aug 2022 07:38
BATS 2b heater test (115 °C setpoint – 3 weeks)	Magenta	07 Sep 2022 14:52	28 Sep 2022 08:02
BATS 2c heater test (130 °C setpoint – 3 weeks)	Dark Blue	12 Oct 2022 10:01	02 Nov 2022 11:43
HP Packer out of borehole	Gray	22 Nov 2022 09:45	30 Nov 2022 08:05
BATS 2d heater test (140 °C setpoint – 3 weeks)	Yellow	08 Mar 2023 09:20	29 Mar 2023 09:36
BATS 2e heater test (140 °C setpoint – 3 weeks)	Orange	16 Nov 2023 09:42	07 Dec 2023 11:37
BATS 2f heater test (140 °C setpoint – 5 weeks)	Purple	27 Mar 2024 08:34	01 May 2024 09:33
BATS 2g heater test (140 °C setpoint – 8 weeks)	Peach	03 Jun 2024 08:34	29 Jul 2024 09:34

Figure 7 shows the time series of air pressure in the tubing between the packer and the switching solenoids for the heated and unheated arrays measured at the MPFM and averaged every 10 minutes on the Campbell dataloggers. The cold-trap sampling periods (listed in Table A-6) are also clearly visible in the pressure data. The combination of higher gas flowrate and different plumbing for the cold trap result in a higher gas pressure in the system. Earlier samples from the cold trap (before March 2024) were conducted at gas flowrates of 2 std L/min, which resulted in the highest observed gas pressures.

Figure 8 shows the time series of air temperature in the tubing upstream and downstream of the HP borehole packer (upstream of the now-fixed switching solenoids), measured at the MPFM and averaged every 10 minutes on the Campbell dataloggers. Gas stream temperatures show effect of changes in ambient drift temperature, with few significant additional fluctuations visible.

In January 2024, there was a drop in circulation gas temperature (the minimum temperature is 22 to 23 °C), at a time when the flowrate dropped below 0.01 std mL/min in both arrays.

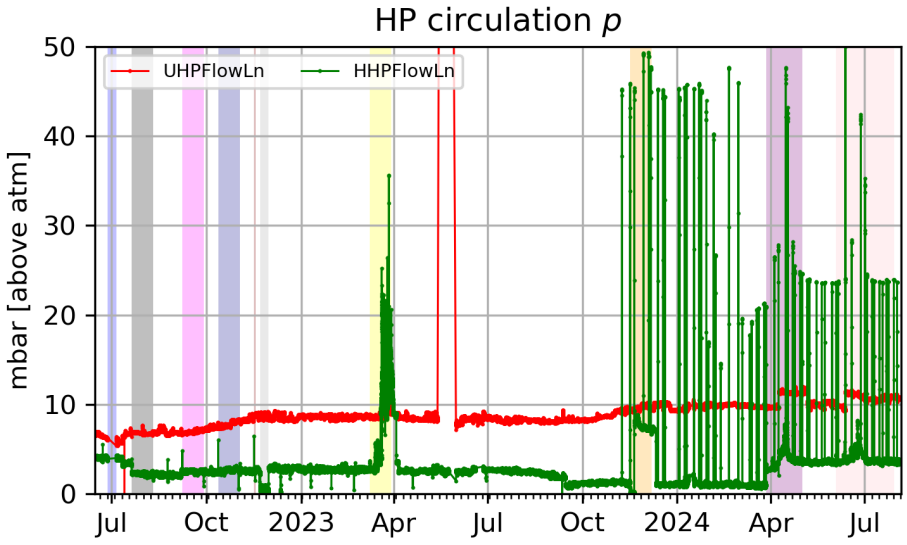

Figure 7. Gas stream pressure downstream of HP packers; "FlowLn" in legend indicates flowline.

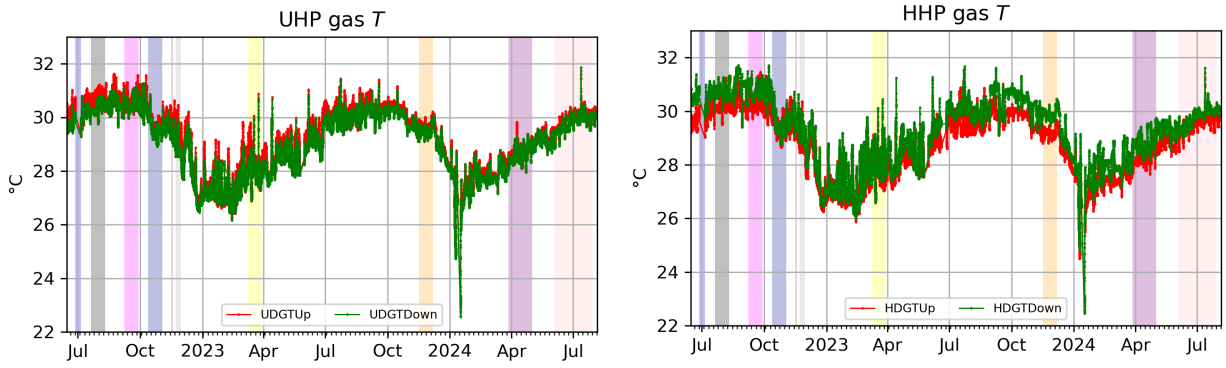

Figure 8. Gas temperature up- (red) and down-stream (green) of HP packers (unheated array left, heated array right).

4.1.2 HP: WATER CONTENT TIME SERIES

Water production from the HP gas stream is estimated using data from multiple observations made in the HP gas stream. Descriptions and assumptions for water production and the system are as follows:

- The gas flowing into the packer-isolated interval is assumed dry (UHP N_2; less than 10^{-5} fraction water).
- The gas mass flowrate leaving the HP packers is measured by MPFM. The water concentration in this gas stream is measured using two different instruments:
  - two LI-COR 850 instruments (both heated and unheated) recording water concentration data at 10-minute averages (Figure 9 and Figure 10).
  - both branches of the gas system have Campbell EE181-L TRH probes measuring in-line air temperature and RH at 10-minute average (Figure 11) before and after desiccant canisters on each branch.
- Desiccant canisters are weighed once or twice weekly (Figure 12) to measure the total mass of water leaving the borehole system.

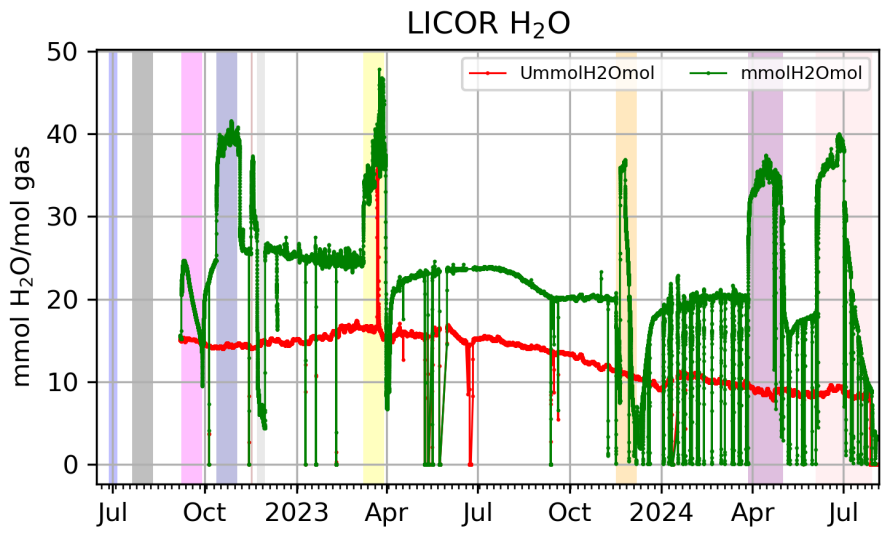

Figure 9. LI-COR water concentrations. Red is unheated array; green is heated array. No initial capital letter is heated array, leading "U" is unheated.

The LI-COR data reported in the FY22 report (Kuhlman et al., 2022) were erroneous (through 6 September 2022) and are left out of Figure 9 and Figure 10. The instruments were far out of calibration and required servicing by the manufacturer.

The water concentrations reported by the LI-COR (Figure 9) show higher water concentration during the BATS 2 heater tests, and lower concentrations between tests. In heater tests BATS 2c, d, and f, the higher water concentration lasted for the entire heating period (3 weeks for BATS 2c and d, and 5 weeks for BATS 2f). In other heater tests water concentration dropped after a few weeks of heating. In the longest and most recent heater test (BATS 2g), the water concentration dropped to levels below the typical background observed between tests.

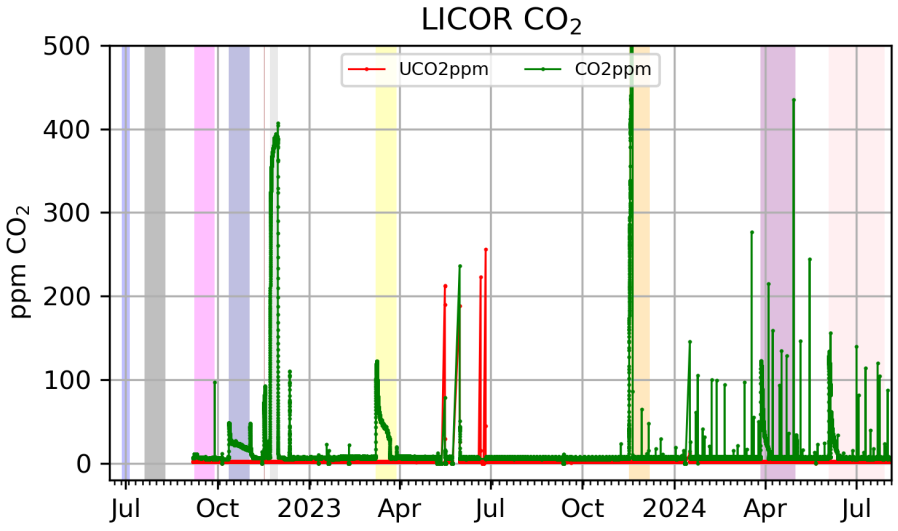

Figure 10.LI-COR CO_2 concentrations. Red is unheated array green is heated array. No initial capital letter is heated array, leading "U" is unheated.

The LI-COR also measures CO_2 concentrations (Figure 10), which were at approximately atmospheric levels while the heated HP packer was out of the borehole (400 ppm), as expected. At the beginning of multiple heating tests, the CO_2 concentrations spike, then rapidly decay. At the beginning of BATS 2e there was a very high peak (green values extend beyond the graph to approximately 2500 ppm), which is believed to be erroneous or possibly due to some other effect on the sensor (e.g., water condensation). These spikes and decays likely are caused by CO_2 desorbing from the borehole wall or exsolving from brine at elevated temperatures.

During cold trap sampling events, the CO_2 level rose for one 10-minute measurement, which is likely due to atmospheric gas (~400 ppm CO_2) in the cold trap being flushed through the system when the cold trap sampling is started.

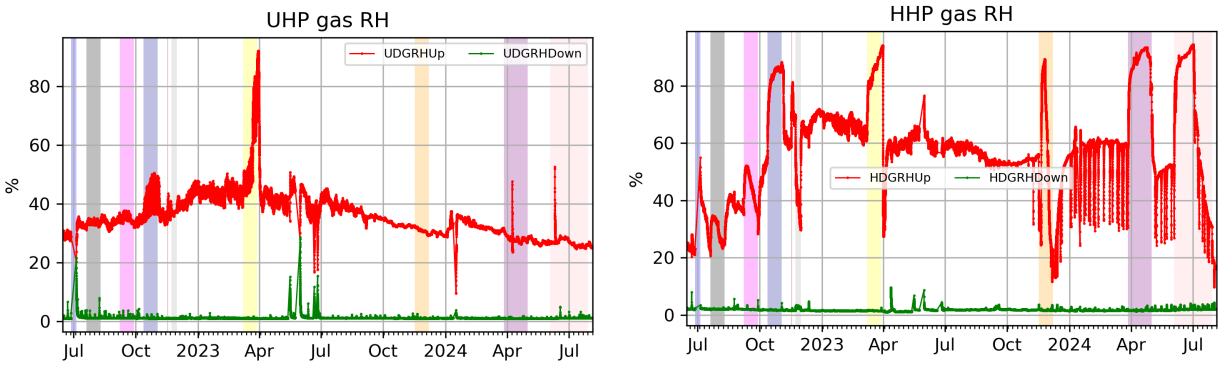

Figure 11. RH up- (red) and down-stream (green) of the unheated array (left) and heated array (right) desiccant.

Relative humidity (RH) time series are measured both upstream and downstream of the Drierite desiccant canisters (Figure 11). These RH sensors are downstream of the second set of solenoid valves (Figure 5), which are now no longer switching in the updated plumbing system (see Section 3.1.1). The upstream RH in the unheated array was elevated at the end of BATS 2d (and to a lesser degree during BATS 2c). The downstream RH is mostly ≤ 1% (green curves).

The desiccant water production data is listed in Table A-4 (heated array) and Table A-5 (unheated array) and presented graphically in Figure 12. The unheated array produced similar water concentration in air from the heated array. Since October 2023, the two arrays are producing approximately the same concentration again. The heated array produced a higher concentration of water in produced air during unheated periods from October 2022 to October 2023 (see aqua-colored horizontal bar). Near the end of the elevated water production period in the heated array (August and September 2023), the water production rate dropped even lower, before recovering to approximately the same rate observed in the unheated array (see purple colored bar).

At early times the newly drilled BATS 2 heated array was producing more brine because the boreholes were fresh (boreholes are drilled with air, but the fresh salt produces more brine initially). After BATS 2b (and even more between BATS 2c and 2d) brine production likely increased due to induced damage from heating and cooling cycles.

The unheated array showed a spike in water production during BATS 2d (see yellow vertical bar in Figure 12), which is like the data seen in the RH sensors and LI-COR during this period. This supports the hypothesis that some of the large amount of water produced during this test went into the unheated array tubing. Water concentration in the unheated array rose to levels in the heated array (~0.025 g H_2O/L air) near the end of the BATS 2d heating period. This is believed to be an artifact or leakage between the two branches through the switching solenoids.

During more recent heating tests (BATS 2e, f, and g), the water production rate has dropped during and through the end of heating tests, with recovering occurring after heating. At least one of the drops in water heated array water production between heater tests (September 2023) occurs the same time as other observed changes in other observations (see Section 5).

Notably, there was not a significant inflow of water observed in the heated array after the shutdown of the heater during any of the BATS 2 heater tests (BATS 2 c and d were the closest to seeing this behavior).

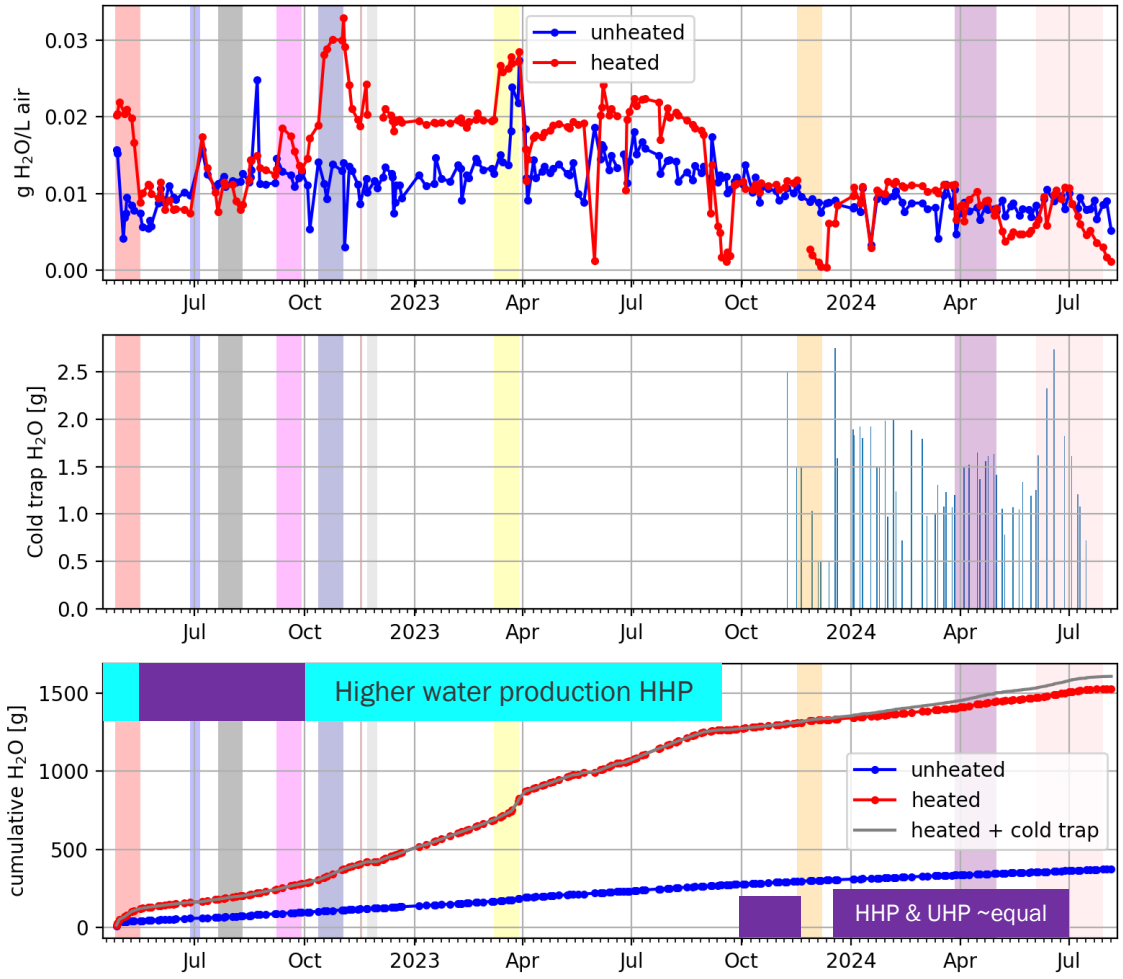

Figure 12. Desiccant water production as instantaneous concentration (top), cold trap sampling events (middle), and desiccant water production as cumulative mass (bottom) data.

4.1.3 HP: WATER ISOTOPIC COMPOSITION TIME SERIES

Only the heated HP borehole is analyzed for water isotopes (the unheated array is no longer tested for water isotopes). The cold trap samples were analyzed at LANL and the detailed results are reported in tabular form in Guiltinan et al. (2024). Figure 13 shows changes in water isotopes measured at LANL using both liquid samples collected from the heated SM borehole (labeled “brine” and indicated with circles) and cold trap samples collected from the heated array gas stream (labeled “vapor” and indicated with triangles). There are changes in the isotopic makeup of the water during heating, assumed to be due to effects of evaporation. See Guiltinan et al. (2024) for more discussion about the water isotope data.

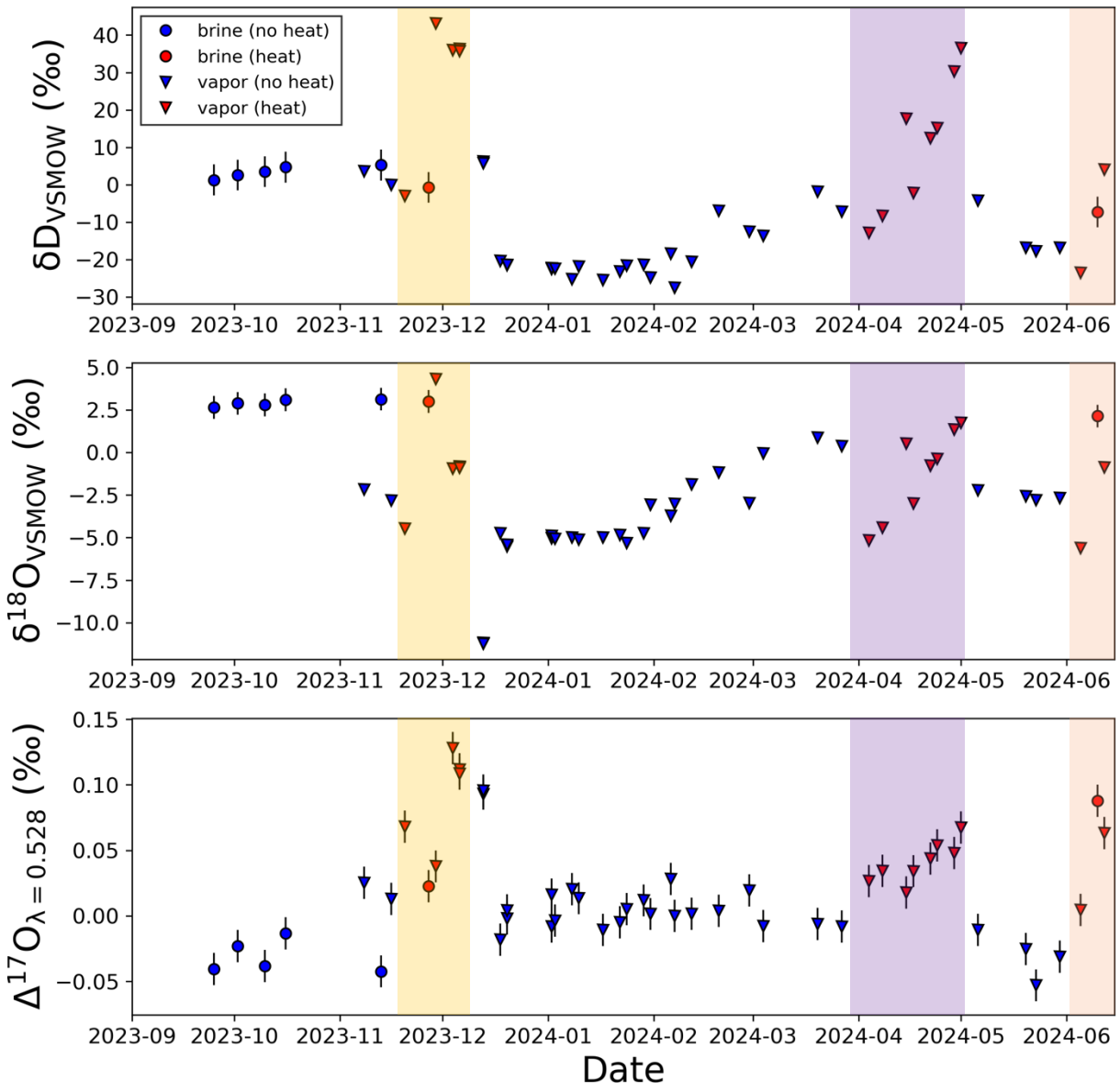

Figure 13.Isotopic measurements made on samples collected from HSM borehole (circles) and the HHP gas stream using cold trap (triangles). VSMOW is Vienna standard mean ocean water (Guiltinan et al., 2024).

Figure 14 shows stable isotope measurements of borehole seep brines collected from HSM during and between BATS 2 heating tests. In general, the brines collected during or between heating phases overlap within measurement uncertainty with brines collected during pre-heating phase (grey circles) indicating minimal contributions from halite fluid inclusions to these borehole seep brines. If significant quantities of halite fluid inclusions were being mobilized during the BATS 2 heating tests, we would expect the isotopic compositions of the evolved borehole brines to trend downward in Figure 14 towards the halite fluid inclusion (HFI) endmember (i.e., similar $\delta^{18}O_{VSMOW}$ but lower δD_{VSMOW}). The one possible exception to the above is the recent borehole brine sample collected during BATS 2g (June 2024). This sample has a δD_{VSMOW} value lower than any borehole brine sample collected to date. If the isotopic mixing framework represented in Figure 14 is correct, the isotopic composition of this brine implies an HFI contribution of ~30%. This simple mixing exercise

assumes no significant isotopic fractionation is associated with the heat-induced mobilization of HFI. Between BATS 2e (November 2023) and 2g (June 2024), not enough brine was retrievable from the sampling borehole for isotopic analysis. Thus, heating phase 2f conducted April-May 2024 was not captured in the borehole brine samples.

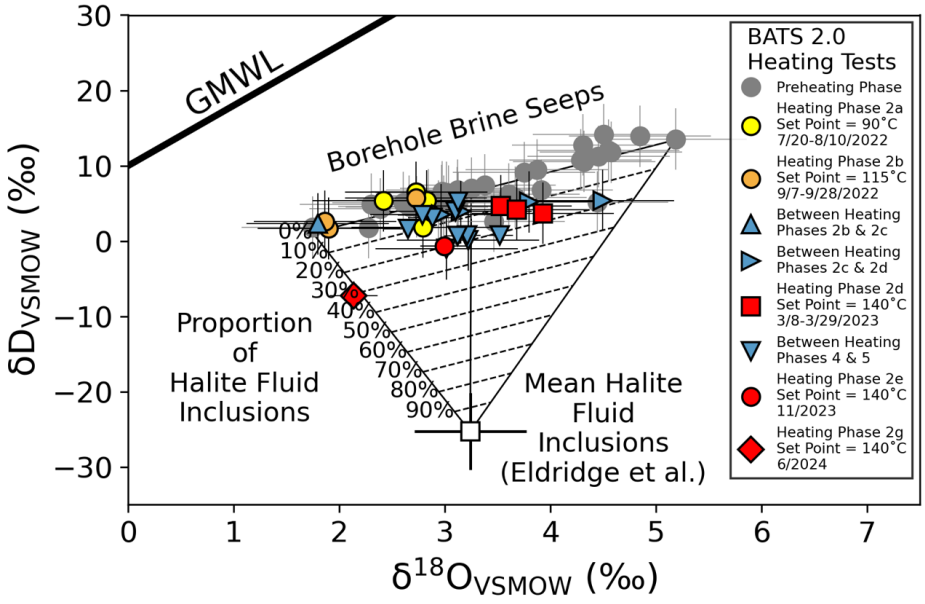

Figure 14: Stable isotope data of heated SM borehole brines. Brine samples collected during most of the BATS 2 heating tests are within measurement uncertainty of the brines collected prior to heating (preheating phase). We interpret this to reflect negligible contributions from any mobilized halite fluid inclusions during most of the heating tests. VSMOW is Vienna standard mean ocean water, and GMWL is the global meteoric water line (Guiltinan et al., 2024).

4.1.4 HP: GAS COMPOSITION TIME SERIES

The SRS QMS-200 gas analyzer monitors the gas stream for compositional changes with time. The gas analyzer is operating in "P vs. T" mode, which monitors the signal at ten specific values of mass divided by charge (i.e., m/z), using the Faraday cup sensor. Figure 15 shows the relative reported ion current for three key gases, normalized by the ion current reported for N_2 (to adjust for differences in pressure of the input gas stream). Assuming N_2 concentration is near 1, the normalized ion current then is essentially the volume fraction of each gas in the overall stream. Argon is added to the system behind the heated D borehole packer, while CO_2 and H_2O are not added to the system.

In August 2023, the SRS QMS-200 gas analyzer failed, and it was swapped out with a similar piece of equipment, while the original unit was sent back to the manufacturer for repairs.

Figure 15 shows the normalized signal associated with CO_2 (m/z=44), Ar (m/z=40), and H_2O (m/z=18). For each of the BATS 2 heating tests shown in Figure 15 (BATS 2e, f, and g) there is a clear peak of argon after heating has ended, when argon gas pressurized behind the HD has flowed to the HHP borehole, once the permeability changes due to contraction associated with cooling.

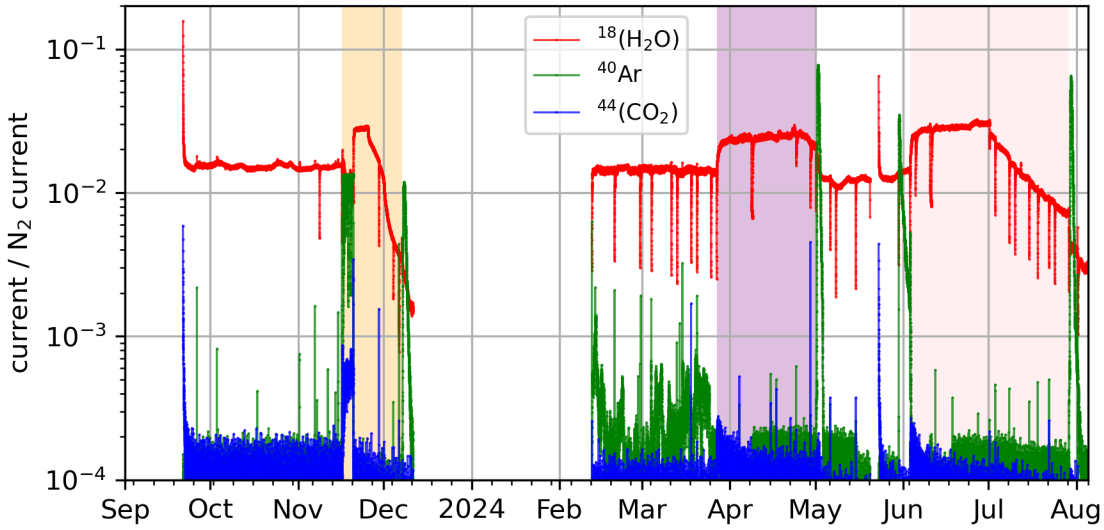

Figure 15.SRS gas analyzer data since September 2023 (after swapping out QMS-200 units). Heated array data shown.

The very high CO_2 levels observed in the LICOR instrument at the beginning of BATS 2e (Figure 10) do not similarly show up in the observations made with the SRS gas analyzer, supporting the statement that these LICOR measurements are likely erroneous. The rise and slow decay of CO2 in heating tests BATS 2f and g are also visible in the SRS gas analyzer data.

Short drops in water concentration shown in Figure 15 are associated with cold trap sampling times. Some of these times (but not all) also have increases in Ar and CO_2 signals, assumed to be due to the small amount of atmospheric air inside the cold trap when it is first connected at each sampling.

Figure 16 shows a more detailed plot (x-axis minor tick marks are every 12 hours) of the gas analyzer results around the three BATS 2 heater tests in FY24. In each of these, a clear breakthrough of argon gas is observed at the end of each heating phase (colored bars). Argon is pressurized behind the HD packer to approximately 138 kPa [20 psi gauge] at the beginning of each heater test.

The observed signal at the beginning of the BATS 2e heater test appears different from the other tests. From the beginning of heating on November 16, until the morning of November 20, Ar levels were high (and quite variable) in the HHP borehole. This could be due to early breakthrough of Ar gas from the HD source borehole, which then is cut off due to closure of fractures during heating. This type of behavior is also observed, over a much shorter timeframe, in the most recent heater test (BATS 2g). The long period of argon breakthrough in BATS 2e does not seem to be consistent with the timescale associated with the closing of fractures in BATS 2g. Also, the difference in the CO_2 and H_2O signals during this same time leads us to believe the gas analyzer system might have been somehow contaminated with atmospheric air (lower H_2O and higher Ar and CO_2) during the first 3 to 4 days of BATS 2e.

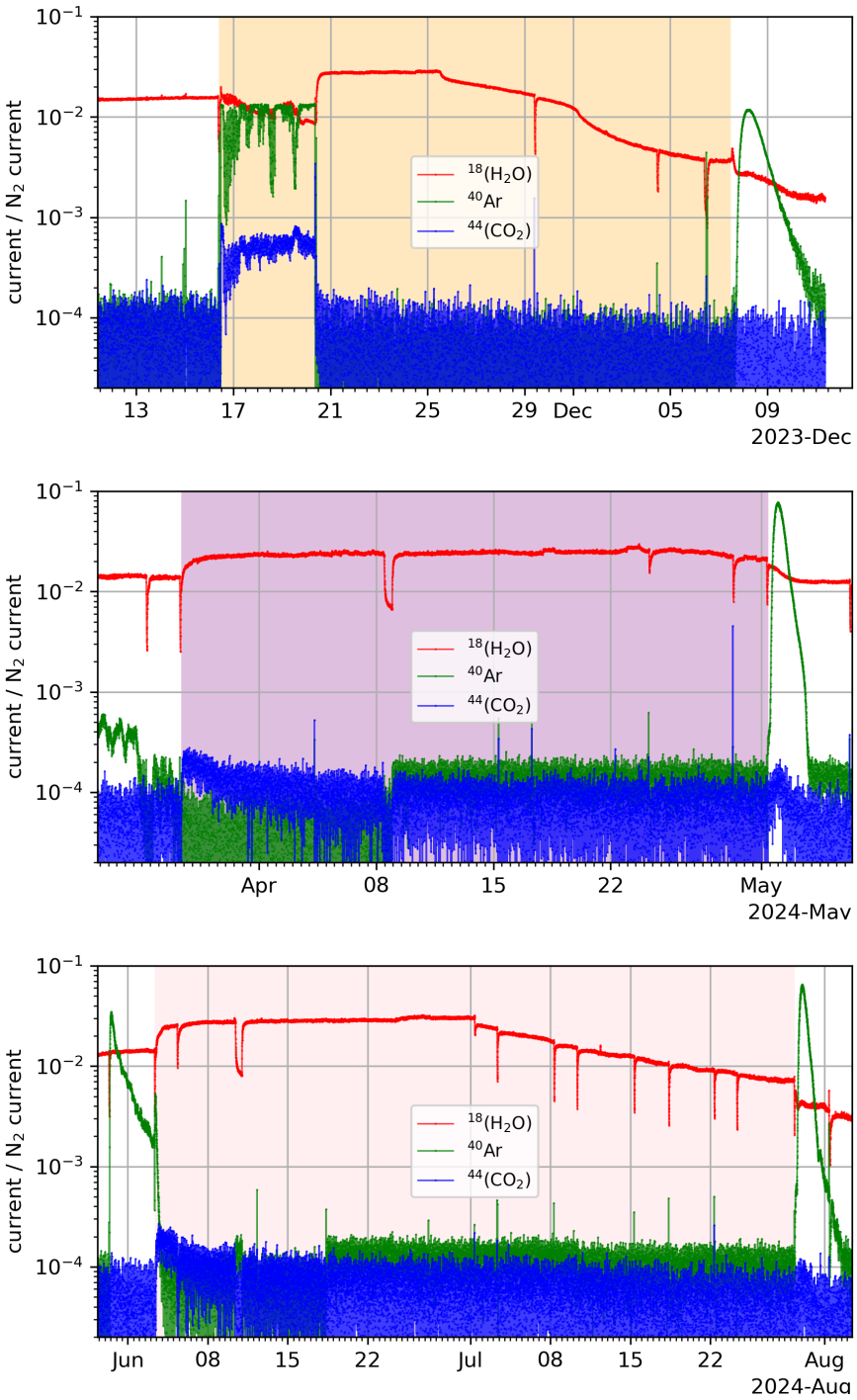

Figure 16.SRS gas analyzer data associated with BATS 2e (top), BATS 2f (middle), and BATS 2g (bottom). Heated periods have colored backgrounds.

4.1.5 HP: BOREHOLE CLOSURE GAUGE TIME SERIES

A linear variable differential transformer (LVDT) was used to measure the diameter of both heated and unheated HP boreholes through time. Figure 17 shows the change in borehole diameter since

the beginning of BATS 2. Both LVDT sensors have failed. The unheated array LVDT stopped working in December 2022, while the heated array LVDT stopped working in December 2023.

The large jump in the heated LVDT measurement in late 2022 was when the packer was taken out of the borehole. Most of the other large jumps in LVDT measurements were associated with heating and cooling (except September 2023 – see discussion in Section 5).

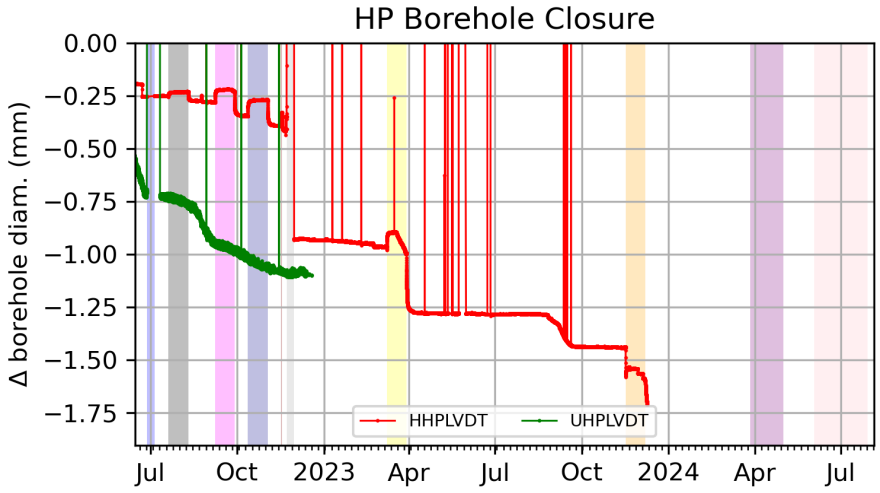

Figure 17.Change in diameter of HP boreholes measured by LVDT. Unheated LVDT failed in December 2022, heated LVDT failed in December 2023.

4.1.6 HP: HEATER POWER AND TEMPERATURE TIME SERIES

The heater controller reports applied current and voltage, apparent heater resistance, and power to the heater (Figure 18). These data are critical to characterizing the applied thermal boundary condition in numerical modeling. The controller also reports the temperature at thermocouples inside the borehole used to control and provide a high temperature safety limit for the heater. In the upper-left subplot of Figure 18, 4TC_C_SP_Max (green) gives the temperature observed on the setpoint thermocouple, while 4TC_C_SP (red) gives the setpoint; they only differ when the borehole is hotter than the heater (i.e., between heating events). Only the heated array HP borehole is collecting this time series.

The power measured by the heater controller can be confirmed by using either $P = VI$ (power from potential and current) or $P = I^2R$ (power from current squared and resistance). Both checks give similar values to those reported directly by the controller, providing some confidence in the internal consistency of the measurements. The heater element resistance increases slightly (33.5 to 34.75 ohm) during the first four heater test episodes but then holds constant, which is a sign the heating element is still behaving nominally. Most of the heater controller parameters (aside from thermocouples) are only reported or only make sense when the heater is on (i.e., the setpoint is greater than the ambient temperature).

The three most recent heater tests (BATS 2e, f, and g) had the same temperature setpoint (140 °C), but the limit thermocouples reported decreasing temperatures (Table 3). This disparity between the temperature at the controller and limit thermocouples may be due to their arrangement and position in the borehole, and how well they contact the borehole wall.

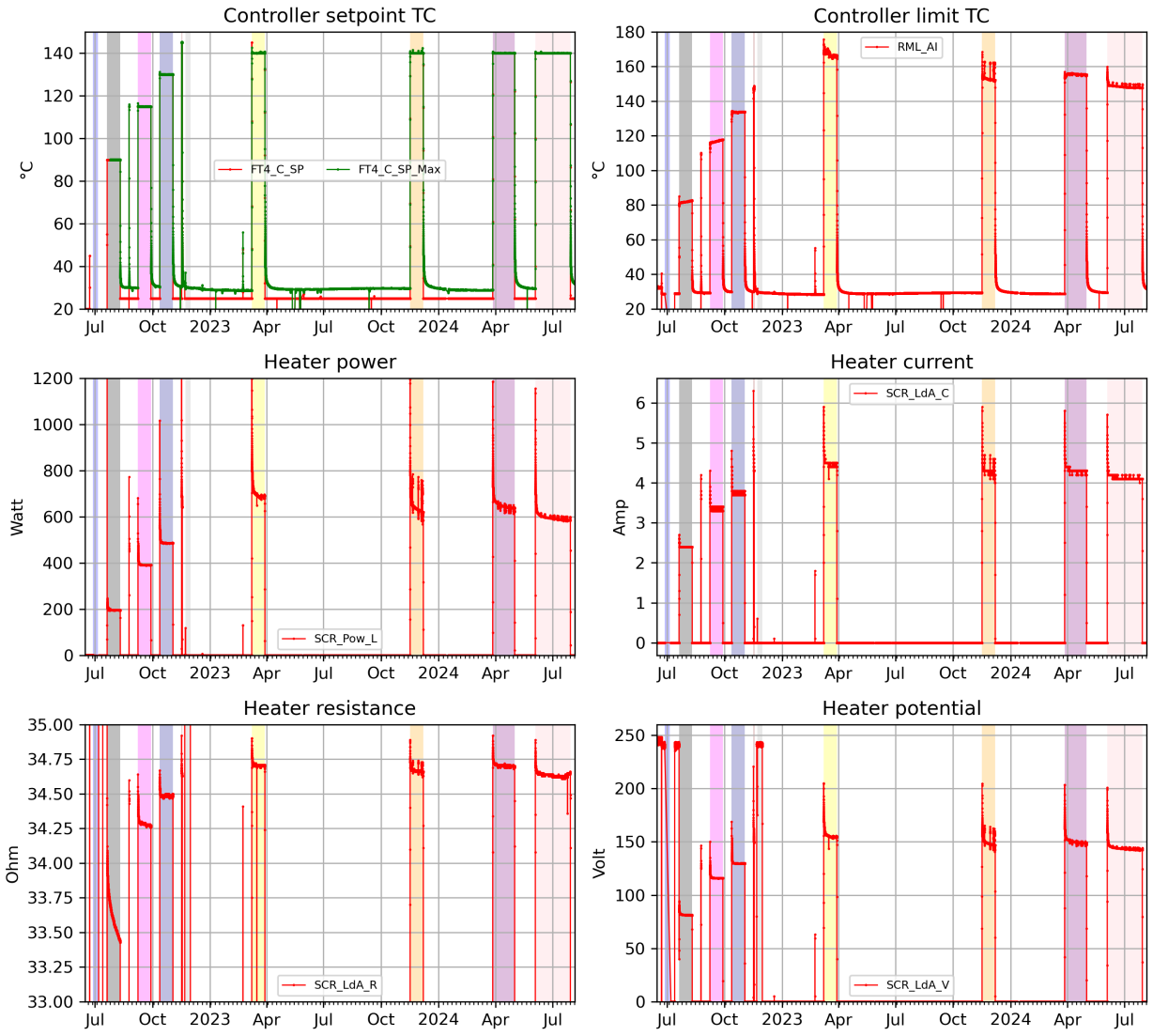

Figure 18.Heater controller parameters from heated borehole.

The average applied power and temperature observed at the closest thermocouple to the heater in another borehole (HF1TC2) are plotted in Figure 19. HF1TC2 is computed to be 19.3 cm [7.6 in] from the center of the heater, which is centered inside a 12.2-cm [4.8 in] diameter borehole. There is approximately 13.2 cm [5.2 in] of salt and grout (in the F1 borehole) between the closest thermocouple and the heater. The power and temperature are averages over the last day of heating for each test. The plot shows there is general agreement between the estimated applied power at the heater and the temperature observed in a nearby borehole.

Table 3. Summary of BATS 2 heating events.

Heating Event	Beginning	Ending	Duration [days]	Setpoint TC temperature [°C]	Applied power* [W]	HF1TC2 temperature* [°C]
BATS 2a	20 Jul 2022 08:29	10 Aug 2022 07:38	21.0	90	195	41
BATS 2b	07 Sep 2022 14:52	28 Sep 2022 08:02	20.9	115	391	56
BATS 2c	12 Oct 2022 10:01	02 Nov 2022 11:43	21.9	130	487	64
BATS 2d (aborted)	16 Nov 2022 07:30	17 Nov 2022 17:02	1.4	145	650	69
BATS 2d	8 Mar 2023 09:20	29 Mar 2023 09:36	21.0	140	690	80
BATS 2e	16 Nov 2023 09:42	07 Dec 2023 11:37	21.1	140	620	76
BATS 2f	27 Mar 2024 08:34	01 May 2024 09:33	35.1	140	640	77
BATS 2g	03 Jun 2024 08:34	29 Jul 2024 09:34	56.0	140	585	74

* average of last day of heating period

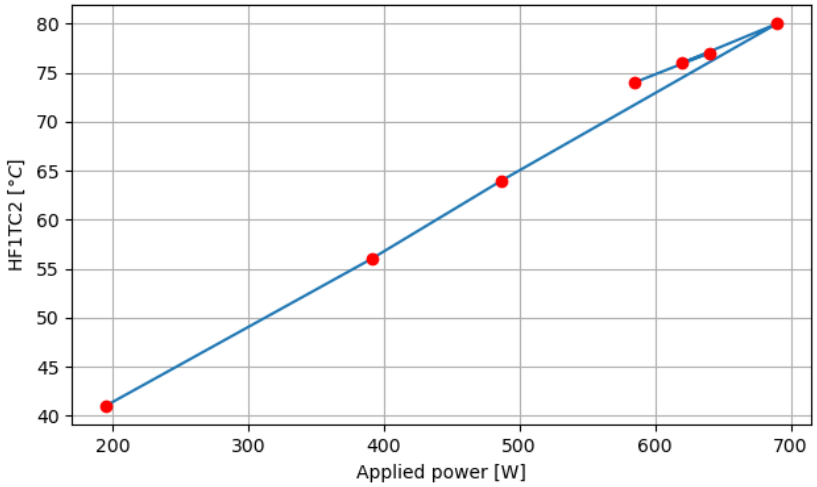

Figure 19. Comparison of applied power and nearest thermocouple in a different borehole (HF1TC2) over last day of all complete heater test periods.

4.2 D: CONTINUOUS GAS PRESSURE TESTING

The interval behind the inflatable IPI packer in the D borehole was pressurized to approximately 20 psi [1.4 bar] above atmospheric pressure and closed in (i.e., disconnected from the inflation tank). The packer inflation pressure (roughly 80 psi [5.5 bar] above atmospheric) and the pressure of gas

in the interval behind the packer are both monitored. Figure 20 shows the gas pressure behind the packer in the D borehole through time.

Initially the interval was pressurized with UHP N_2 (May and July 2022). The drop in pressure just before BATS 2a heater test (20 July) is when N_2-filled interval was depressurized and re-pressurized with UHP Ar to the same pressure. Argon was used to get tracer travel information from the gas permeability tests, when the Ar was observed breaking through by the gas analyzer in the HP borehole.

The slow decrease in pressure behind the D borehole between heating events (Figure 20) can be used to constrain the interval relative gas permeability, which appears to sometimes increase (i.e., steeper declines) and sometimes decrease. Interpretation of these data is more complex than interpreting single-phase pressure decline since this is movement of gas through a variably brine-saturated fracture system. Gas pressure decline is sensitive to the gas relative permeability of the interval. The relative permeability might change due to fractures mechanically opening and closing (i.e., changes in absolute permeability due to thermal expansion and contraction) or due to changes in brine content in fractures (i.e., changes in relative permeability due to migration of liquid).

The rise in pressure during the BATS 2 heater tests is expected due to essentially heating a closed container of gas (i.e., permeability is low enough to prevent significant gas leakage).

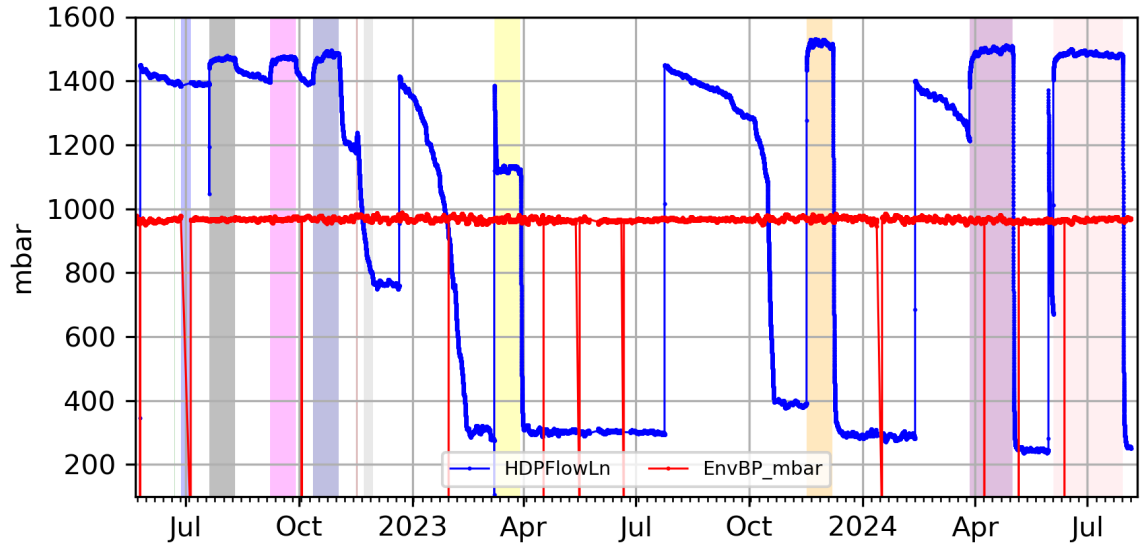

Figure 20. Interval gas pressure (above atmospheric) for heated D borehole and barometric pressure on same scale.

Adding the atmospheric pressure measured in the drift (red line in Figure 20) to the gauge gas pressure measurement behind the packer in the heated D borehole (blue line in Figure 20) produces the absolute pressure (Figure 21), where most of the high-frequency daily fluctuations are now canceled out. Fluctuations of the same magnitude and opposite direction occur in the atmospheric pressure data and the heated D borehole pressure data.

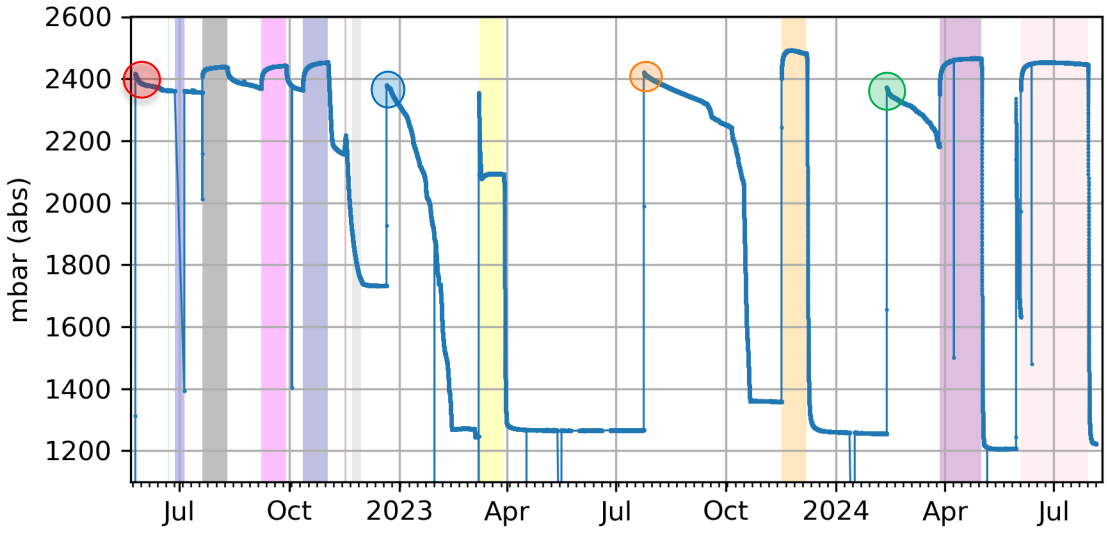

Figure 21.Interval gas pressure (absolute) for heated D borehole. Colored circles correspond to tests plotted in next figure.

Figure 22 shows the change in pressure against relative time, on a log-log scale plot. For a typical (i.e., constant material properties) falling-head pressure test, the curves should deviate to the right (i.e., flatten out), rather than deviate up (i.e., get steeper) at late time. The first test (5/25/22 in red) shows a flattening-out behavior, while later tests show the steepening behavior. It might be that brine is moving around in the fractures (driven by external processes to the pressurization of the heated D borehole), and it is blocking or allowing the migration of gas. In Kuhlman et al. (2023) and Guiltinan et al. (2023) there was also discussion and preliminary analysis of these atypical responses. Section 5 notes some anomalous changes across instrument types, including the drop in pressure in the blue curve in Figure 22. Despite some late-time deviations, the responses of these four pressure tests appear to have similar slopes at early time (Figure 22, <1 day since test began).

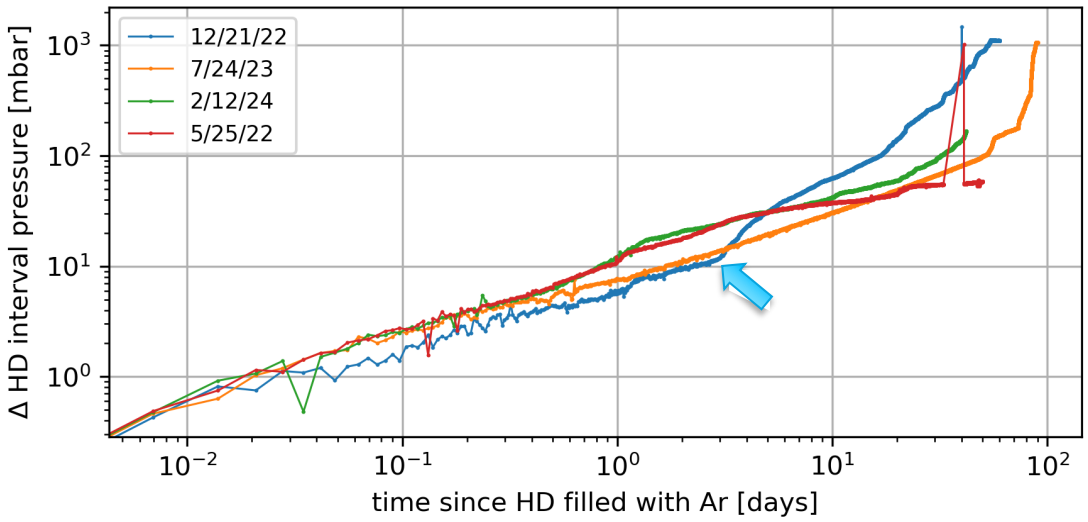

Figure 22.Change in pressure in HD borehole against days since filled for four unheated gas permeability tests (legend indicates start day of each test, corresponding to colored circles in previous figure). Anomalous drop in pressure noted with arrow.

4.3 AE DATA FROM BATS 2 HEATED AE BOREHOLES

This subsection discusses cumulative AE data recorded in the heated BATS 2 array from July 2023 to July 2024. Yellow intervals in the figures indicate the extent of heater tests BATS 2 e through g. Consistent with previous observations, AE activity increases at the onset of heating and further increases at the onset of cooling after each heated interval. Electrical interference from the ERT system and possibly mining activity has continued to create significant noise issues for the AE recordings. Data has been filtered using a partial power frequency method, where the energy content in the 10 to 250 kHz frequency band must be greater than or equal to 50% of the total energy of a recorded waveform to be considered, otherwise data is removed. Data is then filtered with an elevated threshold of 45 dB to be consistent with previous years.

Cumulative hits can be seen in Figure 23 and Figure 24 (the second figure is a zoom into the period after the major activity in September 2023), and daily AE counts can be seen in Figure 25. After a period of elevated AE in late summer of 2023, AE accumulates steadily throughout FY24, with surges in activity associated with changes in heating (Figure 24).

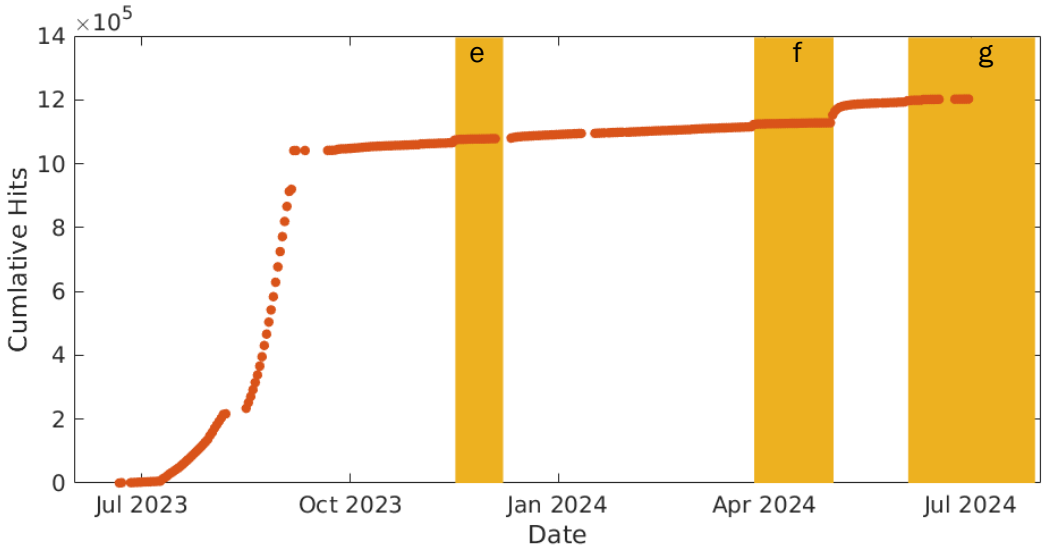

Figure 23.Cumulative AE hits since July 2023. Heated periods are marked in yellow.

Most events since October 2023 occur when heating ceased at the beginning of May 2024 (heater event BATS 2f). The data associated with the ending of the most recent heating test (BATS 2g) are not yet available.

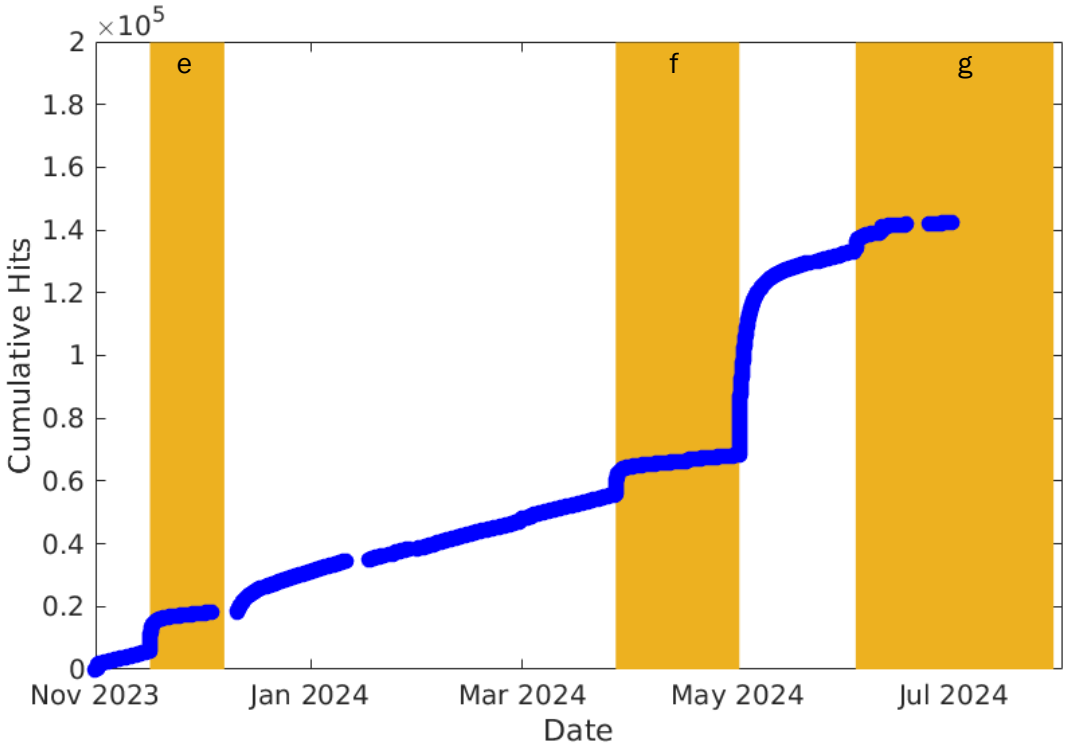

Figure 24.Cumulative AE hits from November 2023 to July 2024 (zoomed into the BATS 2e, f, and g heater tests). Heated periods are marked in yellow.

Most clearly shown in Figure 25, there was a period of elevated AE hits that was not associated with a heating period (July 2023 to September 2023 – indicated in green). The cause of this is not understood, but possible explanations include mining activity associated with the new WIPP utility shaft (see two mentions of mining in the notes -- Table A-1), maintenance activity in the underground near BATS, and drift closure. It is unusual that the elevated activity is not more episodic (like drilling/blasting events or equipment driving by), and appears to be elevated over an extended period, including weekends.

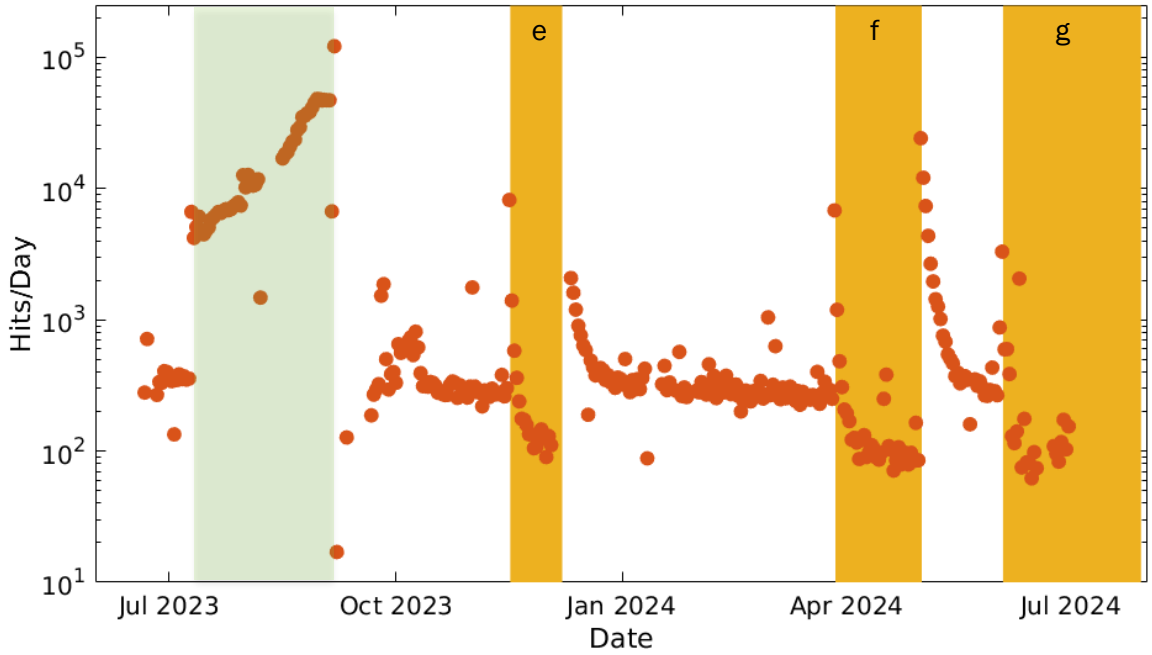

Figure 25. Daily AE hit rate (hits per day) for BATS 2e, f, and g heater tests. Heated periods are marked in yellow. Period with significant number of AE hits/day, that does not correspond to a heater test, is marked in green.

Daily rates increase at the onset of heating, and further increase at the onset of cooling (Figure 25). Rates spike with changes in heater activity and logarithmically decay to a background level. It seems the daily rates decrease to background faster during heated intervals (after the start of heating) compared to cooling periods (after the end of heating). This could be indicative of a low frequency bias, where heating the salt and closing microcracks and pores allows for the transmission of higher frequency content that gets removed by the low frequency filter. However, this trend can also be observed in previous year's data that has not been frequency filtered, but gaps in data recording make it difficult to draw definitive conclusions.

The elevated hit rate during July to mid-September 2023 is clear in Figure 25. The reponse is elevated for several weeks, and does not have an exponential-type decay, as is observed with heating events BATS 2f and 2g.

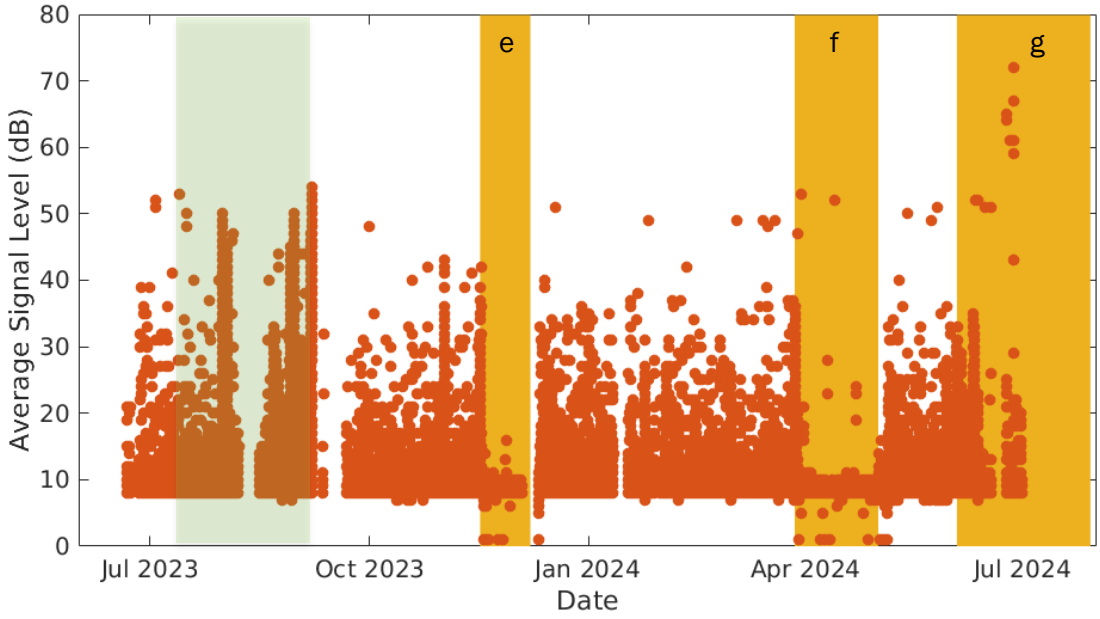

Figure 26.Average signal level (dB) for BATS 2e, f, and g heater tests. Heated periods are marked in yellow. Period with significant number of AE hits, that does not correspond to a heater test, is marked in green.

The average signal level (ASL) is a measure of the continuously varying amplitude that has been averaged over a 500 ms time window. Like daily hit rate observations (Figure 25), ASL increases with changes in heater condition and decays to background levels (Figure 26). Between heating periods, ASL remains high with appreciable variability in values. During heated intervals, ASL levels seem to reduce to lower values and remain relatively constant. Peaks in ASL are associated with the onset of heating. Similar peaks in ASL are not observed at the onset of cooling, despite unheated intervals having higher average ASL activity compared to heated intervals. This may be because the hits at the beginning of heating are closer to the sensors, while the hits at the end of heating are further from the sensors.

There are at least three significant peaks of ASL during the July to September 2023 period marked in green. It is not clear what this means.

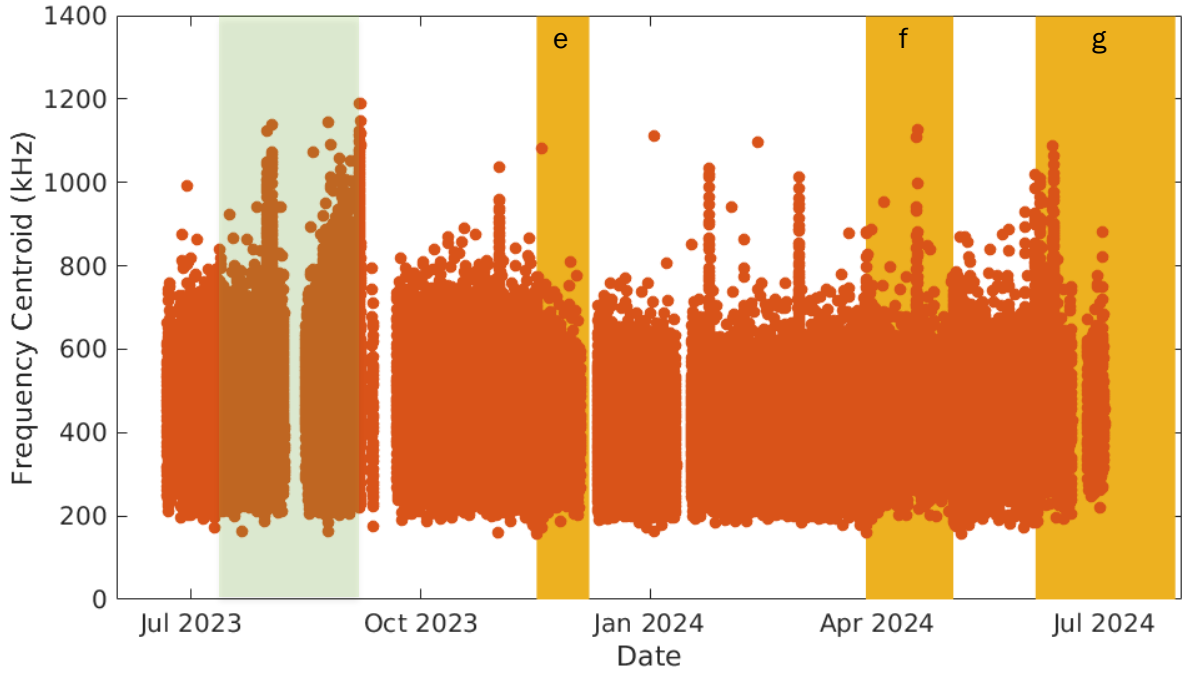

Figure 27.AE frequency centroid for BATS 2e, f, and g heater tests. Heated periods are marked in yellow. Period with significant number of AE hits, that does not correspond to a heater test, is marked in green.

The frequency centroid is derived from fast Fourier transforms on recorded waveforms and represents the average frequency based on the energy of frequency bands. The frequency centroid range increases with changes in heater activity, and decays to steady state levels (Figure 27). The lower bound of the data increases slightly for heated intervals compare to intervals without active heating, but the higher values seem to be consistent throughout.

The period of increased activity from July to October 2023 is also marked in green. There are two or three episodes of higher frequencies during this period, which are also not readily explained.

The data presented here shows clear impacts of the FY24 heater cycles on recorded AE. The onset of heating creates an increase in AE activity, resulting in greater number of hits (Figure 24 and Figure 25), higher averaged amplitudes (Figure 26), and wider frequency ranges (Figure 27). The onset of cooling once heating stops has a similar but greater effect, with higher AE rates and a wider centroid frequency range. Despite surges in AE rates, ASL is lower at the onset of cooling than the onset of heating. ASL at the onset of cooling increases compared to the steady state heated value but is lower than the steady state unheated value (Figure 26). Throughout the three FY24 heater cycles (BATS 2e, f, and g), AE activity is lower during heated intervals than unheated intervals. This could be bias induced from the new frequency-based filter implemented this year, but these trends are also observable in earlier FY23 AE data. Less recording time was lost in FY24 compared to FY23 due to power outages and maintenance, and this more continuous dataset better illustrates the differences between heated and unheated intervals than was seen in previous data (Kuhlman et al., 2023). The lower steady values during heated intervals indicate heating may be stabilizing the borehole region with expanded salt crystals closing microcracks and pores, or that the increase in temperature may be activating a plastic deformation mechanism that does not generate AE.

The elevated activity during the July to September 2023 period when there was no heating going on is unexplained. More discussion of this, along with comparison with other signals is presented in Section 5.

4.4 T: TEMPERATURE TIME SERIES

Thirty-six sealed Type-K thermocouples are grouted into the two T boreholes, and more thermocouples are co-located with other observations in other boreholes (e.g., AE, F, and SL). Resistance temperature detectors (RTDs) are used in place of thermocouples in the ERT boreholes (E1 through E4).

The unheated array (Figure 28) now shows regional fluctuations of temperature in the salt, as ERT survey are no longer being conducted in the unheated array. Most of the thermocouples in the ERT boreholes in the unheated array have failed since they were installed in 2019. The BATS 2 heated array is further away from the BATS 1 unheated array than the BATS 1 heated array was (Figure 2), so the effects of the BATS 2 heating events are not observed in the unheated array, as they were in BATS 1. The unheated T1 borehole shows that the variation of ambient temperature with depth varies with seasons (an unexplained downward shift appears to impact the deepest two thermocouples in the UT2 borehole, compared to the shallower thermocouples). In the summer, the drift air is warmer than the salt and in the winter the salt is warmer than the drift air. A maximum of 1 °C difference is observed between TC1 and TC16 in the summer, and approximately 0.75 °C difference is observed between these thermocouples in the winter. The annual variation in the shallowest thermocouple is approximately 2 °C, and the annual variation in the deepest thermocouple is only 0.7 °C.

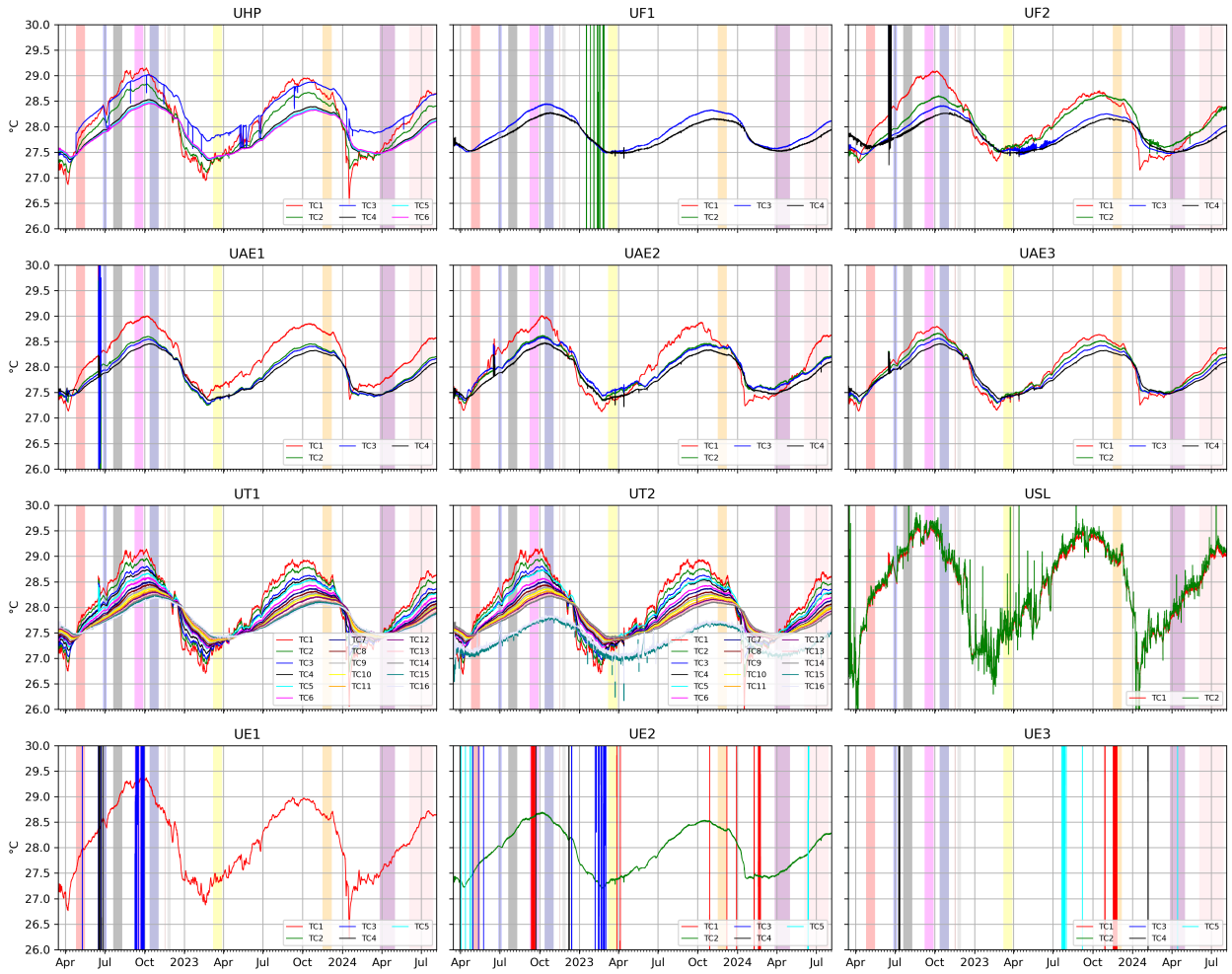

Figure 28.Thermocouple data from unheated array.

An average “deep” salt temperature of 27.77 °C [81.99 °F] is inferred from the average UT1TC16 temperature between 1 June 2022 and 1 June 2024 (two years). This is consistent with what has been observed previously at WIPP, but it is clearer in the unheated array data now than when it was subject to more man-made impacts.

Figure 29 shows temperature data observed in the BATS 2 heated array. Each subplot in the plot is a different borehole; curves within each subplot show data from different thermocouples. In each borehole thermocouple “TC1” is closest to the drift, “TC2” is deeper in the borehole, etc. Thermocouple and RTD data collected during ERT surveys are not deleted from the BATS 2 dataset (some noise is still observed in the data during ERT surveys each night), as was done in BATS 1.

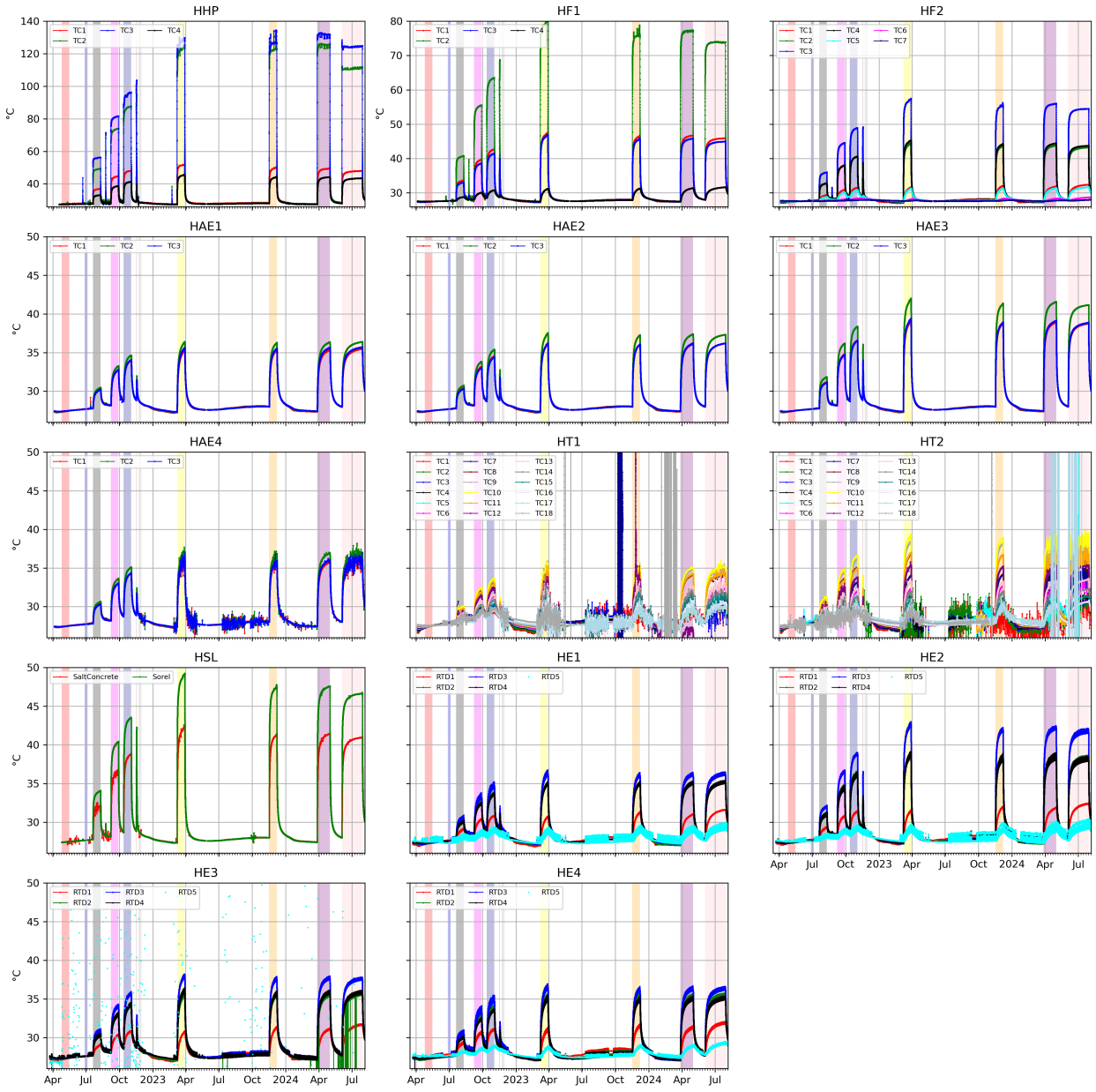

Figure 29. Background temperature data from heated array. Each subplot shows the thermocouples or RTDs from a single borehole.

RTD5 in the BATS 2 heated array AE3 borehole is quite noisy since BATS 2a began, so it was plotted without lines connecting the dots.

The temperature rise observed in TC2 of the heated F1 borehole is the largest temperature rise observed outside the heated HP borehole. This thermocouple is 19.3 cm from the center of the HP heater (13.2 cm from the HHP borehole wall).

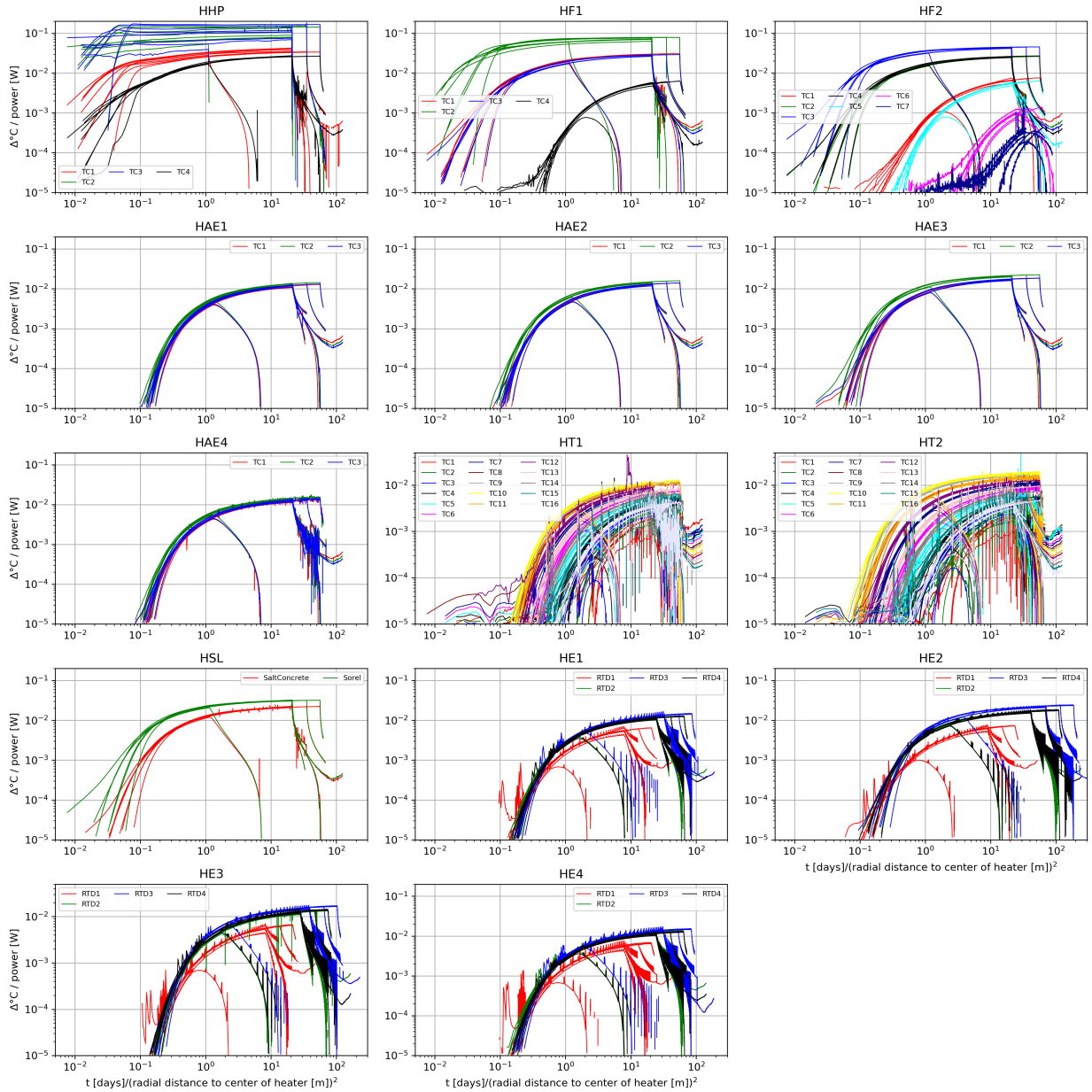

Figure 30.Scaled change in temperature and scaled relative time for BATS 2a-g, including aborted BATS 2d (1.4 day) test. Each subplot shows the thermocouples or RTDs of a different borehole. RTD5 sensors in HE boreholes and TC17-18 from HT boreholes excluded due to low signal and higher noise.

Figure 30 shows the scaled change in temperature (scaled by the applied power at the end of the test) and scaled relative time since the heating test began (scaled by the straight-line distance from the sensor to the midpoint of the heater). In a linear system, the responses from different heating levels would fall on top of one another (since the material properties do not change with temperature). In a system with non-linear thermal conductivity, heat capacity, or other changes with temperature, there will be differences in the responses (the differences appear to be largest at early times). The log-log scale also allows showing short (1.5 day), medium (3 week), and long (8 week) tests on the same scale.

4.5 E: ELECTRICAL RESISTIVITY TOMOGRAPHY (ERT) DATA

Rutqvist et al. (2024) and Chen et al. (2024) provide a detailed summary of data collection, inversion, and analysis of BATS 2 ERT data. Recently, Wang et al. (2023) published an analysis of the ERT data collected as part of BATS 1. Between BATS 1 and BATS 2, improvements were made to the model used to invert the data, and there are more electrodes distributed across four boreholes in BATS 2 as compared to three boreholes in BATS 1.

ERT surveys were nominally conducted nightly, but they were not conducted during power outages or periods when there were equipment issues (see surveys on days with asterisks in Figure 31). The top subplot shows average resistance and temperature, while the middle plot shows lower resistance measurements, and the bottom subplot shows the higher resistance measurements. The low- and high-resistance measurements react differently to the beginning and ending of heating (red stripes). There is one response in the high resistivity data that does not line up with a heating period (July to September 2023); it is discussed more in Section 5.

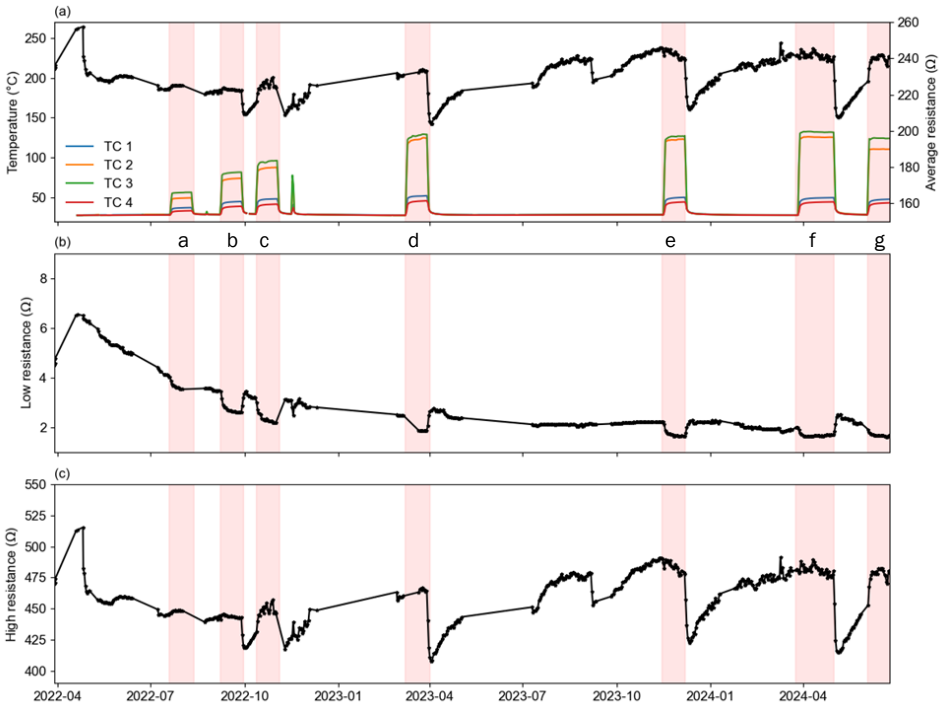

Figure 31. Time-series of temperature and average resistance during BATS 2: (a) daily average temperature data from four thermocouples in HHP and average resistance data from ERT, with asterisks indicating the days when ERT data measurements were taken, (b) the trend of low resistance data (<100 Ω) and (c) the trend of high resistance data (≥100 Ω). Red shading represents heating periods (Rutqvist et al., 2024).

Figure 32 shows the inverted resistivity distribution in a box around the BATS 2 heated array. Like in the averaged raw observations (Figure 31), there are several types of responses to the start and end of heating events (i.e., the red stripe in subplot c).

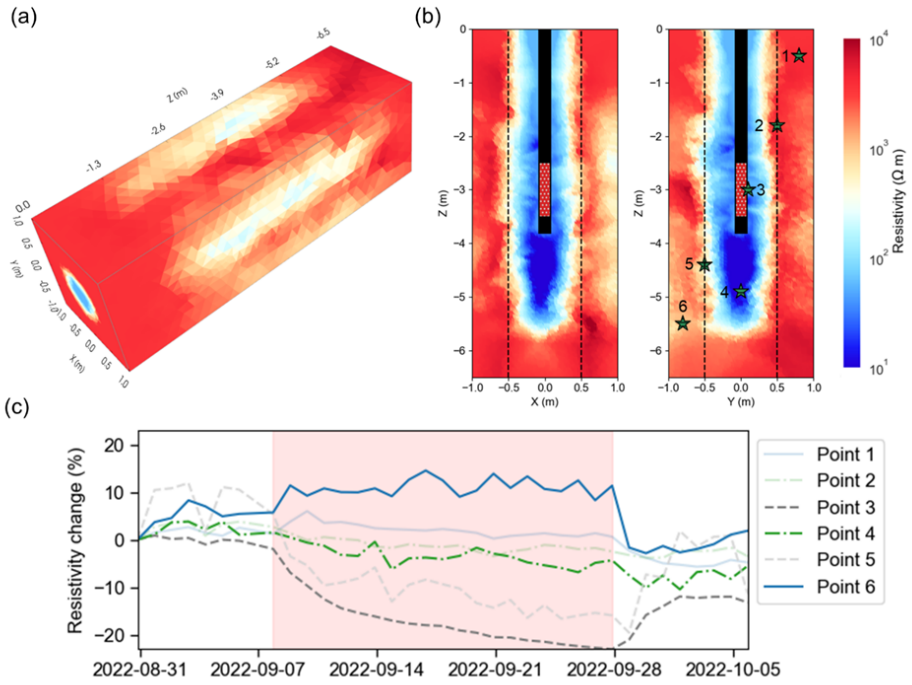

Figure 32. The inverted resistivity distribution from the selected baseline (2022/08/30) in BATS 2b: (a) a three-dimensional perspective, (b) cross-sections along HP borehole with the extent of HHP heater indicated with a red box, and (c) the time evolution of resistivity at the six points shown in (b) during second heating phase (Rutqvist et al., 2024).

Using time-series clustering analysis, several classes of responses were characterized (Figure 33). These response correlate physically with the anticipated distribution of the damaged zone and the distribution of brine in salt surrounding the heated borehole.

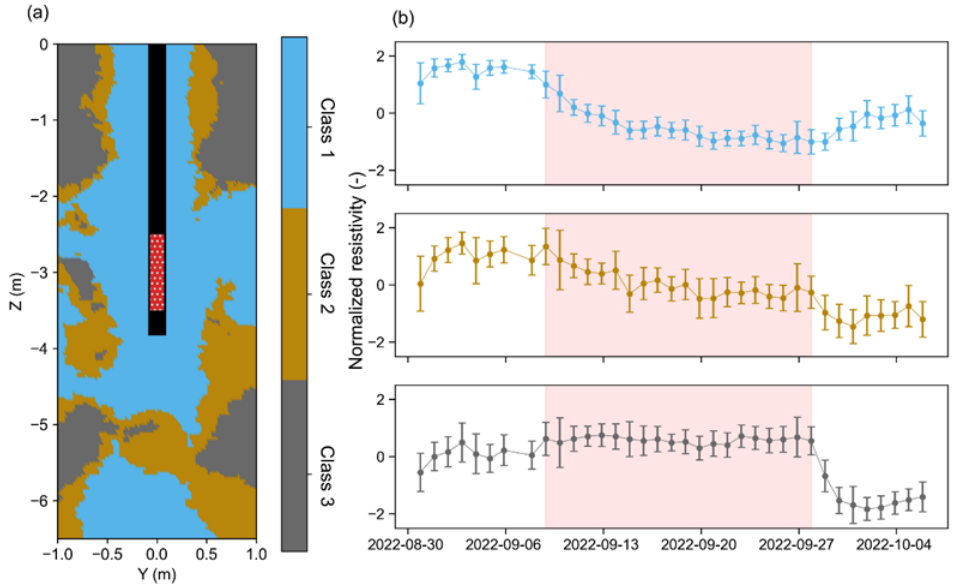

Figure 33. The time-series clustering results: (a) the spatial distribution of classes with HHP borehole and heated interval indicated, and (b) the normalized resistivity changes in each cluster with its uncertainty (one standard deviation). Red shading is BATS 2b heating test (Rutqvist et al., 2024).

Additional data, background, and analysis of the ERT data are presented in Rutqvist et al. (2024). This approach illustrates a way to delineate the 3D distribution of damage in salt, which is a first, and warranted a recent publication in *Geophysical Research Letters* (Chen et al., 2024).

4.6 FIBER OPTIC (F) DATA

A near-continuous recording of fiber optic datasets was observed over nearly two years during the BATS 2 test. The raw data collected are plotted in Figure 34. The point where the fiber first meets grout in the wall of the drift is located at approximately 2 meters along the fiber (large strain anomaly), while the heater location is at about 4.5 to 5 meters along the fiber (large temperature anomaly associated with heating events). The variation in entrance location can be attributed to the differing lengths of optical fiber outside the borehole.

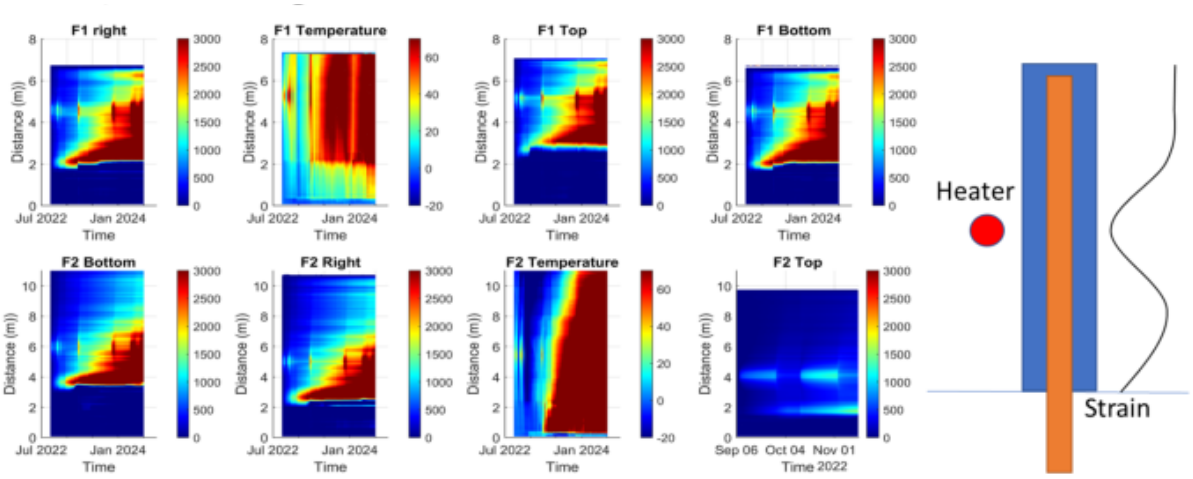

Figure 34. Left: the raw data of the distributed fiber-optic sensing measurement from September 2022 to July 2024. The top, right and bottom indicated the location of the raw microstrain (Δ length/original length, temperature in °C) optical fiber in HF1 and HF2. Right: the illustration plot of the strain distribution in the HF boreholes, relative to the heater and the access drift (Rutqvist et al., 2024).

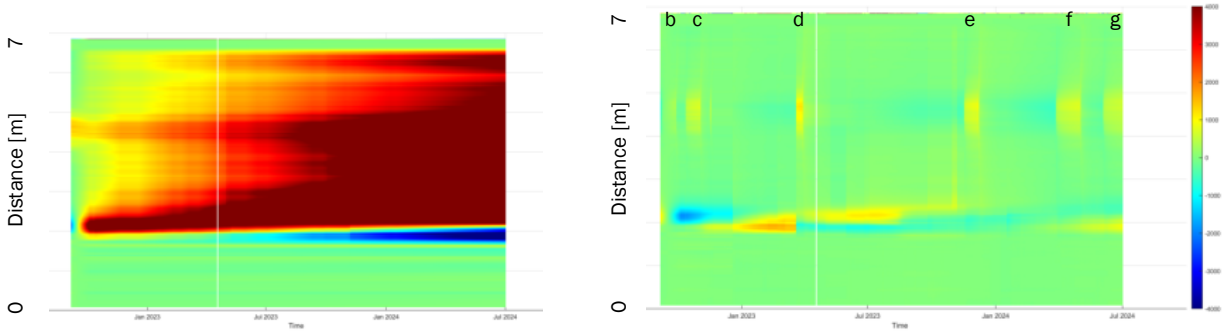

Figure 35. Fiber optic strain response. Left: The strain data (red high, blue low; different scale to right subplot) in HF1 right after low pass filter; Right: The strain data in HF1 right after high pass filter (blue is -4,000 microstrains, red is 4,000 microstrains). Heater tests BATS 2b-g are visible in the filtered data (Rutqvist et al., 2024).

The temperature at both F1 and F2 showed a continuous increase even after the heater was turned off, indicating that the cables are not entirely free of strains due to the large deformation of the rock salt around them (Figure 34). This may be due to bending that pushed the temperature cable away from the heater, a factor that should be addressed in future experiments. Despite the simultaneous measurement of strain and temperature by the strain optical fiber, the drift measured after the heater was turned off can still be considered pure mechanical deformation.

Figure 35 shows an analysis of the measured strain and temperature (both processes are impacting the observed results in the fiber) after applying two different types of filters, revealing a correlation with the heating operation. Specifically, a low pass filter can remove short temporal effects and highlight slow, long-term changes of the system, while a high pass filter has the opposite effect. The strain changes indicate deformation within the two monitoring boreholes when the heater was activated six times: in September and October 2022, and May and November 2023, and May and June 2024. The simultaneous occurrence of maximum strain and temperature changes at the depth of the heater suggests maximum deformation at the heater level, consistent with expected changes.

More detail on the fiber optic data and its analysis is given in Rutqvist et al. (2024).

4.7 LIQUID SAMPLE BOREHOLE (SM) DATA

4.7.1 SM: AIR TEMPERATURE AND RH TIME SERIES

Figure 36 shows the temperature and RH associated with the behind-the packer interval in the SM and SL boreholes. The right subplot shows the air temperature behind the packer rising during the heating portion of the test (red and green curves), while the left subplot shows the RH rising during heating in the heated SL borehole (with the nature of rise being more muted in the heated SM borehole). RH near 75% is indicative of equilibrium between moist air and halite at ambient temperature. These observed RH values indicate there is not a significant amount of dry air getting around the packer.

The rise in RH behind the packer during heating is likely due to liquid brine being present in the seal borehole (SL), but not the sample borehole (SM; because of repeated removal of any standing brine for geochemical sampling). The upward spikes (~1%) in all the RH data (heated and unheated arrays) are in response to power outages. The RH sensor requires a warm-up time each time after the power is disconnected. The early (2022 and 2023) downward spikes (1 to 2%) in the RH data in the SM borehole are associated with sampling attempts. A vacuum pump is connected to the 6.4 mm [0.25 in] tubing to extract any brine standing at the back of the borehole. When air and water are removed from the borehole for sampling, less humid drift air must flow in to replace it.

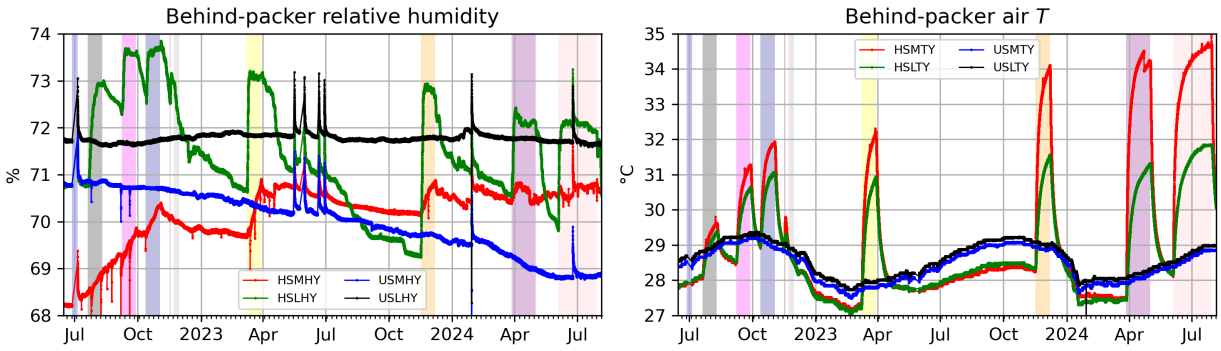

Figure 36.Relative humidity (left) and air temperature (right) for SM and SL boreholes.

4.7.2 SM: LIQUID BRINE SAMPLES

Volumes of brine sampled during BATS 2 are listed Table A-2 for all boreholes. Brine production volumes through time for the heated SM borehole are plotted in Figure 37 (see RH and air temperature in this borehole as red lines in Figure 36). Geochemical data associated with SM samples with enough volume to analyze are listed in

Table A-3 and plotted in Figure 38 and Figure 39. The heated SM borehole was drilled 9 February 2022, and the mechanical packer (as opposed to the initial sewer plug) was installed 13 April 2022 (Table A-1, marked by vertical dashed line in SM brine figures).

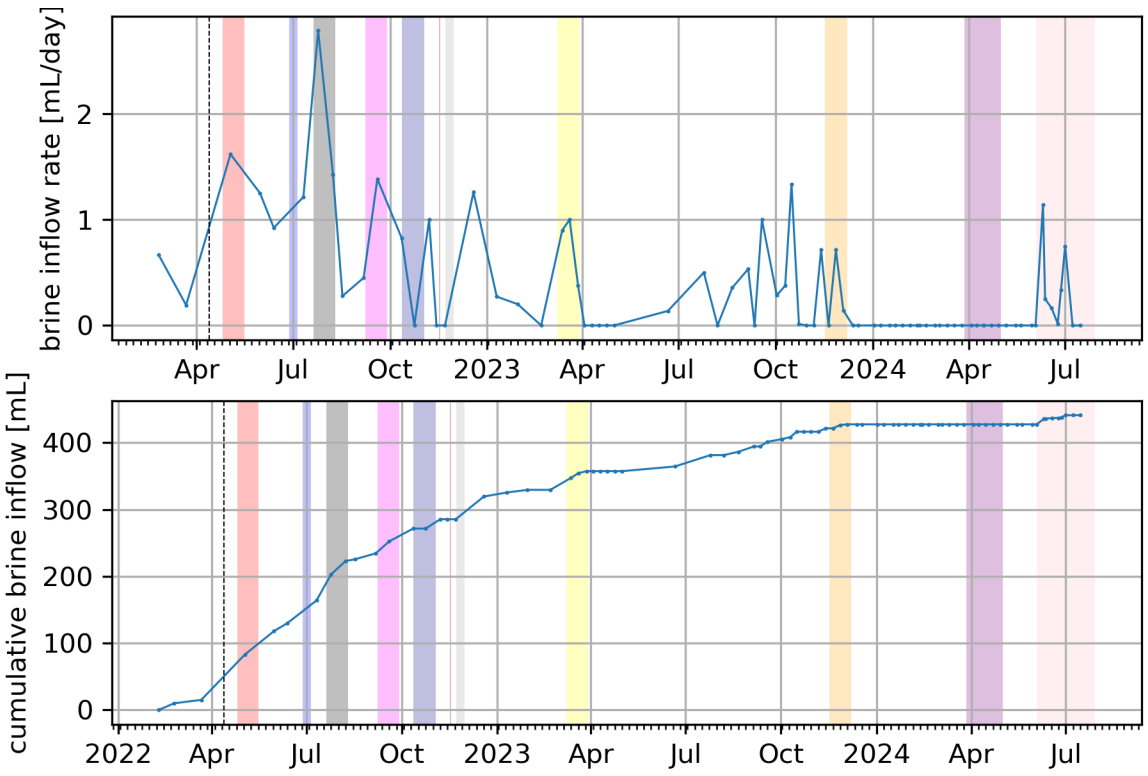

Figure 37.Brine production in heated SM borehole through time.

The highest averaged rate of brine production in the SM borehole was observed during heating event BATS 2a (gray bar). The second highest rate of brine production was just after installing the permanent inflatable packer (April 2022). The third highest rate of brine production was during heating event BATS 2b. Brine production in the heated SM borehole has significantly dropped off since BATS 2e, with a few recent samples of brine during the most recent heating event (BATS 2g).

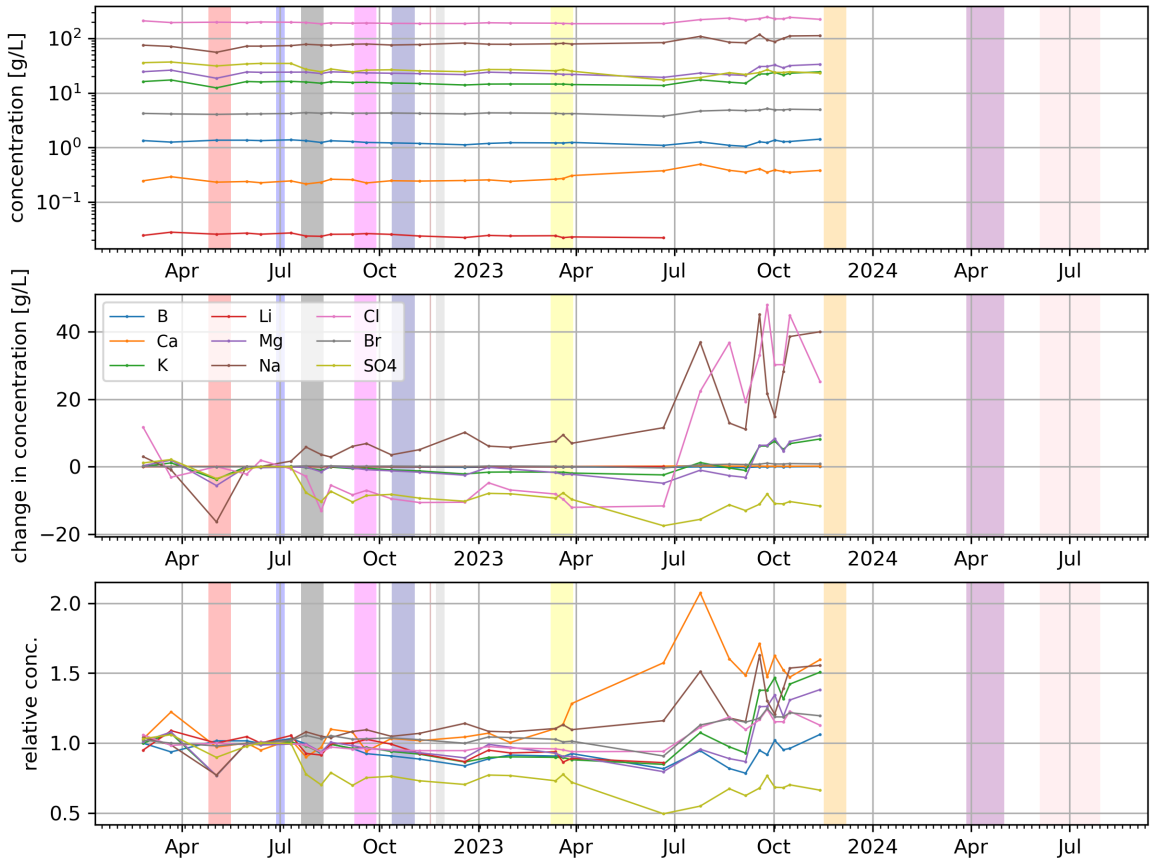

Figure 38. Brine chemistry data through time in heated SM borehole. (top) observed concentrations, (middle) change in concentrations, and (bottom) relative change in concentration.

Figure 38 shows the wide range of dissolved species tracked in BATS brine samples. The top subplot shows over three orders of magnitude between lithium and chloride. Reliable lithium data were not found for the most recent analyzed samples (since July 2023). The middle subplot shows differences in species through time (compared to the median of the first 5 samples), which is mostly dominated by the higher-concentration species (i.e., sodium and chloride), which have deviated in recent data. The bottom subplot shows the relative changes in concentrations (divided by the median of the first 5 samples), which is mostly dominated by changes in more minor species (i.e., calcium), which change most after the BATS 2d heater test. Sulphate appears significant in both the middle and bottom subplots.

Kuhlman et al. (2018) performed laboratory evaporation experiments and numerical modeling to understand evaporation in a closed system, but the borehole is an open system—more brine flows into the borehole during the tests, while the brine concentrates due to heating.

Figure 39 shows ratios of Na/Cl and K/Mg ion concentrations through time at the SM borehole (see

Table A-3 for data in g/L). Molar ratios (computed from value converted from g/L to moles/L through the molar weight) are plotted because they are less sensitive to dilution issues during sample collection (e.g., contamination by a small amount of clean rinse water between sampling events) or during laboratory processing (i.e., during dilution of samples to 100 or 10,000 times, based on requirements of the analytical instrument).

The Na/Cl data show a steady increase with time (the third sample in May 2022 is suspect for cross-contamination during sampling). Recent data also show more variability in the Na/Cl molar ratio. The K/Mg data show a dip after BATS 2c, followed by an increase to higher than the initial level.

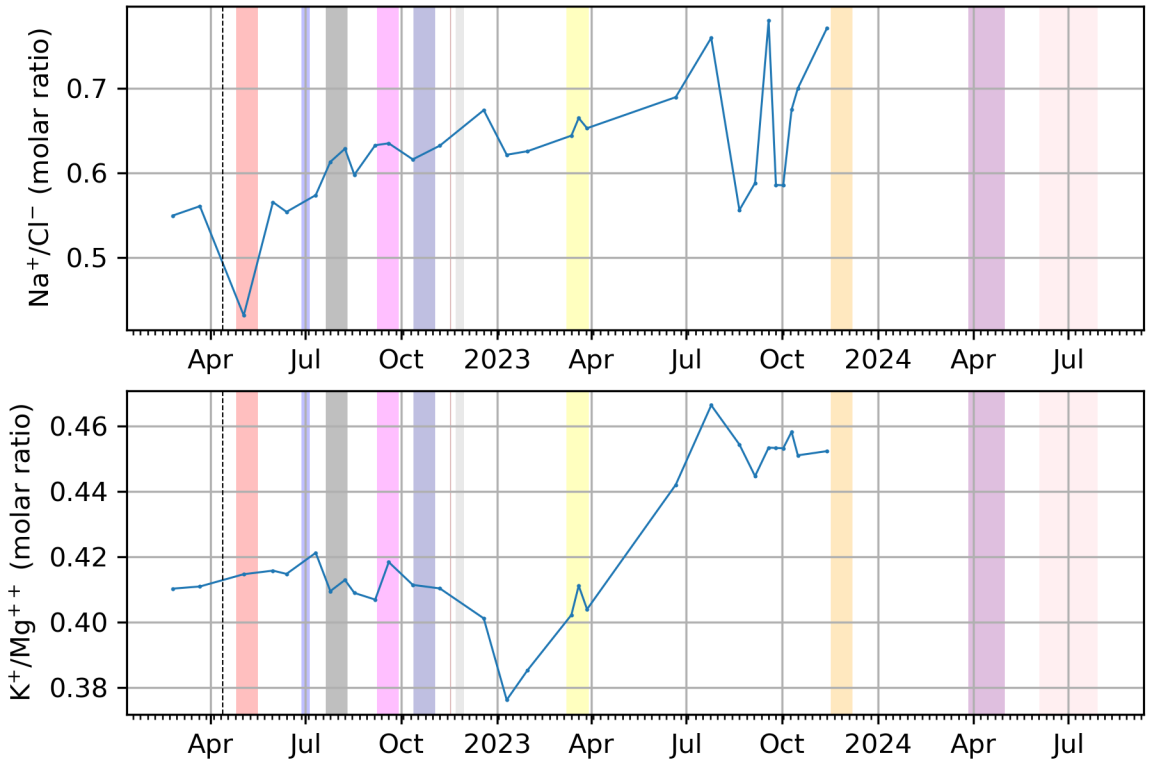

Figure 39.Ratios of ions in heated SM borehole brine samples through time.

To place these values and changes in context, these SM sample data are plotted in Figure 40 against other BATS 1 and BATS 2 samples collected, as well as historical Map Unit 0 (MU-0, where BATS 2 is completed), Marker Bed 139 (MB-139, approximately 1 to 2 m below where BATS 2 is completed), and fluid inclusion data. See Roberts et al. (1999) for a detailed description of WIPP in-repository stratigraphy.

The two samples that show the lowest K/Mg ratio (early 2023) appear more like the BATS 1 data collected previously (see two red dots in Figure 40 that are located inside the pink “BATS 1 MU-3” box). This change in brine chemistry also occurs within a few months after the marked increase in gas permeability (faster declines in argon gas pressure behind the packer, reported in Figure 21) observed in the heated D borehole.

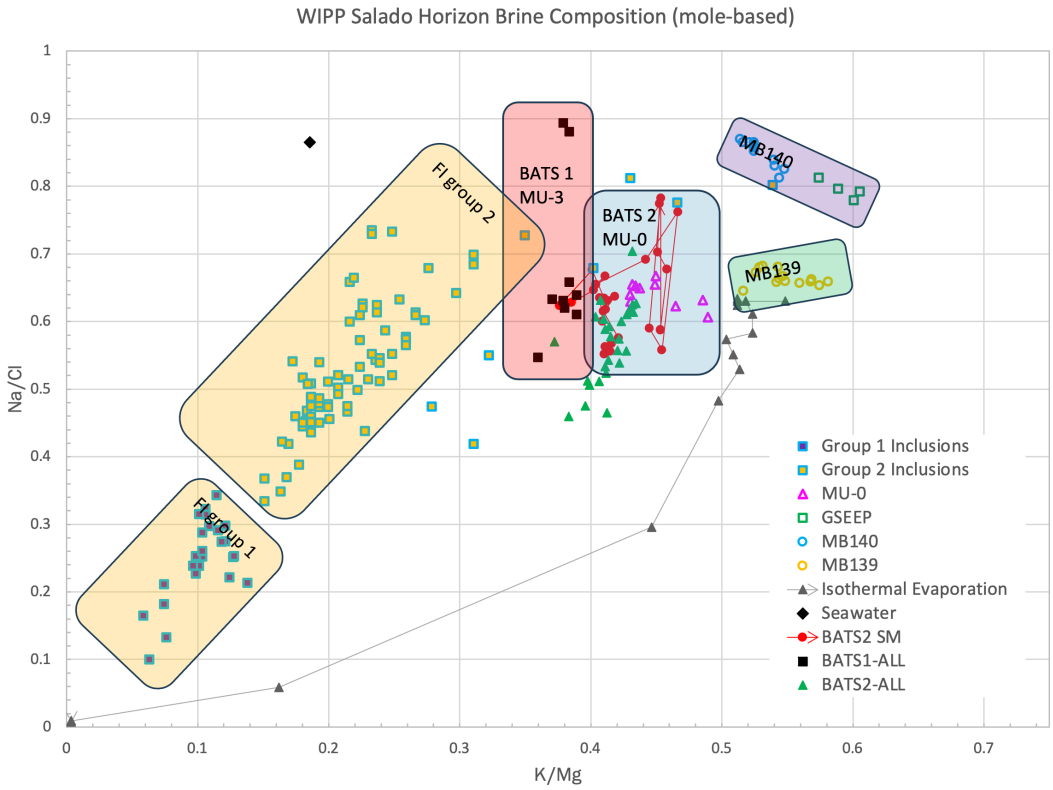

Figure 40.BATS SM brine chemistry timeseries (red filled circles) plotted with historic fluid inclusions, BATS 1, and WIPP historic brine MU-0, MB-139, and MB-140 (Krumhansl et al., 1990).

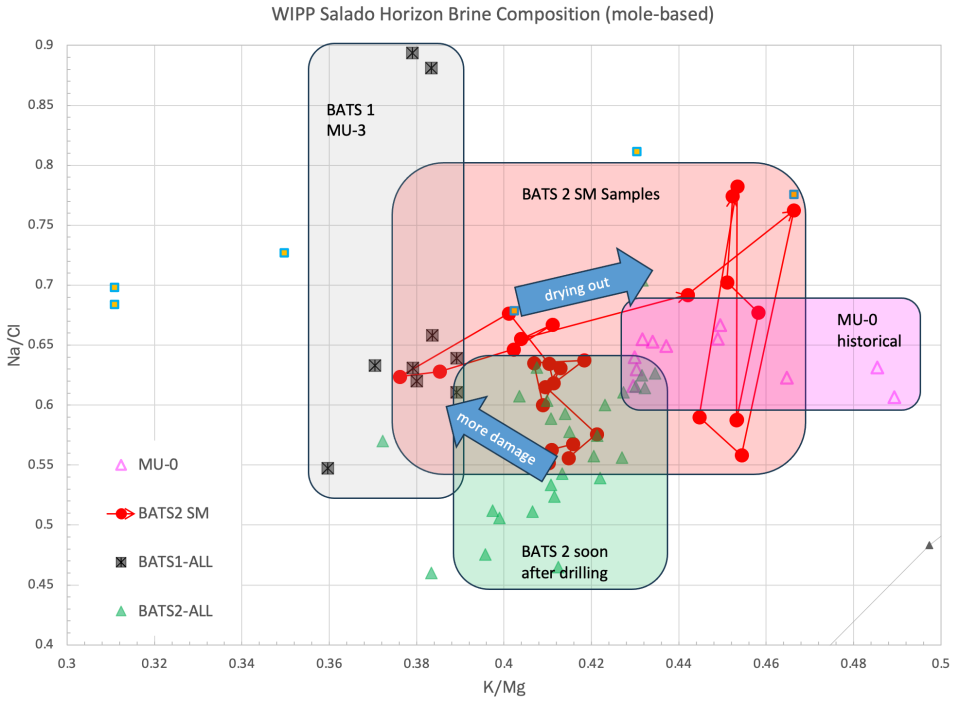

Figure 41.Zoomed in view of BATS SM brine chemistry time series (red filled circles)

Figure 41 shows a zoomed-in view of the same BATS 1 and BATS 2 data shown in Figure 40, with some additional annotations. This figure more clearly shows the evolution of the BATS 2 SM data (red circles) from values that are consistent with the initial observations in BATS 2 boreholes (i.e., soon after drilling, green triangles) to lower values of K/Mg (more indicative of BATS 1 data), which may be related to damage associated with the first few heater tests (BATS 2 a through c), which were seen through the permeability testing to have increased the permeability of the salt (Section 4.2). An increase in permeability may have allowed brine from higher areas (BATS 1 was in MU-3, which is above where BATS 2 is in MU-0) to reach the BATS 2 heated SM borehole.

Since this time, the higher K/Mg values have emerged, which would be more consistent with MU-0 seen in historical unheated boreholes (reported in Deal et al., 1995). Another possible explanation is something caused by the July to September 2023 event described in Section 5. Some of the "up and down" oscillations in more recent data, may be because of the effect evaporation has on brine composition. Evaporation of water from a brine tends to move the data towards the origin (see sequence of black triangles connected by lines in Figure 40, and discussion in Kuhlman et al., 2018).

4.8 SEAL BOREHOLE DATA

The new BATS 2 seals were emplaced as part of the BATS 2 construction, while the unheated seals from BATS 1 are still in place and will remain in place longer, with over-coring of both sets of seals occurring at a future date (possibly during preparations for BATS 3).

4.8.1 SL: AIR TEMPERATURE AND RH TIME SERIES

Figure 36 shows the air temperature and relative humidity data associated with the SL boreholes. Unlike the SM boreholes, the relative humidity behind the packer rises in the SL borehole in response to heating. This is likely due to standing brine in the borehole being removed regularly from the SM borehole by vacuum pump, while any brine that accumulates in the SL borehole would remain and would tend to saturate parts the emplaced seals with time.

4.8.2 SL: STRAIN AND TEMPERATURE TIME SERIES

The lab-constructed seals were instrumented with embedded strain gauges to observe strain in the salt once the borehole has closed in and made contact on the laboratory-fabricated cement plugs. The vibrating-wire GEOKON strain gauges installed in seals as part of BATS 1 in the unheated seal have failed and are no longer reporting valid values. The VPG strain gauges in the unheated seal are still working (blue line in top subplot of Figure 42), and the data show a clear change in slope in December 2022. This is interpreted that the borehole has crept shut against the unheated seal; now the sample is showing a higher steady state strain rate (~570 microstrains per year now, compared to ~140 microstrains per year before) under the now-increased stress (assumed near lithostatic) in the seal. This elevated strain rate would be associated with a steady-state creep rate of the seal material under constant load. This unheated array strain gauge was installed as part of BATS 1 in 2019 and is embedded in the salt concrete portion (see detailed description in Kuhlman et al., 2020) of the unheated SL composite seal. It has taken roughly three years for the borehole to close in on the unheated SL borehole salt concrete seal.

Similar VPG strain gauges in the sorel and salt concrete seals in the heated SL boreholes (red [sorel] and green [salt concrete] lines in Figure 42) show clear straining in response to heating events. The sorel seal experiences higher temperatures than the salt concrete seal, due to each seal's thermocouple's relative distance to the heater. In May 2023, after BATS 2d, the VPG gauge in the heated sorel cement seal saw a similar increase in strain rate, followed by another jump at the end of June 2023 and a drop in September 2023 (see more discussion on this in Section 5). It has taken roughly one year for the borehole to close in on the BATS 2 heated sorel seal, but the nature of the response is clearly different in the heated seal, compared to the unheated seal.

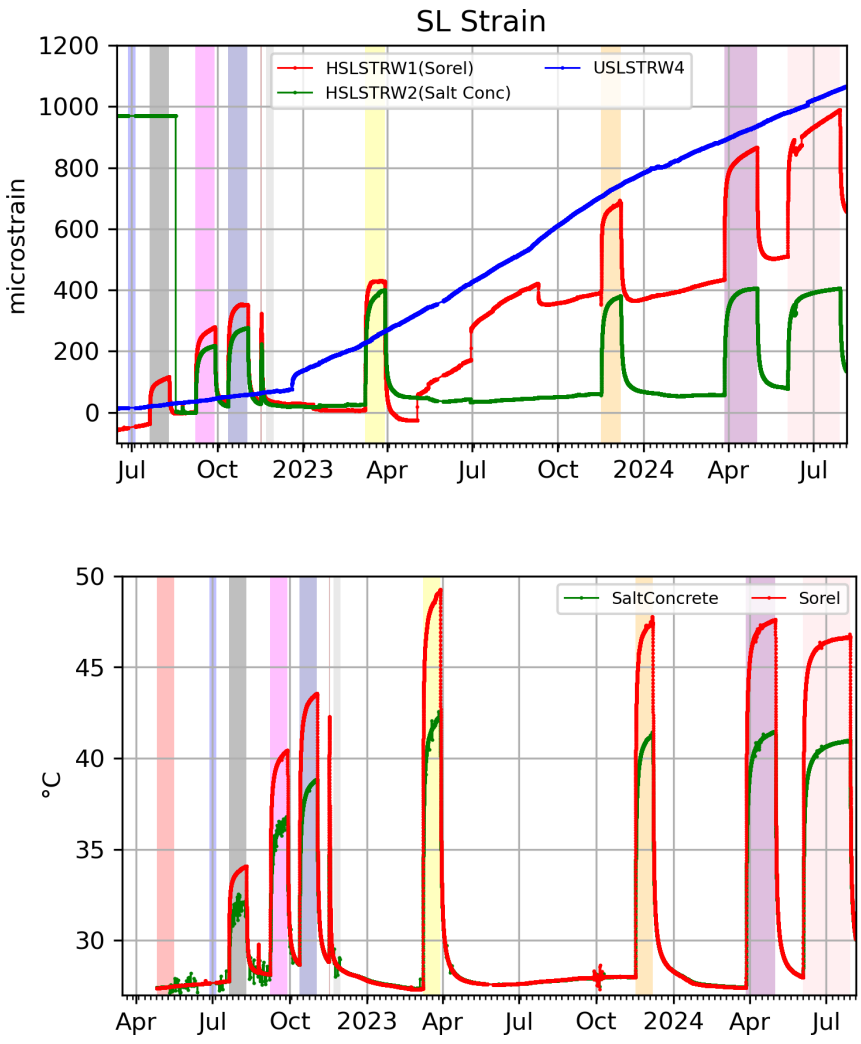

Figure 42.Strain (top) and temperature (bottom) inside cement plugs in SL borehole.

4.9 IN-DRIFT TIME SERIES

Weather station measurements were made in the N-940 drift. Figure 43 shows 10-minute average air temperature, RH, barometric pressure, and air speed near the datalogger enclosures. Drift air temperature increased during the observation period, associated with summer weather. The RH generally rises from spring into summer, associated with changing seasons on the surface, since air from the surface is ventilated through the mine. Large changes in ventilation air speeds are likely due to changes in routing of ventilation in the WIPP underground, which are due to ventilation needs and proximity of other activities in WIPP (e.g., mining or rock bolting). Lower ventilation air speeds occur at night when fewer personnel are underground at WIPP. Barometric pressure fluctuations generally stay between 960 and 970 mbar, with higher-amplitude fluctuations in winter and spring.

The air temperature in the drift fluctuated approximately 3.5 °C through a 12-month period, but there are spikes of higher temperatures observed when the mine ventilation is low, possibly due to heat generated by the instrumentation and computers in the N-940 drift at BATS.

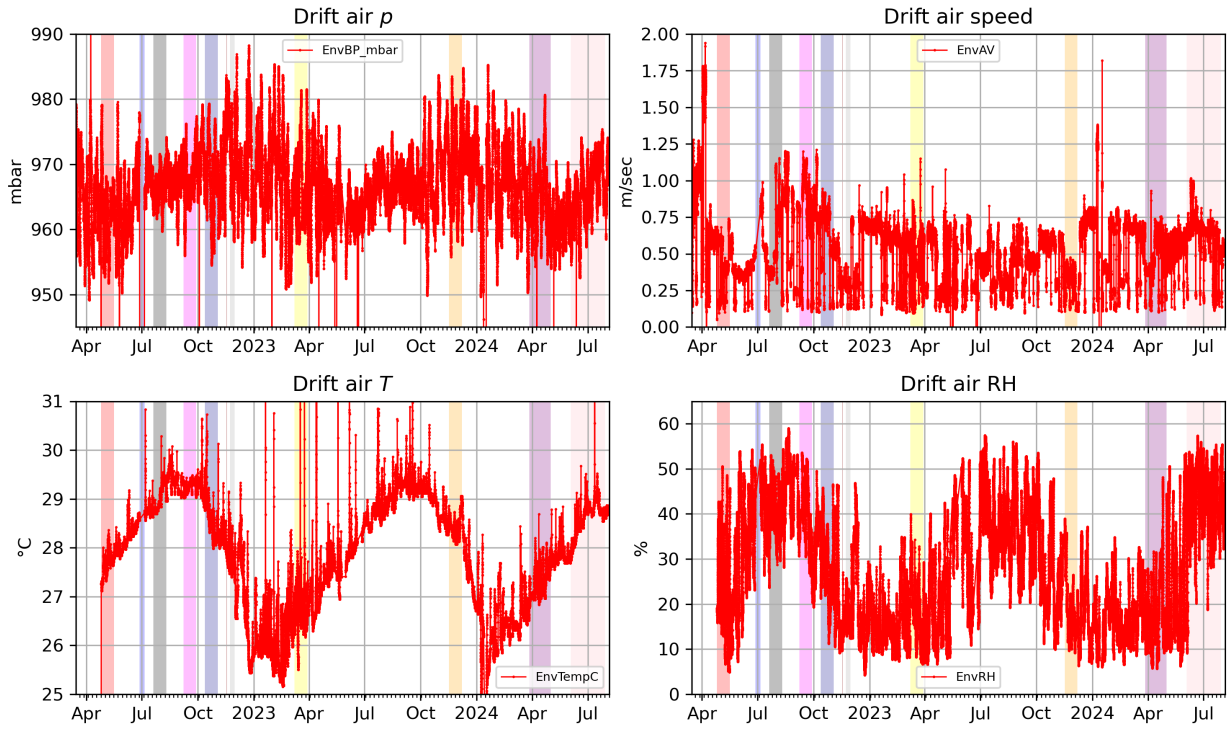

Figure 43.In-drift barometric pressure (top left), air speed (top right), air temperature (bottom left), and RH (bottom right) during BATS 2.

Figure 44 shows the computed dewpoint of the air in the drift. This is computed from the air temperature and RH (both shown in Figure 43), and largely follows the trend in RH. Dewpoint is computed (in °C) from

$$\gamma(T, RH) = \log\left(\frac{RH}{100}\right) + \frac{bT}{c+T}; \qquad T_{\text{dew}} = \frac{c\gamma(T,RH)}{b-\gamma(T,RH)}$$

where $b = 17.625$ and $c = 243.04$ °C. Dewpoint is more of an indicator in the change of water in the air, not just the changes in RH due to changes in temperature.

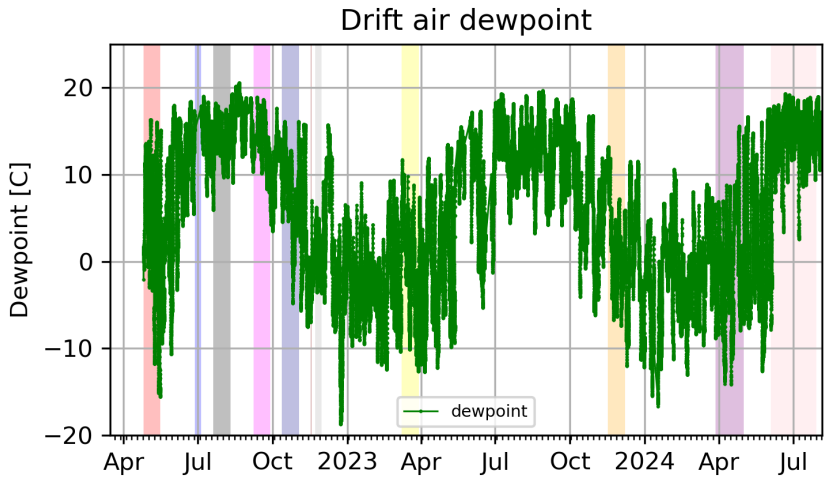

Figure 44.Computed In-drift dewpoint during BATS 2.

5 OBSERVATION ACROSS SENSOR TYPES

During the period between BATS 2d and BATS 2e (April to November 2023), several different observations showed a response from July to September 2023 that appeared in some ways like a heater test, but no heater test was conducted during this time. Figures from earlier in this report are repeated in Figure 45 with this period marked across them.

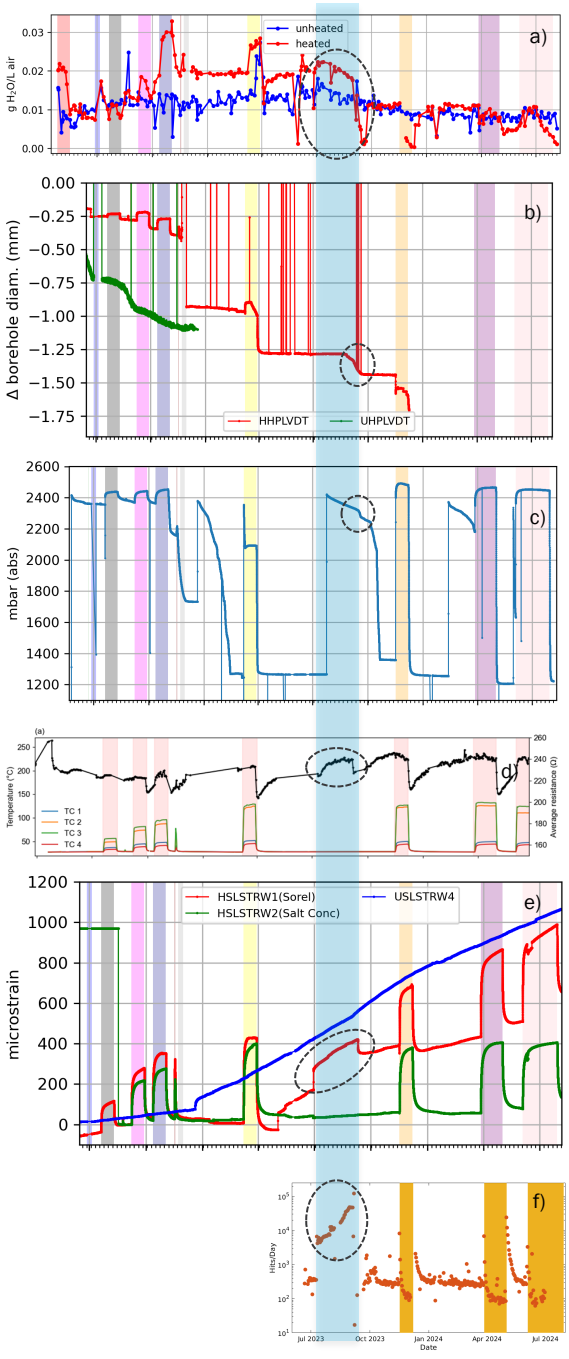

Figure 45. Comparison of multiple sensors with common time axes, highlighting change (blue bar across figures, circled with dashed line) observed July to mid-September 2023: a) desiccant water production from HHP, b) borehole closure in HHP, c) gas pressure in HD, d) average ERT resistance, e) strain in HSL sorel seal, f) AE hits per day.

From July to September 2023, multiple phenomena showed a marked jump or deviation (Figure 45).

a) Water vapor production rate to the HHP borehole, as measured by desiccant and supported by LICOR water concentration measurements -- Figure 9, showed a large drop, which recovered somewhat but has largely sustained until the present.
b) Closure of the HHP borehole, via the LVDT showed a marked decrease in borehole diameter (~0.15 mm) that has been associated with the end of a heating event, every other time it was observed.
c) The argon gas pressure behind the HD packer showed a drop, even after adjusting the data for barometric fluctuations.
d) The heated ERT array (HE1 through HE4) showed an increase in average resistance, with a sudden drop that appears like the type of response observed at the end of heating events. Figure 31 shows this change does not appear in the low resistance measurements, only the higher resistance measurements, which dominate the overall average, shown here.
e) The strain observed in the sorel cement seal has a jump at the beginning of July, and an almost equal magnitude drop in mid-September.
f) The AE hits/day was similar magnitude to levels seen during heating events BATS 2f and 2g, but the hits are sustained for more than a month and the hits/day does not have a smooth fall-off like heating events do.

The fiber optic distributed strain sensors do not show any clear anomalies isolated to this period (Rutqvist et al., 2024). It is possible that the change in brine chemistry (Figure 39) is associated with this, too, but the timing of this is not so directly associated with the July to September 2023 period.

Some of the observations show a change only at the end of this period (borehole closure and HD gas pressure), while the other observations show a change at both the beginning and end of the period.

Considering the types of observations in Figure 45, it is hypothesized that there was a mechanical change in the salt, which may have closed some fractures that were providing brine to HHP borehole, and possibly opened a fracture that was connected to the HD borehole. This change appears to have modified the load being experienced by the sorel seal in the HSL borehole, and somehow modified the apparent resistivity of the formation, as observed by the ERT boreholes. Fractures may significantly modify the electrical properties of the salt, as was used by Chen et al. (2024) to delineate the EDZ, based on the ERT response.

It is possible that drilling and blasting mining for the new WIPP utility shaft (which reached the WIPP level at approximately this time) triggered some change in the salt at the BATS array. It is unusual that the elevated AE activity during this time is not more episodic (like drilling/blasting events or possible movement of equipment), and it stays at elevated over an extended period, including weekends. Review of unpublished WIPP drift closure measurements near BATS (N-940/E-540) show no anomalous drift closure during this period.

Anomalies in any one of these data might have been dismissed as a potential error in a sensor, but the coordinated deviation of multiple disparate sensor types across multiple boreholes in the BATS 2 array point to something larger and more pervasive occurring, like something related to closure in the drift or mining activity.

6 SUMMARY

This report presents the observations from the Brine Availability Test in Salt (BATS) field test in the underground at the Waste Isolation Pilot Plant (WIPP). We presented the motivation and technical background for creating coupled-process field experiments in salt, along with summarizing data collected in FY24 during the most recent three heating phases of BATS 2 (heating events e-g).

Brine migration is important to radioactive waste disposal safety as brine leads to corrosion of waste packages and waste forms, is the primary offsite transport vector, can resist final elimination of excavation porosity by creep closure, and presents a high chlorine concentration environment enabling reduced risk of in-package nuclear criticality.

The main goals of the BATS field test are to collect data that lead to better understanding and possible confirmation of model predictions related to brine availability in bedded salt and to train a new generation of scientists and technicians on the use of underground research labs in the US for radioactive waste disposal.

Eight of the boreholes in the BATS 2 array have instrumentation grouted into them (T1, T2, E1, E2, E3, E4, F1 and F2), while four of the remaining boreholes are isolated with inflatable or mechanical packers (HP, D, SM, SL). The four AE boreholes are not grouted or sealed with packers.

The report describes the most recent three heating events of BATS 2. The BATS 2 tests summarized in last year's milestone report were conducted in 2022 and 2023 over shorter durations (3 weeks) at variable setpoints. In FY24, BATS 2e was three weeks long at a 140 °C setpoint and was conducted in November and December of 2023. BATS 2f was five weeks long at the same setpoint and was conducted March to May 2024. BATS 2g was eight weeks long at the same setpoint and was conducted June and July 2024. BATS 2 explored the effect of different heater controller setpoints (BATS 2 a-c) and different test lengths (BATS 2 e-g) on observed response.

In each array, electrical resistivity electrodes in the four E boreholes are used to interrogate changes in apparent resistivity through time due to brine migration and temperature variation. The ERT system has shown a sensitivity to the migration and distribution of brine during and after heating. The four AE boreholes contain decentralized piezoelectric transducers for monitoring the timing and locating the source of AE in the salt. The two T boreholes, along with temperature measurements in most of the other boreholes, are used to monitor the spatial and temporal variability of temperature around the heater. Aside from a few interactions between the ERT system and the thermocouples (which led to premature failure of most of the thermocouples in the unheated ERT boreholes), the sealed Type-K thermocouples have proven to be generally robust in the salt environment. The ERT boreholes in BATS 2 use RTDs to reduce the noise previously observed during ERT testing each night, but the RTDs still experience some noise. The SL borehole includes a laboratory-created composite seal (salt concrete and sorel cement), instrumented with strain gauges behind a mechanical packer. The D borehole is pressurized with Ar, which is used to test the changing gas permeability of the system (i.e., falling head pressure decay) and monitor breakthrough of gas to the gas analyzer monitoring the HP borehole. The central HP borehole contains a 1250-Watt heater used to heat a 71-cm interval of the borehole, while moisture is removed with flowing dry N_2 for in-drift analyses of gas and water isotope composition.

The AE system saw significant activity at the beginning and end of each heating cycle. The ERT system showed systematic changes in resistivity around the heater associated with each heating event. Samples collected with a cold trap for stable isotopes showed changes in water isotopes, possibly related to the change in the relative contribution of fluid inclusions to the overall brine. Both the unheated and heated seals showed evidence for creep closure of the salt and loading of the plug with increased stress.

The gas permeability of the fractured salt system penetrated by the BATS 2 boreholes changes markedly when the heater is turned on and off. Turning the heater on rapidly stops gas flow between boreholes, and turning the heater off rapidly allows that same gas to flow between boreholes.

Data are presented in this report with some preliminary analyses, but it will take some time to fully understand the coupled thermal, hydrological, mechanical, and chemical processes going on in the BATS 2 array. BATS 1 was the focus of Task E in the DECOVALEX-2023 (DEvelopment of COupled models and their VALidation against EXperiments) international model validation exercise (Kuhlman et al., 2024b). BATS 2 will be the focus of a follow-on task as part of DECOVALEX-2027.

The overall theme in BATS 2 is seeing multiple lines of evidence that an accumulation of damage occurs in the salt associated with both heating and cooling to different temperatures. The BATS tests included:

- thermal (changes in temperature due to a range heater test length; ranging from three to eight weeks);
- hydrological (water production associated with heating and cooling in the HP borehole and gas tracer tests between D and HP boreholes using argon);
- mechanical (closure observations in HP and change in strain rate in the SL boreholes, supplemented by observations of the timing and location of damage through acoustic emissions);
- chemical (water isotope observations through time in HP borehole gas stream and brine chemistry observations through samples made across time in the SM borehole);
- indirect geophysical responses (electrical resistivity tomography changes due to heating and distributed fiber optic strain and temperature measurements showing effects of both heating and drift closure); and
- a possibly coupled response of the system to drift closure or other mechanical change in the system (observed to occur between heating events, in mid-September 2023).

Each of these responses were characteristic of a system changing through damage and brine migration. The focus of BATS is “brine availability”, which is related to the occurrence of brine, and the evolution of the flow networks that bring gas and brine to boreholes and excavations.

The large response of brine inflow after the end of the BATS 1 test (Jan-Mar 2020) has notably not been observed in BATS 2. The difference in the response of the system between these tests is a point which will be investigated further in future work.

7 NEXT STAGES

Additional heater tests are planned for the remainder of 2024 and into 2025, while preparing for BATS 3, building on lessons learned so far during in BATS 1 and BATS 2.

We intend to run a heater test with more gradually increasing start-up and decreasing shut-down heating rates, more characteristic of expected behavior in a real repository. To date, heater tests are essentially a step change on or off (they ramp to the specified setpoint over <10 minutes). We also want to run a cyclic heater test. The heater controller in BATS 2 should allow arbitrary heater power profiles, including gradual ramping up or down over hours or days, or even a smooth sinusoidal heating distribution.

Earlier in FY24, we updated the BATS 5-year plan (Kuhlman et al., 2024a), which included plans for BATS 3. This next phase which will involve a series of smaller tests that are not centered around a single borehole. This approach will reduce scheduling issues and test interference issues. We will continue to develop and test hypotheses associated with brine availability and migration in the salt excavation damaged zone salt.

BATS 1 provided initial key information about the changes in permeability with temperature and damage associated with heating the salt. BATS 2 has further explored the evolution of damage in salt with new instrumentation at a range of heater temperatures. The BATS series of tests continues with BATS 3, that aims to further illuminate the key mechanisms and couplings that govern thermal-hydrological-mechanical-chemical processes and how they relate to key fluid and solid changes (e.g., boiling point of brine or the dewatering point of certain minerals) that would be driven by the emplacement of heat-generating waste into a salt repository.

The specific short-term BATS 3 goals and the corresponding problems being solved are listed below (Kuhlman et al., 2024a). We also indicate how we close out the issues, moving on to the next phase:

- **Conduct heater tests for longer periods** (months to years) **under more representative conditions** (sealed borehole, not removing inflowing water). These tests will demonstrate that brine inflow is small under realistic conditions, where water is not continuously removed. Longer tests with different boundary conditions will explore how long elevated brine production will be maintained from a newly drilled borehole. Tests will compare vertical to horizontal emplacement strategies. These intermediate scale tests will be used to bridge the gap between the smaller and shorter-term BATS 1 and 2 tests (which we are closing out), with the expected disposal scale and conditions. Intermediate scale tests are the next logical phase of testing.
- **Optimize of modern sealings in presence of stress, brine, and heat**. Because the geologic salt barrier is so effective, drift and shaft seals of man-made openings are the focus of repository design optimization efforts. Salt repositories have unique engineered barriers (i.e., crushed salt, salt cements, *no bentonite*), and should leverage improvements in man-made materials from the last 30 years. Developing an optimization framework for the engineered barrier system (e.g., materials and methodologies) is a critical next step beyond the development of basic science, that bridges between science and application, bringing DOE-NE closer to the readiness level needed for implementation. This closes out aspects of the generic pure science investigation of EBS in salt, moving on to the optimization phase.
- **Create easy-to-understand visualizations of processes in salt repositories.** Time-lapse or stop-motion videos of brine seeps, creep closure, and EDZ development. These processes are too slow to see clearly without being sped up, but creating these types of visualizations of field observations is now well within our capabilities. These efforts will help more people (i.e., new staff, regulators, and stakeholders) understand the unique processes ongoing in a salt repository. Creating more outreach-ready materials can be used to build confidence in the

overall program, as we closeout purely theoretical generic investigations and move on to demonstrations and communication our position to stakeholders.

International collaboration in model validation exercises (e.g., DECOVALEX-2027) will continue to build on the incredible feedback between experimentalists and modeling teams to date. BATS and DECOVALEX have also facilitated knowledge transfer between radioactive waste disposal programs and training the next generations of experimentalists and numerical modelers.

The DOE-NE team comprised of WIPP, SNL, LANL, and LBNL will continue our fruitful collaborative teamwork, these collaborations along with the sponsor's funding, have high-quality research results of BATS 1 and 2 possible. We continue to leverage the capabilities of team members and produce results that are useful for both DOE-NE and DOE-EM missions.

8 REFERENCES

Beauheim, R.L. & R.M. Roberts, 2002. Hydrology and hydraulic properties of a bedded evaporite formation, *Journal of Hydrology, 259*(1–4):66–68.

Boukhalfa, H., E. Guiltinan, T. Rahn, D. Weaver, B. Dozier, S. Otto, P.H. Stauffer, M. Mills, K. Kuhlman, E. Matteo, C. Herrick, M. Nemer, J. Heath, Y. Xiong, C. Lopez, J. Rutqvist, Y. Wu & M. Hu, 2019. *2019 LANL Experiments and Simulations in Support of Salt R&D*, (34 p.) M3SF-19LA010303014, LA-UR-19–29830, Los Alamos, NM: Los Alamos National Laboratory.

Chen, H., J. Wang, L. Linqing, S. Otto, J. Davis, K.L. Kuhlman & Y. Wu, 2024. Electrical resistivity changes during heating experiments unravels heterogeneous thermal-hydrological-mechanical processes in salt formations, *Geophysical Research Letters, 51*(14):e2024GL109836.

Davies, C. & F. Bernier [Eds.], 2005. *Impact of the Excavation Disturbed or Damaged Zone (EDZ) on the Performance of Radioactive Waste Geological Repositories*, (359 p.) EUR 21028 EN, Brussels, Belgium: European Commission.

Deal, D.E., R.J. Abitz, D.S. Belski, J.B. Case, M.E. Crawley, C.A. Givens, P.P.J. Lipponer, D.J. Milligan, J. Myers, D.W. Powers and M.A. Valdivia, 1995. *Brine Sampling and Evaluation Program 1992-1993 Report and Summary of BSEP Data since 1982*. DOE-WIPP 94–011, Carlsbad, NM: Westinghouse Electric Corporation.

Guiltinan, E.J., K.L. Kuhlman, J. Rutqvist, M. Hu, H. Boukhalfa, M. Mills, S. Otto, D.J. Weaver, B. Dozier & P.H. Stauffer, 2020. Temperature response and brine availability to heated boreholes in bedded salt, *Vadose Zone Journal, 19*(1):e20019.

Guiltinan, E., H. Boukhalfa, C. Campe, J. Davis, D. Eldridge, O. Marina, H. Miller, S. Otto, T. Rahn, A. Stansberry, P.H. Stauffer, K.L. Kuhlman, M. Mills, R. Jayne, E. Matteo, C. Herrick, M. Nemer, J. Heath, Y. Xiong, C. Choens, M. Paul, J. Rutqvist, Y. Wu, H. Tounsi& M. Hu, 2023. *2023 LANL Contributions to the BATS Test in WIPP*, (67 p.) LA-UR-23–29483. Los Alamos, NM: Los Alamos National Laboratory.

Guiltinan, E., H. Boukhalfa, J. Davis, D. Eldridge, S. Otto, T. Rahn, A. Stansberry, M. Sweeney, A. Migdissov, H. Xu, P.H. Stauffer, K.L. Kuhlman, M. Mills, R. Jayne, E. Matteo, C. Herrick, Y. Xiong, C. Choens, M. Paul, J. Rutqvist, Y. Wu, H. Tounsi & M. Hu, 2024. *2024 LANL Contributions to the BATS Test in WIPP*, (63 p.) LA-UR-24–28851. Los Alamos, NM: Los Alamos National Laboratory.

Kuhlman, K.L., 2019. *Processes in Salt Repositories*, (41 p.) SAND19–6441R, Albuquerque, NM: Sandia National Laboratories. https://doi.org/10.2172/1559569

Kuhlman, K.L. & B. Malama, 2013. *Brine Flow in Heated Geologic Salt*, (128 p.) SAND2013–1944, Carlsbad, NM: Sandia National Laboratories. https://doi.org/10.2172/1095129

Kuhlman, K.L. & S.D. Sevougian, 2013. *Establishing the Technical Basis for Disposal of Heat-Generating Waste in Salt*, (100 p.) SAND2013–6212P, FCRD-UFD-2013–000233. Albuquerque, NM: Sandia National Laboratories.

Kuhlman, K.L., M.M. Mills & E.N. Matteo, 2017. *Consensus on Intermediate Scale Salt Field Test Design*, (95 p.) SAND2017–3179R, Albuquerque, NM: Sandia National Laboratories. https://doi.org/10.2172/1365470

Kuhlman, K.L., C.M. Lopez, M.M. Mills, J.M. Rimsza & D.C. Sassani, 2018. *Evaluation of Spent Nuclear Fuel Disposition in Salt (FY18)*, (83 p.) M2SF-18SN010303031, SAND2018–11355R, Albuquerque, NM: Sandia National Laboratories. https://doi.org/10.2172/1481605

Kuhlman, K., M. Mills, R. Jayne, E. Matteo, C. Herrick, M. Nemer, J. Heath, Y. Xiong, C. Choens, P. Stauffer, H. Boukhalfa, E. Guiltinan, T. Rahn, D. Weaver, B. Dozier, S. Otto, J. Rutqvist, Y. Wu, M. Hu, S. Uhlemann & J. Wang, 2020. *FY20 Update on Brine Availability Test in Salt*, (107 p.) SAND2020–9034R. Albuquerque, NM: Sandia National Laboratories. https://doi.org/10.2172/1657890

Kuhlman, K., M. Mills, R. Jayne, E. Matteo, C. Herrick, M. Nemer, J. Heath, Y. Xiong, C. Choens, M. Paul, P. Stauffer, H. Boukhalfa, E. Guiltinan, T. Rahn, D. Weaver, S. Otto, J. Davis, J. Rutqvist, Y. Wu, M. Hu, S. Uhlemann & J. Wang, 2021b. *Brine Availability Test in Salt (BATS) FY21 Update*, (64 p.) SAND2021–10962R. Albuquerque, NM: Sandia National Laboratories. https://doi.org/10.2172/1821547

Kuhlman, K., M. Mills, R. Jayne, E. Matteo, C. Herrick, M. Nemer, Y. Xiong, C. Choens, M. Paul, C. Downs, D. Fontes, B. Kernen, P. Stauffer, H. Boukhalfa, E. Guiltinan, T. Rahn, S. Otto, J. Davis, M. Carrasco Jr., J. Mata, J. Rutqvist, Y. Wu, H. Tounsi, M. Hu, S. Uhlemann & J. Wang, 2022. *Brine Availability Test in Salt (BATS) FY22 Update*, (82 p.) SAND2022–12142R. Albuquerque, NM: Sandia National Laboratories.

Kuhlman, K., M. Mills, R. Jayne, E. Matteo, C. Herrick, M. Nemer, Y. Xiong, C. Choens, M. Paul, C. Downs, P. Stauffer, H. Boukhalfa, E. Guiltinan, T. Rahn, S. Otto, J. Davis, D. Eldridge, A. Stansberry, J. Rutqvist, Y. Wu, H. Tounsi, M. Hu, S. Uhlemann & J. Wang, 2023. *Brine Availability Test in Salt (BATS) FY23 Update*, (88 p.) SAND2023–08820R. Albuquerque, NM: Sandia National Laboratories. https://doi.org/10.2172/2369628

Kuhlman, K.L., M. Mills, C. Choens, C. Herrick, S. Otto, J. Davis, P. Stauffer & Y. Wu, 2024a. *Summary of the Brine Availability Test in Salt (BATS), Including Extended Plan for Experiments at the Waste Isolation Pilot Plant (WIPP)*, (54 p.) SAND2024–03904R. Albuquerque, NM: Sandia National Laboratories.

Kuhlman, K.L., J. Bartol, S. Benbow, M. Bourret, O. Czaikowski, E. Guiltinan, K. Jantschik, R. Jayne, S. Norris, J. Rutqvist, H. Shao, P. Stauffer, H. Tounsi & C. Watson, 2024b. Synthesis of Results for Brine Availability Test in Salt (BATS) DECOVALEX-2023 Task E, *Geomechanics for Energy and the Environment, 39*:100581.

Kuhlman, K.L., J. Bartol, A. Carter, A. Lommerzheim & J. Wolf, 2024c. Scenario development for safety assessment in deep geologic disposal of high-level radioactive waste and spent nuclear fuel: A review, *Risk Analysis, 44*(8):1850–1864.

Mills, M., K.L. Kuhlman, R.S. Jayne, J.B. Coulibaly & B. Reedlunn, 2024. *Salt International Collaborations FY24 Update*, (26 p.) M3SF-24SN010303063. Albuquerque, NM: Sandia National Laboratories.

Park, H.D, D. Fukuyama, R.C. Leone, C. Madsen, M.J. Paul, A. Salazar & R.P. Rechard, 2024. *FY24 Advancements in PFLOTRAN Development for GDSA Frameworks*, (80 p.) SAND2024–12081R, Albuquerque, NM: Sandia National Laboratories.

Roberts, R.M., R.L. Beauhiem & P.S. Domski, 1999. *Hydraulic Testing of Salado Formation Evaporites at the Waste Isolation Pilot Plant Site: Final Report,* (288 p.) SAND98–2537, Albuquerque, NM: Sandia National Laboratories.

Rutqvist, J., Y. Wu, M. Hu, M. Cao, G. Guo, H. Tounsi, H. Chen, L. Luo & J. Wang, 2024. Salt Coupled THMC Processes Research Activities at LBNL: FY24 Progress, (104 p.) M3SF-24LB010303032, Berkeley, CA: Lawrence Berkeley National Laboratory.

Sandia National Laboratories (SNL), Los Alamos National Laboratory (LANL) & Lawrence Berkeley National Laboratory (LBNL), 2020. *Project Plan: Salt in situ Heater Test*, (20 p.) SAND2020–1251R.

Stauffer, P.H., A.B. Jordan, D.J. Weaver, F.A. Caporuscio, J.A. Ten Cate, H. Boukhalfa, B.A. Robinson, D.C. Sassani, K.L. Kuhlman, E.L. Hardin, S.D. Sevougian, R.J. MacKinnon, Y. Wu, T.A. Daley, B.M. Freifeld, P.J. Cook, J. Rutqvist & J.T. Birkholzer, 2015. *Test Proposal Document for Phased Field Thermal Testing in Salt,* (104 p.) LA-UR-15–23154, FCRD-UFD-2015–000077. Los Alamos, NM: Los Alamos National Laboratory.

Tounsi, H., J. Rutqvist, M. Hu & K. Kuhlman, 2023. Thermo-hydro-mechanical modeling of brine migration in a heated borehole test in bedded salt, *Rock Mechanics and Rock Engineering, 57*:5505–5518.

Wang, J., S. Uhlemann, S. Otto, B. Dozier, K. Kuhlman & Y. Wu, 2023. Joint geophysical and numerical insights of the coupled thermal-hydro-mechanical processes during heating in salt, *Journal of Geophysical Research: Solid Earth, 128*(9):e2023JB026954.

APPENDIX A – TABULAR DATA

Table A-1. TCO BATS 2 major events (SN is serial number).

Date	Activity Category	Description
27-Oct-2021	BATS 2 Drilling & Coring	Drilling started for BATS 2 heated array.
1-Nov-2021	BATS 2 Brine Sampling	Brine samples collected from BATS 2 AE1 and E4 boreholes.
2-Feb-2022	BATS 2 Brine Sampling	Brine samples collected from BATS 2 AE1, AE3, E2, E3, E4, F1, and T1 boreholes.
18-Feb-2022	BATS 2 Drilling & Coring	Drilling completed for BATS 2 heated array.
24-Feb-2022	BATS 2 Brine Sampling	Brine samples collected from BATS 2 AE4, D, F2, SM, E2, and E3 boreholes.
28-Feb-2022	BATS 2 Drilling & Coring	All BATS 2 boreholes blown out with air and cleaned.
1-Mar-2022	BATS 2 Video Logging	Video logging of BATS 2 E1, E2, E3, E4, F1, F2, T1, and T2 boreholes.
3-Mar-2022	BATS 2 Permeability Testing	Permeability testing of BATS 2 SL borehole.
3-Mar-2022	BATS 2 Instrumentation Installation	Installation of the D inflatable packer in the BATS 2 D borehole.
7-Mar-2022	BATS 2 Permeability Testing	Permeability testing of BATS 2 HP borehole.
7-Mar-2022	BATS 2 Instrumentation Installation	Data collection started for datalogger SN 7071 file named BATS2_Array_Unheated_Gas_SN7071.
7-Mar-2022	BATS 2 Instrumentation Installation	Data collection started for datalogger SN 7072 file named BATS2_Array_Unheated_Temperature_SN7072.
8-Mar-2022	BATS 2 Brine Sampling	Brine samples collected from BATS 2 AE2, AE3, AE4, D, E1, E2, E3, E4, F1, F2, HP, SL, SM, T1, AND T2 boreholes.
14-Mar-2022	BATS 2 Video Logging	Video logging of BATS 2 AE1, AE2, AE3, AE4, D, HP, SL, and SM boreholes.
15-Mar-2022	BATS 2 Grouting Instrument Arrays	Instrument arrays grouted in BATS 2 T1, T2, and E1 boreholes.
21-Mar-2022	BATS 2 Grouting Instrument Arrays	Instrument arrays grouted in BATS 2 E2, E3, and E4 boreholes.
22-Mar-2022	BATS 2 Brine Sampling	Brine samples collected from BATS 2 AE2, AE3, AE4, D, F1, F2, HP, SL, AND SM boreholes.
23-Mar-2022	BATS 2 Instrumentation Installation	Data collection started for datalogger SN 29189 file named BATS2_ERT_RTDs_SN29189.
28-Mar-2022	BATS 2 Grouting Instrument Arrays	Instrument arrays grouted in BATS 2 F1 and F2 boreholes.
5-Apr-2022	BATS 2 Instrumentation Installation	Installation of the SL cement plug in the BATS 2 SL borehole.
5-Apr-2022	BATS 2 Instrumentation Installation	Data collection started for datalogger SN 19480 file named BATS2_Heated_Temperature_SN19480.
13-Apr-2022	BATS 2 Instrumentation Installation	Installation of the SM mechanical packer in the BATS 2 SM borehole.
14-Apr-2022	BATS 2 Instrumentation Installation	Installation of the HP packer assembly in the BATS 2 HP borehole.

Date	Activity Category	Description
25-Apr-2022	BATS 2 Instrumentation Installation	The Picarro and Gas Analyzer were started for gas flow measurements and data collection.
25-Apr-2022	BATS 2 Instrumentation Installation	Circulation plumbing completed and circulation flow started to heated and unheated arrays.
25-Apr-2022	BATS 2 Instrumentation Installation	Data collection started for datalogger SN 7069 file named BATS2_Array_D_Borehole_Inflation_SN7069.
25-Apr-2022	BATS 2 Instrumentation Installation	Data collection started for datalogger SN 16312 file named BATS2_Heated_Gas_SN16312.
25-Apr-2022	BATS 2 Instrumentation Installation	Data collection started for datalogger SN 7075 file named BATS2_LVDT_SG_TRH_SN7075.
25-Apr-2022	BATS 2 Instrumentation Installation	Data collection started for datalogger SN 29190 file named BATS2_Power_Controller_SN29190.
3-May-2022	BATS 2 Brine Sampling	Brine sample collected from SM borehole.
9-May-2022	BATS 2 Power Outage	Planned power outage, power restored 5/10/2022.
25-May-2022	BATS 2 Permeability Testing	Permeability testing of BATS 2 D borehole - nitrogen gas.
31-May-2022	BATS 2 Brine Sampling	Brine sample collected from SM borehole.
9-Jun-2022	BATS 2 Power Outage	Planned power outage, power restored 6/13/2022.
13-Jun-2022	BATS 2 Brine Sampling	Brine sample collected from SM borehole.
22-Jun-2022	BATS 2 Instrumentation Installation	Power controller testing and troubleshooting. Power controller issues resolved, and the power controller is ready to use for heating.
27-Jun-2022	BATS 2 Power Outage	Planned power outage, power restored 7/5/2022.
11-Jul-2022	BATS 2 Brine Sampling	Brine sample collected from SM borehole.
11-Jul-2022	BATS 2 Instrumentation Installation	Power controller settings re-configured.
18-Jul-2022	BATS 2 Permeability Testing	Permeability testing of BATS 2 D borehole - nitrogen gas. Test ended and nitrogen vented from the borehole.
18-Jul-2022	BATS 2 Permeability Testing	Permeability testing of BATS 2 D borehole - argon gas. The argon gas will also act as a tracer for the gas analyzer.
20-Jul-2022	BATS 2a Heating Event	The BATS 2 HP borehole heater was set to a 90 °C set point for 3 weeks of scheduled heating.
25-Jul-2022	BATS 2 Brine Sampling	Brine sample collected from SM borehole.
25-Jul-2022	BATS 2 Instrumentation Installation	Datalogger SN 29190 (power controller) was re-configured to capture additional power controller data.
29-Aug-2022	BATS 2 Power Outage	Planned Power Outage, power restored 9/6/2023
6-Sep-2022	BATS 2 Brine Sampling	Brine sample collected from SM borehole. 9 ml sample clear to cloudy in color
7-Sep-2022	BATS 2b Heating Event	The BATS 2 HP borehole heater was set to a 115 °C set point for 3 weeks of scheduled heating.
19-Sep-2022	BATS 2 Brine Sampling	Brine sample collected from SM borehole. 18 ml sample light brown in color
3-Oct-2022	BATS 2 Picarro Issues	Instrument not working as expected, no measurements were being made by the Picarro from 10/3/22 to 11/2/22
5-Oct-2022	BATS 2 Power Outage	Unexpected Power Outage from 10:24 to 11:20

Date	Activity Category	Description
12-Oct-2022	BATS 2 Brine Sampling	Brine sample collected from SM borehole. 19 ml sample light brown in color
12-Oct-2022	BATS 2c Heating Event	The BATS 2 HP borehole heater was set to a 130 °C set point for 3 weeks of scheduled heating.
24-Oct-2022	BATS 2 Brine Sampling	Brine sample collection attempted from SM borehole.
3-Nov-2022	BATS 2 Picarro Issues	Replacement Picarro installed.
7-Nov-2022	BATS 2 Brine Sampling	Brine sample collected from SM borehole. 14 ml sample
7-Nov-2022	BATS 2 ERT Issues	ERT file sizes started decreasing in size. Periodically the ERT is not finishing data runs. Issues persist through 12/5/22
14-Nov-2022	BATS 2 Brine Sampling	Brine sample collection attempted from SM borehole.
14-Nov-2022	BATS 2 Power Outage	Unexpected Power Outage from 07:43 to 09:08
16-Nov-2022	BATS 2d Heating Event	The BATS 2 HP borehole heater was set to a 140 °C set point, but test aborted after ~1.5 days
21-Nov-2022	BATS 2 gas analyzer issues	Gas analyzer is no longer recording data in P vs T mode
22-Nov-2022	BATS 2 Brine Sampling	Brine sample collection attempted from SM borehole.
22-Nov-2022	BATS 2 HP packer	packer removed from HP borehole to check heater, blister in packer rubber prevents re-insertion of packer.
30-Nov-2022	BATS 2 HP packer	packer blister bled using syringe, packer re-inserted into heated HP borehole and re-inflated
5-Dec-2022	BATS 2 ERT Issues	The ERT problem is related to the internal battery. The battery is low. The ERT was turned off to try to re-charge the battery.
7-Dec-2022	BATS 2 ERT Issues	The ERT was re-started. The small file size issue continued and the internal battery was low. Issue persisted through 12/14/22
7-Dec-2022	BATS 2 Gas Analyzer Issues	Gas analyzer is returning errors about RGA head
14-Dec-2022	BATS 2 ERT Issues	The ERT was removed from service and a replacement ERT will be installed in February.
14-Dec-2022	BATS 2 Gas Analyzer Issues	Gas analyzer is removed from service
19-Dec-2022	BATS 2 Brine Sampling	Brine sample collected from SM borehole. 34 ml sample
21-Dec-2022	BATS 2 HD Perm Test	Filled interval behind HD packer with argon to ~20 psi
9-Jan-2023	BATS 2 Power Outage	Unexpected Power Outage from 19:20 to 20:06
10-Jan-2023	BATS 2 Brine Sampling	Brine sample collected from SM borehole. 6 ml sample light brown in color
18-Jan-2023	BATS 2 Gas Analyzer Issues	Repaired gas analyzer is re-connected and started in P vs T mode
20-Jan-2023	BATS 2 Power Outage	Unexpected Power Outage from 00:49 to 08:55
30-Jan-2023	BATS 2 Brine Sampling	Brine sample collected from SM borehole. 4 ml sample clear to colorless
21-Feb-2023	BATS 2 Brine Sampling	Brine sample collection attempted from SM borehole.
27-Feb-2023	BATS 2 ERT Issues	The replacement ERT was installed and ERT data collection resumed.
8-Mar-2023	BATS 2d Heating Event	The BATS 2 HP borehole heater was set to a 140 °C set point for 3 weeks of scheduled heating.
13-Mar-2023	BATS 2 Brine Sampling	Brine sample collected from SM borehole. 18 ml sample light brown in color
16-Mar-2023	BATS 2 Power Outage	Unexpected Power Outage, power restored 3/20/23

Date	Activity Category	Description
20-Mar-2023	BATS 2 Brine Sampling	Brine sample collected from SM borehole. 7 ml sample clear to colorless
28-Mar-2023	BATS 2 Brine Sampling	Brine sample collected from SM borehole. 3 ml sample clear to colorless
1-Apr-2023	BATS 2 Picarro Issues	Instrument has intermittent errors and is repeatedly not operating as expected. Errors continue through 7/2/23
3-Apr-2023	BATS 2 Brine Sampling	Brine sample collection attempted from SM borehole.
10-Apr-2023	BATS 2 Brine Sampling	Brine sample collection attempted from SM borehole.
10-Apr-2023	BATS 2 Power Outage	Unexpected Power Outage, power restored 4/17/23
17-Apr-2023	BATS 2 Brine Sampling	Brine sample collection attempted from SM borehole.
24-Apr-2023	BATS 2 Brine Sampling	Brine sample collection attempted from SM borehole.
1-May-2023	BATS 2 Brine Sampling	Brine sample collection attempted from SM borehole.
1-May-2023	BATS 2 Power Outage	Unexpected Power Outage, power restored 5/8/23
8-May-2023	BATS 2 Power Outage	Planned Power Outage, power restored 11:05
8-May-2023	BATS 2 Power Outage	Unexpected Power Outage, power restored 5/9/23
10-May-2023	BATS 2 ERT Issues	The ERT stopped working due to low internal battery voltage. The ERT was re-started.
12-May-2023	BATS 2 Power Outage	Unexpected Power Outage, power restored 5/16/23
16-May-2023	BATS 2 Power Outage	Multiple unexpected Power Outages during the day
17-May-2023	BATS 2 ERT Issues	The ERT stopped working due to low internal battery voltage. The ERT was turned off. A replacement ERT is installed in July.
23-May-2023	BATS 2 Power Outage	Unexpected Power Outage, power restored 5/24/23
12-Jun-2023	WIPP Shaft Activities	Approximately at 8:30, there was a 2 to 4 second noise in the N940 drift that sounded like a potential back fall. The UFE was contacted and the noise was from the blast at the exhaust shaft excavation.
19-Jun-2023	BATS 2 Power Outage	Planned Power Outage, power restored 6/21/23
21-Jun-2023	BATS 2 Brine Sampling	Brine sample collected from SM borehole. 7 ml sample light brown in color
22-Jun-2023	BATS 2 Power Outage	Unexpected Power Outage from 23:20 to 23:30
2-Jul-2023	BATS 2 Picarro Issues	Picarro is no longer working. All troubleshooting and attempted fixes did not resolve instrument issues. Picarro removed from service.
10-Jul-2023	BATS 2 ERT Issues	The replacement ERT was installed and ERT data collection resumed.
24-Jul-2023	BATS 2 HD Perm Test	Filled interval behind HD packer with argon to ~21 psi
24-Jul-2023	BATS 2 Power Outage	Planned Power Outage at 08:45
25-Jul-2023	BATS 2 Brine Sampling	Brine sample collected from SM borehole. 17 ml sample light brown in color
7-Aug-2023	BATS 2 Brine Sampling	Brine sample collection attempted from SM borehole.
7-Aug-2023	BATS 2 Power Outage	Planned Power Outage at 08:45
7-Aug-2023	BATS 2 Picarro Issues	The Picarro was removed from the underground.
21-Aug-2023	BATS 2 Brine Sampling	Brine sampling of the heated SM borehole. 5 mL of brine was collected, and it was lt. brown in color.
21-Aug-2023	BATS 2 Gas Analyzer Issues	The gas analyzer was re-started. The turbo pump did not sound normal when the GA was re-starting. Normal sound is a loud and winding pitch. Like a jet engine

Date	Activity Category	Description
		getting louder as the rpm's increase. There was little to no sound for the turbo pump.
23-Aug-2023	WIPP Shaft Activities	At 11:09, blasting from shaft 5 was heard and felt in the north end of the WIPP underground. This time can be used by the AE PI to evaluate the AE data for a better understanding of how shaft 5 blasting affects AE data.
29-Aug-2023	BATS 2 Gas Analyzer Issues	From 12:00 to 12:20 the gas analyzer was disconnected and removed from the gas circulation plumbing. After the GA was removed the circulation inlet and outlet for the gas analyzer were plugged to close the circulation plumbing circuit.
5-Sep-2023	BATS 2 Plumbing	Datalogger sn 16312 for the heated gas array was re-configured to remove the solenoid switching. The solenoids will no longer switch, and the heated array gas stream is permanently flowing to the GA system.
5-Sep-2023	BATS 2 Brine Sampling	Brine sampling of the heated SM borehole. 8 mL of brine was collected, and it was lt. brown in color.
5-Sep-2023	BATS 2 Brine Sampling	Brine sampling of the unheated SM borehole. 0 mL of brine was collected.
11-Sep-2023	BATS 2 Brine Sampling	Brine sampling of the heated SM borehole. 0 mL of brine was collected.
11-Sep-2023	BATS 2 AE Issues	The heated AE was off, and data were not being collected. Data collection stopped on 9/7/2023 at 17:35. The external hard drive disk was full.
13-Sep-2023	BATS 2 Power Outage	Started to investigate reported power outage that was reported yesterday afternoon. All instruments using computers/laptops were down. The GA laptop was OFF. All other computers were running, but the cold and hot AE programs were not. The ERT program showed "failed run" and was in idle mode. The FO program was in a "1 second pause" mode and was not recording data. U/G Electrical Maintenance indicated that they would need to reconfigure our electrical feed due to an MSHA citation concerning a ground control problem near the PPC that was providing power.
18-Sep-2023	BATS 2 Brine Sampling	Brine sampling of the heated SM borehole. 7 mL of brine was collected. The brine was lt. brown in color.
18-Sep-2023	BATS 2 Power Outage	Data review of CSI sn16312 1-minute data shows that there was an unexpected power outage on 9/15/2023 from 08:58 to 09:06.
25-Sep-2023	BATS 2 Brine Sampling	Brine sampling the heated SM borehole. 9 mL of brine, clear to colorless in color, was collected.
25-Sep-2023	BATS 2 ERT Issues	The ERT was on, and the next data collection was scheduled for 9/25/2023 at 17:00, however there were no data files written since the ERT was re-started on 9/21/2023.
2-Oct-2023	BATS 2 Brine Sampling	Brine sampling the heated SM borehole. 4 mL of brine, clear to colorless in color, was collected.
10-Oct-2023	BATS 2 Brine Sampling	Brine sampling the heated SM borehole. 3 mL of brine, clear to colorless in color, was collected.
16-Oct-2023	BATS 2 Brine Sampling	Brine sampling of the heated SM borehole was stopped after 10 minutes of sampling. 8 mL of brine was collected, and the brine was clear to colorless in color.
23-Oct-2023	BATS 2 Brine Sampling	Brine sampling of the heated SM borehole ended. Sampling time was 10 minutes. Two drops of brine were collected (<1 mL, maybe 0.1 mL). No sample was collected due to an insufficient amount.
30-Oct-2023	BATS 2 Brine Sampling	Brine sampling of the heated SM borehole was stopped. 0 mL of brine was collected - no sample.
1-Nov-2023	BATS 2 Cold Trap	The cold trap items were added, and the heated circulation gas flow was returned to normal.

Date	Activity Category	Description
6-Nov-2023	BATS 2 Brine Sampling	Brine sampling of the heated SM borehole was stopped. 0 mL of brine was collected - no sample.
6-Nov-2023	BATS 2 AE Issues	The unheated AE screen showed that the instrument was on and working. However, there were no new data files since 10/30/2023. The unheated AE was re-started, and data collection resumed.
8-Nov-2023	BATS 2 Cold Trap	Approximately 2 to 3 mL of liquid was collected from the heated HP borehole by the cold trap.
13-Nov-2023	BATS 2 Brine Sampling	Brine sampling of the heated SM borehole was stopped after 10 minutes. 5 mL of brine was collected. Brine was relatively clear.
16-Nov-2023	BATS 2 Plumbing	A new gas cylinder was added to the heated circulation flow line. Two full gas cylinders are in place for the heated circulation flow line.
16-Nov-2023	BATS 2 Cold Trap	The cold trap gas flow was stopped. Approximately 1.5 mL of brine was collected. The valves were returned to the normal position.
16-Nov-2023	BATS 2 Permeability	Argon gas flow to the heated HD borehole. The borehole pressure was 20.81 psi. Approximately 6.98 L of argon was used to recharge the borehole.
16-Nov-2023	BATS 2 Heater Test	The heated HP borehole power controller (heater controller) setpoint was changed from 25 °C to 140 °C. The PV temperature at startup was 30 °C. The power output started to increase.
20-Nov-2023	BATS 2 Plumbing	Check of the heated circulation flow rate at the flow controller showed that the flow was 0 mL/min. The two UHP cylinders were checked, and the valves were open and both cylinders had gas. Further checks showed that the valve by the pressure transducer was closed. The wrong valve was closed after the permeability test on 11/16/2023. Data review shows that gas flowed to the heated circulation flow line for ~20 minutes at 400 mL/min before the valve was accidentally closed. The valves were labeled to avoid making this mistake in the future. The valve that was supposed to be closed was on the heated D argon flow line. Since the gas cylinder valve to the heated D flow line was closed, the permeability test was not negatively impacted.
20-Nov-2023	BATS 2 Cold Trap	Approximately 1.5 to 2.0 g of brine water were collected in the cold trap.
20-Nov-2023	BATS 2 Brine Sampling	Brine sampling of the heated SM borehole. 0 mL of brine was collected.
27-Nov-2023	BATS 2 Brine Sampling	Brine sampling of the heated SM borehole. 5 mL of brine was collected. The color was clear to colorless.
29-Nov-2023	BATS 2 Cold Trap	The heated circulation flow rate was changed from 2 L/min to 400 mL/min. The heated circulation valves were turned to direct flow to the main heated circulation flow line. Approximately 1.03 g of water was collected in the cold trap.
4-Dec-2023	BATS 2 Brine Sampling	Brine sampling of the heated SM borehole. Approx. 1mL of brine was collected. The color was clear.
4-Dec-2023	BATS 2 Cold Trap	Approximately 0.5 g of water was collected in the cold trap.
6-Dec-2023	BATS 2 Cold Trap	Approximately 0.5 g of water was collected in the cold trap.
13-Dec-2023	BATS 2 Brine Sampling	Brine sampling for the heated SM borehole. 0 mL of brine was collected - no sample.
13-Dec-2023	BATS 2 Cold Trap	Approximately 0.5 g of water was collected in the cold trap.
18-Dec-2023	BATS 2 Brine Sampling	Brine sampling for the heated SM borehole. 0 mL of brine was collected - no sample.
18-Dec-2023	BATS 2 Cold Trap	2.75 g of water was collected in the cold trap.
20-Dec-2023	BATS 2 Cold Trap	1.59 g of water was collected in the cold trap.

Date	Activity Category	Description
2-Jan-2024	BATS 2 Brine Sampling	Brine sampling for the heated SM borehole. 0 mL of brine was collected - no sample.
2-Jan-2024	BATS 2 Cold Trap	1.89 g of water was collected in the cold trap.
3-Jan-2024	BATS 2 Cold Trap	1.83 g of water was collected in the cold trap.
8-Jan-2024	BATS 2 Brine Sampling	Brine sampling for the heated SM borehole. 0 mL of brine was collected - no sample.
8-Jan-2024	BATS 2 Cold Trap	1.92 g of water was collected in the cold trap.
10-Jan-2024	BATS 2 Cold Trap	1.80 g of water was collected in the cold trap.
17-Jan-2024	BATS 2 Cold Trap	1.92 g of water was collected in the cold trap.
22-Jan-2024	BATS 2 Cold Trap	Approximately 1.5 g of water was collected in the cold trap.
22-Jan-2024	BATS 2 Brine Sampling	Brine sampling for the heated SM borehole. 0 mL of brine was collected - no sample.
24-Jan-2024	BATS 2 Power Outage	Unplanned power outage on reconfigured power feed. Gas Analyzer turbopump was very audible compared to a controlled power down. Notified underground electrician.
24-Jan-2024	BATS 2 Cold Trap	Approximately 1.5 g of water was collected in the cold trap.
29-Jan-2024	BATS 2 Brine Sampling	The heated SM borehole packer can't be removed from the borehole. The sampling tubing can't be tested. The sampling tubing is possibly clogged and not working.
29-Jan-2024	BATS 2 Brine Sampling	Brine sampling for the heated SM borehole. 0 mL of brine was collected - no sample.
29-Jan-2024	BATS 2 Cold Trap	1.98 g of water was collected in the cold trap.
31-Jan-2024	BATS 2 Cold Trap	0.97 g of water was collected in the cold trap.
5-Feb-2024	BATS 2 Brine Sampling	Brine sampling for the heated SM borehole. 0 mL of brine was collected - no sample.
5-Feb-2024	BATS 2 Cold Trap	2.00 g of water was collected in the cold trap.
7-Feb-2024	BATS 2 Cold Trap	1.24 g of water was collected in the cold trap.
12-Feb-2024	BATS 2 Cold Trap	Check of the cold trap showed that the inflow was 2.0940 L/min and the outflow was 0.4740 L/min. The large difference is most likely due to the missing O-rings in the ultra torr fittings.
12-Feb-2024	BATS 2 Brine Sampling	Brine sampling for the heated SM borehole. 0 mL of brine was collected - no sample.
12-Feb-2024	BATS 2 Cold Trap	0.72 g of water was collected in the cold trap.
12-Feb-2024	BATS 2 Permeability	The flow valve to the heated D borehole was closed. Prior to closing the valve, the flow was 0.0002 L/min (set point was 2 L/min) and the pressure was 20.32 psi.
14-Feb-2024	BATS 2 Brine Sampling	3/8-inch tubing was passed thru the heated SM borehole packer pass thru to check for clearance. The tubing did pass thru and reached the end of the borehole. Some obstructions were felt in the borehole, possibly precipitated brine nodules. When the tubing was removed it was wet and there was brown clay on the tubing.
14-Feb-2024	BATS 2 Brine Sampling	Brine sampling for the heated SM borehole. 0 mL of brine was collected - no sample.
20-Feb-2024	BATS 2 Cold Trap	Replacement O-rings were inserted into the cold trap ultra torr fittings.

Date	Activity Category	Description
20-Feb-2024	BATS 2 Brine Sampling	Brine sampling for the heated SM borehole. 0 mL of brine was collected - no sample.
20-Feb-2024	BATS 2 Cold Trap	1.88 g of water was collected in the cold trap.
29-Feb-2024	BATS 2 Brine Sampling	Brine sampling for the heated SM borehole. 0 mL of brine was collected - no sample.
29-Feb-2024	BATS 2 Cold Trap	1.79 g of water was collected in the cold trap.
4-Mar-2024	BATS 2 Brine Sampling	Brine sampling for the heated SM borehole. 0 mL of brine was collected - no sample.
4-Mar-2024	BATS 2 Cold Trap	0.98 g of water was collected in the cold trap.
11-Mar-2024	BATS 2 Brine Sampling	Brine sampling for the heated SM borehole. 0 mL of brine was collected - no sample.
11-Mar-2024	BATS 2 Cold Trap	1.01 g of water was collected in the cold trap.
18-Mar-2024	BATS 2 Brine Sampling	Brine sampling for the heated SM borehole. 0 mL of brine was collected - no sample.
18-Mar-2024	BATS 2 Cold Trap	1.08 g of water was collected in the cold trap.
20-Mar-2024	BATS 2 Cold Trap	1.23 g of water was collected in the cold trap.
25-Mar-2024	BATS 2 Brine Sampling	Brine sampling for the heated SM borehole. 0 mL of brine was collected - no sample.
25-Mar-2024	BATS 2 Cold Trap	1.07 g of water was collected in the cold trap.
27-Mar-2024	BATS 2 Permeability	Argon flow to the heated D borehole was stopped. The heated D borehole pressure was 20.02 psi.
27-Mar-2024	BATS 2 Heater Test	The heated HP borehole power controller set point was changed from 25 °C to 140 °C.
1-Apr-2024	BATS 2 Packer	Based on the amount of gas flowed to the heated HP packer, the packer may have a leak.
3-Apr-2024	BATS 2 Brine Sampling	Brine sampling of the heated SM borehole. 0 mL of brine was collected.
4-Apr-2024	BATS 2 Cold Trap	1.49 g of water was collected in the cold trap.
8-Apr-2024	BATS 2 data issues	The heated circulation (outflow side) flow controller was not reading properly. The reading was well above the high-end range of 2 L/min. Most likely, the additional water in the system, higher temperatures from the heating cycle, and the change for when the cold trap is in use are causing the flow controller to read erratically.
8-Apr-2024	BATS 2 Brine Sampling	Brine sampling of the heated SM borehole. 0 mL of brine was collected.
8-Apr-2024	BATS 2 Cold Trap	1.52 g of water was collected in the cold trap.
15-Apr-2024	BATS 2 Cold Trap	1.65 g of water was collected in the cold trap.
17-Apr-2024	BATS 2 Cold Trap	1.37 g of water was collected in the cold trap.
22-Apr-2024	BATS 2 Brine Sampling	Brine sampling of the heated SM borehole. 0 mL of brine was collected.
22-Apr-2024	BATS 2 Cold Trap	1.56 g of water was collected in the cold trap.
29-Apr-2024	BATS 2 Cold Trap	1.56 g of water was collected in the cold trap.
29-Apr-2024	BATS 2 Brine Sampling	Brine sampling of the heated SM borehole. 0 mL of brine was collected.
29-Apr-2024	BATS 2 Cold Trap	1.63 g of water was collected in the cold trap.

Date	Activity Category	Description
29-Apr-2024	BATS 2 Battery Backup	Data review shows that the unheated array gas datalogger (sn7071) 12Vdc/100 Ah AGM battery was not being charged. There could be an issue with the fuses or NOCO Genius GEN5X2 smart charger. The LED lights on the smart charger have been showing green since installation and that indicates the battery is 100% Charged.
1-May-2024	BATS 2 Battery Backup	Data logger sn7071 shows the battery voltage at 12.7VDC this morning for the unheated array gas. Battery does not appear to be fully charged even though the NOCO charger indicator lights indicate full charge. NOCO charger power cycled and appeared to start charging. 7071 data downloaded for examination in the office.
1-May-2024	BATS 2 Battery Backup	1.41 g of water was collected in the cold trap.
1-May-2024	BATS 2 Heater Test	HP borehole power controller setpoint was changed from 140 to 25 °C to terminate heating. The control thermocouple started dropping slowly indicating that the heating cycle was ending.
1-May-2024	BATS 2 Battery Backup	Examination of the downloaded data from sn7071 shows that the NOCO Genius GEN5X2 smart charger was providing charge to the battery but then appears to have stopped charging the battery late yesterday or early this morning around midnight. We should plan on replacing the charger as soon as possible as it appears to be defective.
6-May-2024	BATS 2 Cold Trap	1.06 g of water was collected in the cold trap.
8-May-2024	BATS 2 Cold Trap	0.78 g of water was collected in the cold trap.
15-May-2024	BATS 2 Brine Sampling	Brine sampling of the heated SM borehole. 0 mL of brine was collected.
15-May-2024	BATS 2 Cold Trap	1.07 g of water was collected in the cold trap.
20-May-2024	BATS 2 Brine Sampling	Brine sampling of the heated SM borehole. 0 mL of brine was collected.
20-May-2024	BATS 2 Cold Trap	1.05 g of water was collected in the cold trap.
23-May-2024	BATS 2 Power Outage	Instrumentation status suggests that there was an unexpected power outage.
23-May-2024	BATS 2 Cold Trap	1.34 g of water was collected in the cold trap.
30-May-2024	BATS 2 Brine Sampling	Brine sampling of the heated SM borehole. 0 mL of brine was collected.
30-May-2024	BATS 2 Cold Trap	1.19 g of water was collected in the cold trap.
30-May-2024	BATS 2 Permeability	Pressurized HD borehole with Argon to 20psi. Mass flow controller (MFC) was set to 1 L/min and valves were opened. MFC and data logger were observed as borehole was pressurized.
3-Jun-2024	BATS 2 Brine Sampling	Brine sampling of the heated SM borehole. 0 mL of brine was collected.
3-Jun-2024	BATS 2 Permeability	The heated D borehole pressure was 20.8 psi. The flow controller was reading ~0 L/min.
3-Jun-2024	BATS 2 Heater Test	The heated HP borehole power controller setpoint was changed from 25 °C to 140 °C.
5-Jun-2024	BATS 2 Cold Trap	1.62 g of water was collected in the cold trap.
10-Jun-2024	BATS 2 Brine Sampling	Brine sampling of the heated SM borehole. 8 mL of brine was collected, and it was lt. brown in color.
12-Jun-2024	BATS 2 Brine Sampling	Brine sampling of the heated SM borehole. <1 mL of brine was collected, and it was lt. brown in color.
12-Jun-2024	BATS 2 Battery Backup	The new charge controller for the unheated array gas datalogger was installed and the datalogger was connected to the AGM battery for power.
12-Jun-2024	BATS 2 Cold Trap	2.32 g of water was collected in the cold trap.

Date	Activity Category	Description
18-Jun-2024	BATS 2 Cold Trap	2.73 g of water was collected in the cold trap.
18-Jun-2024	BATS 2 Brine Sampling	Borehole video logging of the heated SM borehole showed standing brine in the back of the borehole and video also showed that the sampling tubing was in the back of the borehole in contact with the brine.
24-Jun-2024	BATS 2 Brine Sampling	Brine sampling of the heated SM borehole. ~2 to 3 drops of brine was collected. There was not enough brine for a sample.
27-Jun-2024	BATS 2 Brine Sampling	Brine sampling of the heated SM borehole. 1 mL of brine was collected. The brine was clear to colorless. Note - the camera was in the borehole during sample collection.
27-Jun-2024	BATS 2 Cold Trap	1.82 g of water was collected in the cold trap.
1-Jul-2024	BATS 2 Battery Backup	The fuse in the NOCO charger to the AGM battery was removed and then re-inserted into the fuse holder. The charging cycle for the NOCO charger started.
1-Jul-2024	BATS 2 Brine Sampling	Brine sampling of the heated SM borehole. 3 mL of brine was collected. The brine was light brown in color.
1-Jul-2024	BATS 2 Cold Trap	1.70 g of water was collected in the cold trap.
3-Jul-2024	BATS 2 Cold Trap	1.61 g of water was collected in the cold trap.
8-Jul-2024	BATS 2 Brine Sampling	Brine sampling of the heated SM borehole. 0 mL of brine was collected -no sample.
8-Jul-2024	BATS 2 Cold Trap	1.21 g of water was collected in the cold trap. The temperature of the cold trap was -37.0 °C since there was no more dry ice.
10-Jul-2024	BATS 2 Cold Trap	1.08 g of water was collected in the cold trap.
15-Jul-2024	BATS 2 Brine Sampling	Brine sampling of the heated SM borehole. 0 mL of brine was collected -no sample.
15-Jul-2024	BATS 2 Cold Trap	0.72 g of water was collected in the cold trap.

Table A-2. BATS 2 brine production and sample collection log.

Date	ID	Volume Collected, mL	Notes
11/01/21	AE1	5	Vacuum pump: 2 sample bottles used for collection.
11/01/21	E4	3	Vacuum pump: 2 sample bottles used for collection. More brine in the borehole that the tubing and pump could not collect.
02/02/22	AE1	3	Brine squeezed from sponge directly into sample vials.
02/02/22	AE2	1.5	No sample retrieved from sponge due to insufficient brine volume. Sponge saved in plastic bag.
02/02/22	AE3	8	Brine squeezed from sponge directly into sample vials.
02/02/22	E2	20	Brine squeezed from sponge directly into sample vials.
02/02/22	E3	12	Brine squeezed from sponge directly into sample vials.
02/02/22	E4	1.5	Brine squeezed from sponge directly into sample vials.
02/02/22	F1	12	Brine squeezed from sponge directly into sample vials.
02/02/22	T1	8	Brine squeezed from sponge directly into sample vials.
02/02/22	T1	8	Brine squeezed from sponge directly into sample vials.
02/24/22	AE4	10	Brine squeezed from sponge directly into sample vials. Liquid is brown - most likely due to salt drill cuttings.
02/24/22	D	10	Brine squeezed from sponge directly into sample vials. Liquid is brown - most likely due to salt drill cuttings.
02/24/22	E1	1	Sample volume is too small for getting brine into sample vial. Sponge with brine was saved and bagged.
02/24/22	E2	10	Brine squeezed from sponge directly into sample vials. Liquid is cloudy - most likely due to salt drill cuttings.
02/24/22	E3	12	Brine squeezed from sponge directly into sample vials. Liquid is cloudy - most likely due to salt drill cuttings.
02/24/22	F2	8	Brine squeezed from sponge directly into sample vials. Liquid is brown - most likely due to salt drill cuttings.
02/24/22	SM	10	Brine squeezed from sponge directly into sample vials. Liquid is brown in color - most likely due to salt cuttings in the borehole from drilling.
02/24/22	T2	2	Sample volume is too small for getting brine into sample vial. Sponge with brine was saved and bagged.
03/22/22	AE1	1	Not enough sample for transfer to vial.
03/22/22	AE2	5	Brine squeezed from sponge directly into sample vials. Cloudy in color.
03/22/22	AE3	8	Brine squeezed from sponge directly into sample vials. Brown in color.
03/22/22	AE4	8	Brine squeezed from sponge directly into sample vials. Brown in color.
03/22/22	D	10	Brine squeezed from sponge directly into sample vials. Brown in color.
03/22/22	F1	8	Brine squeezed from sponge directly into sample vials. Light brown in color.
03/22/22	F2	8	Brine squeezed from sponge directly into sample vials. Brown in color.
03/22/22	HP	2	Brine squeezed from sponge directly into sample vials. Brown in color. Only 1 or 2 drops transferred to vial.

Date	ID	Volume Collected, mL	Notes
03/22/22	SL	3	Brine squeezed from sponge directly into sample vials. Brown in color.
03/22/22	SM	5	Brine squeezed from sponge directly into sample vials. Brown in color.
05/03/22	SM	68	Brine sampled behind mechanical packer (installed 4/13/22), collected with vacuum pump.
05/31/22	SM	35	Light brown brine sample collected with vacuum pump.
06/13/22	SM	12	Brine sample collected with vacuum pump.
07/11/22	SM	34	Light brown brine sample collected with vacuum pump.
07/25/22	SM	39	Light brown to clear brine sample collected with vacuum pump.
08/08/22	SM	20	Brine sample collected with vacuum pump.
08/17/22	SM	2.5	Light brown brine sample collected with vacuum pump.
9/6/2022	SM	9	Clear to cloudy sample collected with vacuum pump
9/19/2022	SM	18	Light brown sample collected with vacuum pump
10/12/2022	SM	19	Light brown sample collected with vacuum pump
10/24/2022	SM	0	Vacuum pump, no sample collected
11/7/2022	SM	14	Sample collected with vacuum pump
11/14/2022	SM	0	Vacuum pump, no sample collected
11/22/2022	SM	0	Vacuum pump, no sample collected
12/19/2022	SM	34	Sample collected with vacuum pump
1/10/2023	SM	6	Light brown sample collected with vacuum pump
1/30/2023	SM	4	Clear to colorless sample collected with vacuum pump
2/21/2023	SM	0	Vacuum pump, no sample collected
3/13/2023	SM	18	Light brown sample collected with vacuum pump
3/20/2023	SM	7	Clear to colorless sample collected with vacuum pump
3/28/2023	SM	3	Clear to colorless sample collected with vacuum pump
4/3/2023	SM	0	Vacuum pump, no sample collected
4/10/2023	SM	0	Vacuum pump, no sample collected
4/17/2023	SM	0	Vacuum pump, no sample collected
4/24/2023	SM	0	Vacuum pump, no sample collected
5/1/2023	SM	0	Vacuum pump, no sample collected
6/21/2023	SM	7	Light brown sample collected with vacuum pump
7/25/2023	SM	17	Vacuum pump
8/7/2023	SM	0	Vacuum pump, no sample collected

Date	ID	Volume Collected, mL	Notes
8/21/2023	SM	5	Light brown sample collected with vacuum pump
9/5/2023	SM	8	Light brown sample collected with vacuum pump
9/5/2023	SM	0	Vacuum pump, no sample collected
9/11/2023	SM	0	Vacuum pump, no sample collected
9/18/2023	SM	7	Light brown sample collected with vacuum pump
9/25/2023	SM	9	Clear sample collected with vacuum pump
10/2/2023	SM	4	Clear sample collected with vacuum pump
10/10/2023	SM	3	Clear sample collected with vacuum pump
10/16/2023	SM	8	Clear sample collected with vacuum pump
10/23/2023	SM	0.1	Vacuum pump, no sample collected
10/30/2023	SM	0	Vacuum pump, no sample collected
11/6/2023	SM	0	Vacuum pump, no sample collected
11/20/2023	SM	0	Vacuum pump, no sample collected
12/13/2023	SM	0	Vacuum pump, no sample collected
12/18/2023	SM	0	Vacuum pump, no sample collected
1/2/2024	SM	0	Vacuum pump, no sample collected
1/8/2024	SM	0	Vacuum pump, no sample collected
1/17/2024	SM	0	Vacuum pump, no sample collected
1/22/2024	SM	0	Vacuum pump, no sample collected
1/29/2024	SM	0	Vacuum pump, no sample collected
2/5/2024	SM	0	Vacuum pump, no sample collected
2/12/2024	SM	0	Vacuum pump, no sample collected
2/14/2024	SM	0	Vacuum pump, no sample collected
2/20/2024	SM	0	Vacuum pump, no sample collected
2/29/2024	SM	0	Vacuum pump, no sample collected
3/4/2024	SM	0	Vacuum pump, no sample collected
3/11/2024	SM	0	Vacuum pump, no sample collected
3/18/2024	SM	0	Vacuum pump, no sample collected
3/25/2024	SM	0	Vacuum pump, no sample collected
4/3/2024	SM	0	Vacuum pump, no sample collected

Date	ID	Volume Collected, mL	Notes
4/8/2024	SM	0	Vacuum pump, no sample collected
4/22/2024	SM	0	Vacuum pump, no sample collected
4/29/2024	SM	0	Vacuum pump, no sample collected
5/15/2024	SM	0	Vacuum pump, no sample collected
5/20/2024	SM	0	Vacuum pump, no sample collected
5/30/2024	SM	0	Vacuum pump, no sample collected
6/3/2024	SM	0	Vacuum pump, no sample collected
6/10/2024	SM	8	Light brown sample collected with vacuum pump
6/12/2024	SM	0.5	Light brown sample collected with vacuum pump
6/24/2024	SM	0.1	Vacuum pump, no sample collected
6/27/2024	SM	1	Clear sample collected with vacuum pump while camera was in borehole
7/1/2024	SM	3	Light brown sample collected with vacuum pump
7/8/2024	SM	0	Vacuum pump, no sample collected
7/15/2024	SM	0	Vacuum pump, no sample collected

Table A-3. BATS 2 brine ionic species composition data for heated SM borehole, values in g/L. Dashed line indicated end of data reported in Kuhlman et al. (2023). No reliable lithium data from recent samples.

	B	Ca	K	Li	Mg	Na	Cl	Br	SO_4
2/24/22	1.339	0.245	16.16	0.025	24.48	74.92	209.4	4.217	35.85
3/22/22	1.255	0.292	17.26	0.028	26.12	71.00	194.6	4.127	36.85
5/31/22	1.361	0.238	16.18	0.027	24.20	71.94	195.5	4.117	34.00
6/13/22	1.337	0.226	15.93	0.026	23.88	71.96	199.6	4.143	34.76
7/11/22	1.383	0.244	16.28	0.027	24.03	73.58	197.0	4.202	34.68
7/25/22	1.332	0.215	15.85	0.024	24.06	77.74	194.8	4.356	27.03
8/8/22	1.236	0.231	15.05	0.024	22.66	75.52	184.6	4.251	24.39
8/17/22	1.329	0.262	16.01	0.026	24.34	74.78	192.2	4.347	27.44
9/6/22	1.287	0.257	15.56	0.026	23.77	77.97	189.3	4.244	24.27
9/19/22	1.238	0.225	15.67	0.027	23.29	78.80	190.7	4.254	26.17
10/12/22	1.216	0.246	15.19	0.026	22.95	75.44	188.2	4.282	26.53
11/7/22	1.187	0.243	14.88	0.024	22.55	76.97	187.1	4.228	25.41
12/19/22	1.122	0.249	13.97	0.022	21.65	82.11	187.1	4.124	24.49
1/10/23	1.189	0.255	14.51	0.025	23.99	78.03	192.9	4.308	26.83
1/30/23	1.225	0.240	14.57	0.024	23.51	77.69	190.8	4.291	26.70
3/13/23	1.215	0.263	14.52	0.024	22.44	79.47	189.6	4.240	25.41
3/20/23	1.211	0.271	14.50	0.022	21.92	81.36	188.0	4.164	26.98
3/28/23	1.239	0.306	14.24	0.023	21.91	78.87	185.6	4.185	25.03
6/21/23	1.094	0.375	13.70	0.022	19.27	83.49	186.0	3.747	17.21
7/25/23	1.267	0.494	17.36	-	23.141	108.78	220.0	4.661	19.11
8/21/23	1.096	0.382	15.73	-	21.520	84.88	234.5	4.837	23.43
9/5/23	1.052	0.354	15.02	-	21.000	83.01	216.9	4.746	21.74
9/18/23	1.270	0.408	22.25	-	30.508	117.13	230.8	4.859	23.60
9/25/23	1.229	0.351	22.27	-	30.544	93.66	245.6	5.150	26.64
10/2/23	1.366	0.387	23.72	-	32.534	86.84	227.9	4.902	23.79
10/10/23	1.276	0.363	21.24	-	28.816	100.11	228.0	4.898	23.71
10/16/23	1.289	0.351	22.97	-	31.659	110.53	242.6	5.025	24.40
11/13/23	1.422	0.381	24.35	-	33.461	111.93	223.0	4.933	23.07

Table A-4. Desiccant water production data for heated array. Dashed line marks end of data reported in Kuhlman et al. (2023).

Date Time Start	Date Time End	ΔTime [day]	ΔH_2O mass [g]	Rate of change H_2O mass [g/day]	Upstream gas mass flow rate [std mL/min]
4/26/22 12:46	4/27/22 10:00	0.8847	13.03	14.7278	500
4/27/22 10:10	4/29/22 00:15	1.5868	25.08	15.8053	500
5/2/22 08:40	5/3/22 12:04	1.1417	16.8	14.7153	500
5/3/22 12:04	5/4/22 07:53	0.8257	4.91	5.9465	200
5/4/22 07:53	5/5/22 07:43	0.9931	6	6.042	200
5/5/22 07:48	5/9/22 08:10	4.0153	22.91	5.7057	200
5/10/22 07:55	5/11/22 09:15	1.0556	5.07	4.8032	200
5/11/22 09:15	5/16/22 08:30	4.9688	12.6	2.5358	200
5/16/22 08:30	5/18/22 09:51	2.0563	2.23	1.0845	75
5/18/22 09:51	5/23/22 08:14	4.9326	5.96	1.2083	75
5/23/22 08:14	5/24/22 13:51	1.234	1.47	1.1912	75
5/24/22 13:51	5/25/22 07:45	0.7458	0.8	1.0726	75
5/25/22 07:45	5/31/22 08:03	6.0125	6.11	1.0162	75
5/31/22 08:03	6/2/22 09:06	2.0437	2.53	1.2379	75
6/2/22 09:06	6/6/22 07:54	3.95	3.38	0.8557	75
6/6/22 07:54	6/9/22 08:33	3.0271	2.97	0.9811	75
6/9/22 08:33	6/13/22 08:00	3.9771	3.4	0.8549	75
6/13/22 08:00	6/15/22 07:55	1.9965	1.73	0.8665	75
6/15/22 07:55	6/22/22 08:11	7.0111	5.98	0.8529	75
6/22/22 08:11	6/27/22 08:00	4.9924	3.99	0.7992	75
7/5/22 09:45	7/7/22 08:24	1.9437	3.66	1.883	75
7/7/22 08:24	7/11/22 07:55	3.9799	5.75	1.4448	75
7/11/22 07:55	7/18/22 08:14	7.0132	7.72	1.1008	75
7/18/22 08:14	7/20/22 07:56	1.9875	1.64	0.8252	75
7/20/22 07:56	7/25/22 08:02	5.0042	6.21	1.241	75
7/25/22 08:02	7/26/22 11:32	1.1458	1.37	1.1956	75
7/26/22 11:32	8/1/22 07:54	5.8486	7.06	1.2071	75
8/1/22 07:54	8/4/22 10:34	3.1111	3.02	0.9707	75
8/4/22 10:34	8/8/22 07:56	3.8903	3.32	0.85	75
8/8/22 07:56	8/10/22 07:47	1.9938	1.84	0.92	75
8/10/22 07:55	8/15/22 07:45	4.9931	6.34	1.27	75
8/15/22 07:45	8/16/22 10:42	1.1229	1.74	1.55	75
8/16/22 10:42	8/17/22 07:34	0.8694	1.34	1.5412	75
8/17/22 07:34	8/22/22 07:45	5.0076	8.1	1.6175	75
8/22/22 07:45	8/24/22 07:25	1.9861	2.87	1.445	75
8/24/22 07:25	8/29/22 07:39	5.0097	7.08	1.4133	75

Date Time Start	Date Time End	ΔTime [day]	ΔH_2O mass [g]	Rate of change H_2O mass [g/day]	Upstream gas mass flow rate [std mL/min]
8/29/22 07:39	9/6/22 08:45	8.0458	10.83	1.346	75
9/6/22 08:45	9/7/22 14:55	1.2569	1.79	1.4241	75
9/7/22 14:55	9/12/22 08:57	4.7514	9.52	2.0036	75
9/12/22 08:57	9/19/22 08:30	6.9812	13.18	1.8879	75
9/19/22 08:30	9/22/22 09:36	3.0458	5.1	1.6744	75
9/22/22 09:36	9/26/22 07:38	3.9181	5.79	1.4778	75
9/26/22 07:38	9/28/22 08:20	2.0292	2.86	1.4094	75
9/28/22 08:20	10/3/22 07:48	4.9778	7.84	1.575	75
10/3/22 07:48	10/5/22 08:08	2.0139	3.75	1.8621	75
10/5/22 08:08	10/12/22 09:54	7.0736	14.47	2.0456	75
10/12/22 09:54	10/17/22 07:31	4.9007	14.86	3.0322	75
10/17/22 07:31	10/19/22 07:55	2.0167	6.29	3.119	75
10/19/22 07:55	10/24/22 07:33	4.9847	16.22	3.2539	75
10/24/22 07:33	11/1/22 08:40	8.0465	26.04	3.2362	75
11/1/22 08:40	11/2/22 11:46	1.1292	4.01	3.5513	75
11/2/22 11:46	11/3/22 07:54	0.8389	2.64	3.1470	75
11/3/22 07:54	11/7/22 07:50	3.9972	10.45	2.6143	75
11/7/22 07:50	11/9/22 08:44	2.0375	4.64	2.2773	75
11/9/22 08:44	11/14/22 10:00	5.0528	10.71	2.1196	75
11/14/22 10:00	11/16/22 07:37	1.9007	3.87	2.0361	75
11/16/22 07:37	11/21/22 08:10	5.0229	13.15	2.6180	75
11/21/22 08:10	11/22/22 07:47	0.9840	2.16	2.1951	75
11/22/22 07:47	11/28/22 10:00	6.0924	0.34	0.0558	0
11/28/22 10:00	11/30/22 08:07	1.9215	0.03	0.0156	0
11/30/22 08:07	12/5/22 08:46	5.0271	14.44	2.8724	100
12/5/22 08:46	12/7/22 08:59	2.0090	6.1	3.0363	100
12/7/22 08:59	12/11/22 20:20	4.4729	13.03	2.9131	100
12/12/22 10:10	12/13/22 08:40	0.9375	2.63	2.8053	100
12/13/22 08:40	12/14/22 08:55	1.0104	2.64	2.6128	100
12/14/22 08:55	12/15/22 11:13	1.0958	3.06	2.7924	100
12/15/22 11:13	12/16/22 08:18	0.8785	2.47	2.8117	100
12/16/22 08:18	12/19/22 07:25	2.9632	8.4	2.8348	100
12/19/22 07:25	12/21/22 08:10	2.0313	5.63	2.7717	100
12/21/22 08:10	1/4/23 08:55	14.0313	39.43	2.8102	100
1/6/23 09:05	1/10/23 08:30	3.9757	10.86	2.7316	100
1/10/23 08:30	1/17/23 07:54	6.9750	19.35	2.7742	100
1/17/23 07:54	1/18/23 09:00	1.0458	2.89	2.7633	100
1/18/23 09:00	1/23/23 08:50	4.9931	13.87	2.7779	100

Date Time Start	Date Time End	ΔTime [day]	ΔH2O mass [g]	Rate of change H2O mass [g/day]	Upstream gas mass flow rate [std mL/min]
1/23/23 08:50	1/30/23 09:40	7.0347	19.43	2.7620	100
1/30/23 09:40	2/6/23 08:15	6.9410	19.59	2.8224	100
2/6/23 08:15	2/8/23 08:29	2.0097	5.75	2.8611	100
2/8/23 08:29	2/9/23 07:53	0.9750	2.71	2.7795	100
2/9/23 07:53	2/13/23 07:40	3.9910	10.71	2.6836	100
2/13/23 07:40	2/15/23 07:45	2.0035	5.6	2.7951	100
2/15/23 07:45	2/21/23 08:05	6.0139	17.04	2.8334	100
2/21/23 08:05	2/22/23 08:40	1.0243	3.03	2.9581	100
2/22/23 08:40	2/27/23 08:04	4.9750	14.01	2.8161	100
2/27/23 08:04	3/6/23 07:35	6.9799	19.55	2.8009	100
3/6/23 07:35	3/8/23 07:37	2.0014	5.67	2.8330	100
3/8/23 07:37	3/13/23 07:44	5.0049	19.22	3.8403	100
3/13/23 07:44	3/15/23 08:33	2.0340	7.57	3.7217	100
3/15/23 08:48	3/20/23 07:47	4.9576	18.78	3.7881	100
3/20/23 07:47	3/22/23 07:50	2.0021	8.02	4.0058	100
3/22/23 07:50	3/23/23 12:00	1.1736	9.13	7.7794	200
3/23/23 12:00	3/28/23 08:35	4.8576	57.05	11.7444	300
3/28/23 08:35	3/29/23 09:19	1.0306	16.94	16.4377	400
3/29/23 09:19	4/3/23 08:45	4.9764	45.41	9.1251	400
4/3/23 08:45	4/4/23 08:35	0.9931	2.51	2.5276	150
4/4/23 08:35	4/5/23 07:37	0.9597	3	3.1259	150
4/5/23 07:37	4/10/23 08:27	5.0347	12.56	2.4947	100
4/10/23 08:27	4/12/23 07:38	1.9660	4.98	2.5331	100
4/12/23 07:38	4/17/23 07:55	5.0118	12.55	2.5041	100
4/17/23 07:55	4/19/23 08:40	2.0313	5.26	2.5895	100
4/19/23 08:40	4/24/23 08:05	4.9757	13.08	2.6288	100
4/24/23 08:05	4/26/23 07:55	1.9931	5.43	2.7245	100
4/26/23 07:55	5/1/23 09:18	5.0576	13.9	2.7483	100
5/1/23 09:18	5/8/23 08:45	6.9771	18.81	2.6960	100
5/8/23 08:45	5/10/23 08:03	1.9708	5.25	2.6638	100
5/10/23 08:03	5/13/23 03:37	2.8153	7.87	2.7955	100
5/16/23 12:48	5/17/23 08:50	0.8347	2.28	2.7314	100
5/17/23 08:50	5/22/23 08:21	4.9799	13.74	2.7591	100
5/22/23 08:21	5/31/23 07:57	8.9833	1.57	0.1748	100
5/31/23 07:57	6/5/23 08:30	5.0229	14.63	2.9127	100
6/5/23 08:30	6/6/23 09:00	1.0208	3.13	3.0661	100
6/6/23 09:00	6/7/23 10:27	1.0604	3.69	3.4798	100
6/7/23 10:27	6/12/23 07:59	4.8972	14.29	2.9180	100

Date Time Start	Date Time End	ΔTime [day]	ΔH2O mass [g]	Rate of change H2O mass [g/day]	Upstream gas mass flow rate [std mL/min]
6/12/23 08:07	6/14/23 08:24	2.0118	6.1	3.0321	100
6/14/23 08:24	6/19/23 07:44	4.9722	14.42	2.9001	100
6/19/23 07:44	6/21/23 08:00	2.0111	0.5	0.2486	0
6/21/23 08:00	6/26/23 08:03	5.0021	7.53	1.5054	100
6/26/23 08:13	6/27/23 07:40	0.9771	2.77	2.8350	100
6/27/23 07:40	6/29/23 08:35	2.0382	6.06	2.9732	100
6/29/23 08:35	7/3/23 07:43	3.9639	12.79	3.2266	100
7/3/23 07:43	7/5/23 09:09	2.0597	6.37	3.0927	100
7/5/23 09:09	7/10/23 08:37	4.9778	15.98	3.2103	100
7/10/23 08:37	7/12/23 07:58	1.9729	6.35	3.2186	100
7/12/23 07:58	7/24/23 07:25	11.9771	37.77	3.1535	100
7/24/23 07:25	7/25/23 07:45	1.0139	2.49	2.4559	100
7/25/23 07:45	7/31/23 08:07	6.0153	18.33	3.0472	100
7/31/23 08:07	8/2/23 07:26	1.9715	5.66	2.8709	100
8/2/23 07:26	8/7/23 07:40	5.0097	14.86	2.9662	100
8/7/23 07:40	8/9/23 07:56	2.0111	5.85	2.9088	100
8/9/23 07:56	8/16/23 07:39	6.9882	19.73	2.8233	100
8/16/23 07:39	8/21/23 08:15	5.0250	13.72	2.7303	100
8/21/23 08:15	8/23/23 09:15	2.0417	5.44	2.6645	100
8/23/23 09:15	8/28/23 08:41	4.9764	13.06	2.6244	100
8/28/23 08:41	8/30/23 09:23	2.0292	5.17	2.5478	100
8/30/23 09:23	9/5/23 08:12	5.9507	6.39	1.0738	100
9/5/23 08:12	9/6/23 08:18	1.0042	1.99	1.9817	100
9/6/23 08:18	9/11/23 08:25	5.0049	4.17	0.8332	100
9/11/23 08:25	9/13/23 08:06	1.9868	1.39	0.6996	100
9/13/23 08:06	9/14/23 13:32	1.2264	0.3	0.2446	100
9/14/23 13:32	9/18/23 08:15	3.7799	0.3	0.0794	50
9/18/23 08:15	9/19/23 08:07	0.9944	0.17	0.1709	50
9/19/23 08:07	9/21/23 09:40	2.0646	0.28	0.1356	50
9/21/23 09:40	9/25/23 08:31	3.9521	3.15	0.7970	50
9/25/23 08:31	9/27/23 07:48	1.9701	1.6	0.8121	50
9/27/23 07:48	10/2/23 08:02	5.0097	4.17	0.8324	50
10/2/23 08:02	10/4/23 08:27	2.0174	1.55	0.7683	50
10/4/23 08:27	10/10/23 09:07	6.0278	4.58	0.7598	50
10/10/23 09:07	10/12/23 10:04	2.0396	1.64	0.8041	50
10/12/23 10:04	10/16/23 08:45	3.9451	2.88	0.7300	50
10/16/23 08:45	10/17/23 08:46	1.0007	0.82	0.8194	50
10/17/23 08:46	10/23/23 08:18	5.9806	4.73	0.7909	50

Date Time Start	Date Time End	ΔTime [day]	ΔH2O mass [g]	Rate of change H2O mass [g/day]	Upstream gas mass flow rate [std mL/min]
10/23/23 08:18	10/30/23 08:00	6.9875	5.62	0.8043	50
10/30/23 08:00	11/1/23 09:47	2.0743	1.57	0.7569	50
11/1/23 09:47	11/6/23 09:54	5.0049	3.89	0.7772	50
11/6/23 09:54	11/8/23 10:54	2.0417	1.72	0.8424	50
11/8/23 10:54	11/13/23 09:08	4.9264	4.04	0.8201	50
11/13/23 09:08	11/16/23 08:47	2.9854	2.52	0.8441	50
11/16/23 08:47	11/20/23 08:10	3.9743	1.68	0.4227	0
11/20/23 08:10	11/27/23 07:50	6.9861	10.91	1.5617	400
11/27/23 07:50	11/29/23 08:41	2.0354	2.34	1.1496	400
11/29/23 09:41	12/4/23 09:54	5.0090	3.02	0.6029	400
12/4/23 09:54	12/6/23 09:38	1.9889	0.54	0.2715	400
12/6/23 11:51	12/11/23 08:00	4.8396	1.01	0.2087	400
12/11/23 10:06	12/13/23 08:00	1.9125	0.84	0.4392	50
12/13/23 10:15	12/18/23 08:04	4.9090	2.15	0.4380	50
12/18/23 10:26	12/20/23 07:36	1.8819	1.15	0.6111	50
12/20/23 08:53	1/2/24 10:32	13.0687	9.1	0.6963	50
1/2/24 11:43	1/3/24 07:24	0.8201	0.64	0.7804	50
1/3/24 08:48	1/8/24 07:38	4.9514	3.11	0.6281	50
1/8/24 08:51	1/10/24 07:34	1.9465	1.53	0.7860	50
1/10/24 08:50	1/17/24 07:37	2.5600	1.44	0.5625	50
1/17/24 08:47	1/22/24 09:08	5.0146	3.78	0.7538	50
1/22/24 10:17	1/24/24 11:18	2.0424	1.49	0.7295	50
1/24/24 12:22	1/29/24 08:15	4.8285	3.46	0.7166	50
1/29/24 09:28	1/31/24 07:44	1.9278	1.6	0.8300	50
1/31/24 08:56	2/5/24 10:25	5.0618	4.13	0.8159	50
2/5/24 11:32	2/7/24 08:02	1.8542	1.54	0.8306	50
2/7/24 09:13	2/12/24 07:42	4.9368	3.91	0.7920	50
2/12/24 08:53	2/14/24 07:41	1.9500	1.52	0.7795	50
2/14/24 07:41	2/20/24 07:43	6.0014	4.8	0.7998	50
2/20/24 08:47	2/29/24 07:45	8.9569	7.09	0.7916	50
2/29/24 09:00	3/4/24 07:11	3.9243	2.9	0.7390	50
3/4/24 08:22	3/11/24 08:00	6.9847	5.27	0.7545	50
3/11/24 09:15	3/13/24 08:27	1.9667	1.43	0.7271	50
3/13/24 09:56	3/18/24 07:52	4.9139	3.95	0.8038	50
3/18/24 09:01	3/20/24 08:38	1.9840	1.59	0.8014	50
3/20/24 09:53	3/25/24 07:18	4.8924	3.9	0.7972	50
3/25/24 08:27	3/27/24 07:23	1.9556	1.58	0.8080	50
3/27/24 08:27	3/28/24 09:01	1.0236	0.97	0.9476	100

Date Time Start	Date Time End	ΔTime [day]	ΔH_2O mass [g]	Rate of change H_2O mass [g/day]	Upstream gas mass flow rate [std mL/min]
3/28/24 09:01	4/1/24 13:06	4.1701	5.03	1.2062	100
4/1/24 13:06	4/3/24 07:57	1.7854	2.2	1.2322	100
4/3/24 07:57	4/4/24 08:20	1.0160	0.94	0.9252	100
4/4/24 09:27	4/8/24 10:18	4.0354	5.38	1.3332	100
4/8/24 11:33	4/15/24 08:22	6.8674	10.14	1.4765	100
4/15/24 09:29	4/17/24 07:59	1.9375	2.36	1.2181	100
4/17/24 09:17	4/22/24 07:28	4.9243	6.41	1.3017	100
4/22/24 08:40	4/24/24 07:33	1.9535	2.56	1.3105	100
4/24/24 09:06	4/29/24 08:21	4.9688	5.09	1.0244	100
4/29/24 09:21	5/1/24 08:42	1.9729	2.29	1.1607	100
5/1/24 09:45	5/6/24 07:52	4.9215	3.61	0.7335	100
5/6/24 08:52	5/8/24 07:15	1.9326	1.06	0.5485	100
5/8/24 08:15	5/13/24 10:00	5.0729	3.23	0.6367	100
5/13/24 10:00	5/15/24 07:33	1.8979	1.36	0.7166	100
5/15/24 08:47	5/20/24 08:10	4.9743	3.39	0.6815	100
5/20/24 09:22	5/23/24 07:33	2.9243	1.98	0.6771	100
5/23/24 08:46	5/28/24 08:35	4.9924	3.47	0.6951	100
5/28/24 09:29	5/30/24 08:15	1.9486	1.46	0.7493	100
5/30/24 09:30	6/3/24 08:02	3.9389	3.35	0.8505	100
6/3/24 09:12	6/5/24 07:35	1.9326	1.84	0.9521	100
6/5/24 08:41	6/10/24 08:09	4.9778	6.86	1.3781	100
6/10/24 08:09	6/12/24 07:42	1.9812	1.66	0.8379	100
6/12/24 09:02	6/18/24 08:27	5.9757	8.52	1.4258	100
6/18/24 09:45	6/20/24 08:38	1.9535	2.94	1.5050	100
6/20/24 08:38	6/24/24 09:47	4.0479	5.42	1.3390	100
6/24/24 09:47	6/27/24 07:38	2.9104	4.54	1.5599	100
6/27/24 08:50	7/1/24 08:09	3.9715	6.16	1.5510	100
7/1/24 09:20	7/3/24 08:00	1.9444	2.43	1.2497	100
7/3/24 09:07	7/8/24 07:35	4.9361	5.03	1.0190	100
7/8/24 08:38	7/10/24 07:58	1.9722	1.71	0.8670	100
7/10/24 09:04	7/15/24 07:58	4.9542	3.28	0.6621	100
7/15/24 09:05	7/18/24 08:43	2.9847	2.24	0.7505	100
7/18/24 09:49	7/24/24 07:46	5.9146	3.09	0.5224	100
7/24/24 08:57	7/29/24 08:16	4.9715	2.18	0.4385	100
7/29/24 09:29	8/1/24 09:30	3.0007	0.74	0.2466	100
8/1/24 11:45	8/5/24 07:53	3.8389	0.65	0.1693	100

Table A-5. Desiccant water production data for unheated array. Dashed line marks end of data reported in Kuhlman et al. (2023).

Date Time Start	Date Time End	ΔTime [day]	ΔH2O mass [g]	Rate of change H2O mass [g/day]	Upstream gas mass flow rate [std mL/min]
4/26/22 12:46	4/27/22 10:00	0.8847	9.7	10.9639	500
4/27/22 10:10	5/2/22 08:30	4.9306	14.61	2.9632	500
5/2/22 08:30	5/3/22 12:04	1.1486	0.57	0.4963	50
5/3/22 12:04	5/4/22 07:53	0.8257	0.44	0.5329	50
5/4/22 07:53	5/5/22 07:43	0.9931	0.68	0.6848	50
5/5/22 07:43	5/9/22 08:10	4.0188	2.44	0.6072	50
5/10/22 07:55	5/11/22 09:22	1.0604	0.6	0.5658	50
5/11/22 09:22	5/16/22 08:30	4.9639	2.67	0.5379	50
5/16/22 08:36	5/18/22 09:52	2.0528	0.83	0.4043	50
5/18/22 09:52	5/23/22 08:15	4.9326	1.93	0.3913	50
5/23/22 08:15	5/24/22 13:51	1.2333	0.58	0.4703	50
5/24/22 13:51	5/25/22 07:48	0.7479	0.31	0.4145	50
5/25/22 07:48	5/31/22 08:04	6.0111	1.89	0.3144	25
5/31/22 08:04	6/2/22 09:08	2.0444	0.78	0.3815	25
6/2/22 09:08	6/6/22 08:00	3.9528	1.25	0.3162	25
6/6/22 08:00	6/9/22 08:33	3.0229	1.2	0.397	25
6/9/22 08:33	6/13/22 08:00	3.9771	1.36	0.342	25
6/13/22 08:00	6/15/22 07:55	1.9965	0.66	0.3306	25
6/15/22 07:55	6/22/22 08:30	7.0243	2.58	0.3673	25
6/22/22 08:30	6/27/22 08:00	4.9792	1.75	0.3515	25
7/5/22 09:45	7/7/22 08:30	1.9479	1.1	0.5647	25
7/7/22 08:30	7/11/22 07:55	3.9757	1.79	0.4502	25
7/11/22 07:55	7/18/22 08:18	7.016	2.74	0.3905	25
7/18/22 08:18	7/20/22 07:58	1.9861	0.81	0.4078	25
7/20/22 07:58	7/25/22 08:09	5.0076	2.21	0.4413	25
7/25/22 08:09	7/26/22 11:32	1.141	0.45	0.3944	25
7/26/22 11:32	8/1/22 07:55	5.8493	2.46	0.4206	25
8/1/22 07:55	8/4/22 10:34	3.1104	1.29	0.4147	25
8/4/22 10:34	8/8/22 08:15	3.9035	1.62	0.42	25
8/8/22 08:15	8/10/22 07:47	1.9806	0.9	0.45	25
8/10/22 07:47	8/15/22 07:45	4.9986	2.07	0.41	25
8/15/22 07:45	8/16/22 10:42	1.1229	0.49	0.44	25
8/16/22 10:42	8/17/22 07:34	0.8694	0.41	0.4716	25
8/17/22 07:34	8/22/22 07:40	5.0042	4.48	0.8953	25
8/22/22 07:40	8/24/22 07:28	1.9917	0.81	0.4067	25
8/24/22 07:28	8/29/22 07:28	5	2.02	0.404	25

Date Time Start	Date Time End	ΔTime [day]	ΔH_2O mass [g]	Rate of change H_2O mass [g/day]	Upstream gas mass flow rate [std mL/min]
8/29/22 07:28	9/6/22 08:45	8.0535	3.3	0.4098	25
9/6/22 08:45	9/7/22 14:55	1.2569	0.66	0.5251	25
9/7/22 14:55	9/12/22 08:40	4.7396	2.2	0.4642	25
9/12/22 08:40	9/19/22 08:30	6.9931	3.12	0.4462	25
9/19/22 08:30	9/22/22 09:27	3.0396	1.19	0.3915	25
9/22/22 09:27	9/26/22 07:30	3.9187	1.7	0.4338	25
9/26/22 07:30	9/28/22 08:20	2.0347	0.94	0.462	25
9/28/22 08:20	10/3/22 07:48	4.9778	1.99	0.3998	25
10/3/22 07:48	10/5/22 08:05	2.0118	0.39	0.1939	25
10/5/22 08:05	10/12/22 09:54	7.0757	3.6	0.5088	25
10/12/22 09:54	10/17/22 07:31	4.9007	1.99	0.4061	25
10/17/22 07:31	10/19/22 07:58	2.0187	0.68	0.3368	25
10/19/22 07:58	10/24/22 07:33	4.9826	2.48	0.4977	25
10/24/22 07:33	11/1/22 08:40	8.0465	3.75	0.4660	25
11/1/22 08:40	11/2/22 11:46	1.1292	0.57	0.5048	25
11/2/22 11:46	11/3/22 07:54	0.8389	0.09	0.1073	25
11/3/22 07:54	11/7/22 07:50	3.9972	1.95	0.4878	25
11/7/22 07:50	11/9/22 08:44	2.0375	0.95	0.4663	25
11/9/22 08:44	11/14/22 10:00	5.0528	2.04	0.4037	25
11/14/22 10:00	11/16/22 07:37	1.9007	0.59	0.3104	25
11/16/22 07:37	11/21/22 08:10	5.0229	2.16	0.4300	25
11/21/22 08:10	11/22/22 07:47	0.9840	0.36	0.3658	25
11/22/22 07:47	11/28/22 10:00	6.0924	2.55	0.4186	25
11/28/22 10:00	11/30/22 08:07	1.9215	0.74	0.3851	25
11/30/22 08:07	12/5/22 08:46	5.0271	2.2	0.4376	25
12/5/22 08:46	12/7/22 08:59	2.0090	0.97	0.4828	25
12/7/22 08:59	12/12/22 10:10	5.0493	2.29	0.4535	25
12/12/22 10:10	12/13/22 08:40	0.9375	0.41	0.4373	25
12/13/22 08:40	12/14/22 08:55	1.0104	0.27	0.2672	25
12/14/22 08:55	12/15/22 11:13	1.0958	0.35	0.3194	25
12/15/22 11:13	12/16/22 08:18	0.8785	0.35	0.3984	25
12/16/22 08:18	12/19/22 07:25	2.9632	1.18	0.3982	25
12/19/22 07:25	12/21/22 08:10	2.0313	0.69	0.3397	25
12/21/22 08:10	1/4/23 08:55	14.0313	6.26	0.4461	25
1/4/23 08:55	1/10/23 08:30	5.9826	2.37	0.3961	25
1/10/23 08:30	1/17/23 07:54	6.9750	2.83	0.4057	25
1/17/23 07:54	1/18/23 08:50	1.0389	0.55	0.5294	25
1/18/23 08:50	1/23/23 08:50	5.0000	2.15	0.4300	25

Date Time Start	Date Time End	ΔTime [day]	ΔH_2O mass [g]	Rate of change H_2O mass [g/day]	Upstream gas mass flow rate [std mL/min]
1/23/23 08:50	1/30/23 09:40	7.0347	2.93	0.4165	25
1/30/23 09:40	2/6/23 08:15	6.9410	3.43	0.4942	25
2/6/23 08:15	2/8/23 08:29	2.0097	0.96	0.4777	25
2/8/23 08:29	2/9/23 07:53	0.9750	0.32	0.3282	25
2/9/23 07:53	2/13/23 07:45	3.9944	1.79	0.4481	25
2/13/23 07:45	2/15/23 07:49	2.0028	0.87	0.4344	25
2/15/23 07:49	2/21/23 08:08	6.0132	3.16	0.5255	25
2/21/23 08:08	2/22/23 08:40	1.0222	0.52	0.5087	25
2/22/23 08:40	2/27/23 08:04	4.9750	2.35	0.4724	25
2/27/23 08:04	3/6/23 07:35	6.9799	3.34	0.4785	25
3/6/23 07:35	3/8/23 07:37	2.0014	0.91	0.4547	25
3/8/23 07:37	3/13/23 07:44	5.0049	2.71	0.5415	25
3/13/23 07:44	3/15/23 08:33	2.0340	1.03	0.5064	25
3/15/23 08:33	3/20/23 07:47	4.9681	2.45	0.4932	25
3/20/23 07:47	3/22/23 07:50	2.0021	1.31	0.6543	25
3/22/23 07:50	3/23/23 12:00	1.1736	1.01	0.8606	25
3/23/23 12:00	3/28/23 08:35	4.8576	7.64	1.5728	50
3/28/23 08:35	3/29/23 09:19	1.0306	2.03	1.9698	50
3/29/23 09:19	4/3/23 08:45	4.9764	6.6	1.3263	50
4/3/23 08:45	4/4/23 08:35	0.9931	0.86	0.8660	50
4/4/23 08:38	4/5/23 07:45	0.9632	0.63	0.6541	50
4/5/23 07:45	4/10/23 08:32	5.0326	2.6	0.5166	25
4/10/23 08:32	4/12/23 07:43	1.9660	0.85	0.4324	25
4/12/23 07:43	4/17/23 08:02	5.0132	2.32	0.4628	25
4/17/23 08:02	4/19/23 08:45	2.0299	0.99	0.4877	25
4/19/23 08:45	4/24/23 08:09	4.9750	2.27	0.4563	25
4/24/23 08:09	4/26/23 08:00	1.9938	0.95	0.4765	25
4/26/23 08:00	5/1/23 09:22	5.0569	2.52	0.4983	25
5/1/23 09:22	5/8/23 08:55	6.9813	3.17	0.4541	25
5/8/23 08:55	5/10/23 08:06	1.9660	0.88	0.4476	25
5/10/23 08:06	5/13/23 09:00	3.0375	1.53	0.5037	25
5/16/23 12:48	5/17/23 08:53	0.8368	0.3	0.3585	25
5/17/23 08:53	5/22/23 08:21	4.9778	1.58	0.3174	25
5/22/23 08:21	5/31/23 07:57	8.9833	6.03	0.6712	25
5/31/23 07:57	6/5/23 08:34	5.0257	2.62	0.5213	25
6/5/23 08:34	6/6/23 09:03	1.0201	0.6	0.5882	25
6/6/23 09:03	6/7/23 10:31	1.0611	0.61	0.5749	25
6/7/23 10:31	6/12/23 07:59	4.8944	2.31	0.4720	25

Date Time Start	Date Time End	ΔTime [day]	ΔH2O mass [g]	Rate of change H2O mass [g/day]	Upstream gas mass flow rate [std mL/min]
6/12/23 08:07	6/14/23 08:24	2.0118	1.08	0.5368	25
6/14/23 08:24	6/19/23 07:44	4.9722	2.39	0.4807	25
6/19/23 07:44	6/21/23 08:00	2.0111	0.06	0.0298	0
6/21/23 08:00	6/24/23 06:10	2.9236	1.59	0.5438	25
6/26/23 08:15	6/27/23 07:42	0.9771	0.4	0.4094	25
6/27/23 07:42	6/29/23 08:37	2.0382	1.04	0.5103	25
6/29/23 08:37	7/3/23 07:43	3.9625	2.57	0.6486	25
7/3/23 07:43	7/5/23 08:58	2.0521	1.12	0.5458	25
7/5/23 09:09	7/10/23 08:41	4.9806	3.01	0.6044	25
7/10/23 08:41	7/12/23 08:09	1.9778	1.13	0.5713	25
7/12/23 08:09	7/24/23 07:31	11.9736	6.44	0.5378	25
7/24/23 07:31	7/25/23 07:47	1.0111	0.46	0.4549	25
7/25/23 07:47	7/31/23 08:07	6.0139	3.1	0.5155	25
7/31/23 08:07	8/2/23 07:26	1.9715	1.02	0.5174	25
8/2/23 07:26	8/7/23 07:40	5.0097	2.56	0.5110	25
8/7/23 07:40	8/9/23 07:56	2.0111	0.84	0.4177	25
8/9/23 07:56	8/16/23 07:39	6.9882	3.23	0.4622	25
8/16/23 07:39	8/21/23 08:15	5.0250	2.13	0.4239	25
8/21/23 08:15	8/23/23 09:15	2.0417	1	0.4898	25
8/23/23 09:15	8/28/23 08:41	4.9764	2.27	0.4562	25
8/28/23 08:41	8/30/23 09:23	2.0292	0.99	0.4879	25
8/30/23 09:23	9/5/23 08:12	5.9507	2.44	0.4100	25
9/5/23 08:12	9/6/23 08:18	1.0042	0.63	0.6274	25
9/6/23 08:18	9/11/23 08:25	5.0049	2.07	0.4136	25
9/11/23 08:25	9/13/23 08:06	1.9868	0.89	0.4480	25
9/13/23 08:06	9/14/23 13:32	1.2264	0.53	0.4322	25
9/14/23 13:32	9/18/23 08:15	3.7799	1.67	0.4418	25
9/18/23 08:15	9/19/23 08:07	0.9944	0.36	0.3620	25
9/19/23 08:07	9/21/23 09:40	2.0646	0.78	0.3778	25
9/21/23 09:40	9/25/23 08:31	3.9521	1.64	0.4150	25
9/25/23 08:31	9/27/23 07:48	1.9701	0.86	0.4365	25
9/27/23 07:48	10/2/23 08:02	5.0097	2.02	0.4032	25
10/2/23 08:02	10/4/23 08:27	2.0174	1	0.4957	25
10/4/23 08:27	10/10/23 09:07	6.0278	2.21	0.3666	25
10/10/23 09:07	10/12/23 10:04	2.0396	0.89	0.4364	25
10/12/23 10:04	10/16/23 08:45	3.9451	1.26	0.3194	25
10/16/23 08:45	10/17/23 08:46	1.0007	0.39	0.3897	25
10/17/23 08:46	10/23/23 08:18	5.9806	2.28	0.3812	25

Date Time Start	Date Time End	ΔTime [day]	ΔH_2O mass [g]	Rate of change H_2O mass [g/day]	Upstream gas mass flow rate [std mL/min]
10/23/23 08:18	10/30/23 08:00	6.9875	2.6	0.3721	25
10/30/23 08:00	11/1/23 09:47	2.0743	0.68	0.3278	25
11/1/23 09:47	11/6/23 09:54	5.0049	1.75	0.3497	25
11/6/23 09:54	11/8/23 10:51	2.0396	0.79	0.3873	25
11/8/23 10:51	11/13/23 09:08	4.9285	1.79	0.3632	25
11/13/23 09:08	11/16/23 08:47	2.9854	1.17	0.3919	25
11/16/23 08:47	11/20/23 08:10	3.9743	1.38	0.3472	25
11/20/23 08:10	11/27/23 07:50	6.9861	2.24	0.3206	25
11/27/23 07:50	11/29/23 08:41	2.0354	0.68	0.3341	25
11/29/23 08:41	12/4/23 09:46	5.0451	1.6	0.3171	25
12/4/23 09:46	12/6/23 09:28	1.9875	0.54	0.2717	25
12/6/23 09:28	12/11/23 08:00	4.9389	1.55	0.3138	25
12/11/23 08:00	12/13/23 08:10	2.0069	0.64	0.3189	25
12/13/23 08:10	12/18/23 08:04	4.9958	1.65	0.3303	25
12/18/23 08:04	12/20/23 07:36	1.9806	0.61	0.3080	25
12/20/23 07:45	1/2/24 10:32	13.1160	3.8	0.2897	25
1/2/24 10:32	1/3/24 07:24	0.8694	0.26	0.2990	25
1/3/24 07:24	1/8/24 07:38	5.0097	1.38	0.2755	25
1/8/24 07:38	1/10/24 07:34	1.9972	0.77	0.3855	25
1/10/24 07:34	1/17/24 07:37	2.6500	0.84	0.3170	25
1/17/24 07:37	1/22/24 11:18	5.1535	1.73	0.3357	25
1/22/24 11:18	1/24/24 11:18	2.0000	0.72	0.3600	25
1/24/24 11:18	1/29/24 08:15	4.8729	1.59	0.3263	25
1/29/24 08:15	1/31/24 07:44	1.9785	0.68	0.3437	25
1/31/24 07:44	2/5/24 10:25	5.1118	1.79	0.3502	25
2/5/24 10:25	2/7/24 08:02	1.9007	0.71	0.3735	25
2/7/24 08:02	2/12/24 07:42	4.9861	1.59	0.3189	25
2/12/24 07:42	2/14/24 07:41	1.9993	0.55	0.2751	25
2/14/24 07:41	2/20/24 07:43	6.0014	1.89	0.3149	25
2/20/24 07:43	2/29/24 07:45	9.0014	2.84	0.3155	25
2/29/24 07:45	3/4/24 07:11	3.9764	1.14	0.2867	25
3/4/24 07:11	3/11/24 08:00	7.0340	2.08	0.2957	25
3/11/24 08:00	3/13/24 08:27	2.0187	0.3	0.1486	25
3/13/24 08:27	3/18/24 07:52	4.9757	1.75	0.3517	25
3/18/24 07:52	3/20/24 08:38	2.0319	0.82	0.4036	25
3/20/24 08:38	3/25/24 07:18	4.9444	1.49	0.3013	25
3/25/24 07:18	3/27/24 07:23	2.0035	0.76	0.3793	25
3/27/24 07:23	3/28/24 09:01	1.0681	0.18	0.1685	25

Date Time Start	Date Time End	ΔTime [day]	ΔH_2O mass [g]	Rate of change H_2O mass [g/day]	Upstream gas mass flow rate [std mL/min]
3/28/24 09:01	4/1/24 13:06	4.1701	1.21	0.2902	25
4/1/24 13:06	4/3/24 07:57	1.7854	0.48	0.2688	25
4/3/24 08:06	4/4/24 08:20	1.0097	0.32	0.3169	25
4/4/24 08:20	4/8/24 10:18	4.0819	1.13	0.2768	25
4/8/24 10:18	4/15/24 08:22	6.9194	2.03	0.2934	25
4/15/24 08:22	4/17/24 07:59	1.9840	0.47	0.2369	25
4/17/24 07:59	4/22/24 07:28	4.9785	1.49	0.2993	25
4/22/24 07:28	4/24/24 07:33	2.0035	0.57	0.2845	25
4/24/24 07:33	4/29/24 08:21	5.0333	1.45	0.2881	25
4/29/24 08:21	5/1/24 08:42	2.0146	0.56	0.2780	25
5/1/24 08:42	5/6/24 07:52	4.9653	1.64	0.3303	25
5/6/24 07:52	5/8/24 07:15	1.9743	0.5	0.2533	25
5/8/24 07:15	5/13/24 10:00	5.1146	1.54	0.3011	25
5/13/24 10:00	5/15/24 07:40	1.9028	0.6	0.3153	25
5/15/24 07:40	5/20/24 08:10	5.0208	1.29	0.2569	25
5/20/24 08:10	5/23/24 07:33	2.9743	0.86	0.2891	25
5/23/24 07:33	5/28/24 08:36	5.0437	1.44	0.2855	25
5/28/24 08:36	5/30/24 08:15	1.9854	0.5	0.2518	25
5/30/24 08:15	6/3/24 08:02	3.9910	1.22	0.3057	25
6/3/24 08:02	6/5/24 07:35	1.9812	0.48	0.2423	25
6/5/24 07:35	6/10/24 08:09	5.0236	1.69	0.3364	25
6/10/24 08:09	6/12/24 07:44	1.9826	0.75	0.3783	25
6/12/24 07:44	6/18/24 08:27	6.0299	1.96	0.3250	25
6/18/24 08:27	6/20/24 08:38	2.0076	0.69	0.3437	25
6/20/24 08:38	6/24/24 09:48	4.0486	1.41	0.3483	25
6/24/24 09:48	6/27/24 07:41	2.9118	0.84	0.2885	25
6/27/24 07:41	7/1/24 08:09	4.0194	1.46	0.3632	25
7/1/24 08:09	7/3/24 08:00	1.9938	0.62	0.3110	25
7/3/24 08:00	7/8/24 07:35	4.9826	1.45	0.2910	25
7/8/24 08:03	7/10/24 07:58	1.9965	0.68	0.3406	25
7/10/24 07:58	7/15/24 08:00	5.0014	1.42	0.2839	25
7/15/24 08:00	7/18/24 08:43	3.0299	0.87	0.2871	25
7/18/24 08:43	7/22/24 08:02	3.9715	1.3	0.3273	25
7/22/24 08:02	7/24/24 07:46	1.9889	0.48	0.2413	25
7/24/24 07:46	7/29/24 08:16	5.0208	1.54	0.3067	25
7/29/24 08:16	8/1/24 09:30	3.0514	0.99	0.3244	25
8/1/24 09:30	8/5/24 07:57	3.9354	0.74	0.1880	25

Table A-6. Heated HP circulation cold trap samples.

Date	Start Time	End Time	Flow Rate, L/min	Approximate Volume Collected, mL	Heat or Ambient	Comments
8-Nov-2023	10:48	11:48	2	2 to 3	Ambient	visual estimate
16-Nov-2023	07:52	09:01	2	1.5	Ambient	weighed with balance
20-Nov-2023	08:05	09:03	2	1.5	Heat	weighed with balance
29-Nov-2023	08:40	09:41	2	1.03	Heat	weighed with balance
4-Dec-2023	09:47	10:47	2	0.5	Heat	weighed with balance
6-Dec-2023	08:41	11:45	2	0.5	Heat	weighed with balance
13-Dec-2023	08:16	10:15	2	0.5	Ambient	weighed with balance
18-Dec-2023	08:24	10:25	2	2.75	Ambient	weighed with balance
20-Dec-2023	07:52	08:52	2	1.59	Ambient	weighed with balance
2-Jan-2024	10:42	11:41	2	1.89	Ambient	weighed with balance
3-Jan-2024	07:47	08:47	2	1.83	Ambient	weighed with balance
8-Jan-2024	07:49	08:49	2	1.92	Ambient	weighed with balance
10-Jan-2024	07:48	08:48	2	1.8	Ambient	weighed with balance
17-Jan-2024	07:46	08:46	2	1.92	Ambient	weighed with balance
22-Jan-2024	09:08	10:08	2	1.5	Ambient	weighed with balance
24-Jan-2024	11:22	12:22	2	1.5	Ambient	weighed with balance
29-Jan-2024	08:25	09:25	2	1.98	Ambient	weighed with balance
31-Jan-2024	07:53	08:53	2	0.97	Ambient	weighed with balance
5-Feb-2024	10:25	11:25	2	2	Ambient	weighed with balance
7-Feb-2024	08:11	09:11	2	1.24	Ambient	weighed with balance
12-Feb-2024	07:50	08:50	2	0.72	Ambient	Weighed with balance, O-rings in ultra torr fittings are missing and the system leaks. New O-rings are needed before the next cold trap sample is collected.
20-Feb-2024	07:45	08:45	2	1.88	Ambient	weighed with balance
29-Feb-2024	07:53	08:53	2	1.79	Ambient	weighed with balance, sample leaking from bottle (bad cap?)
4-Mar-2024	07:19	08:19	1	0.98	Ambient	weighed with balance, sample leaking from bottle (bad cap?)
11-Mar-2024	08:11	09:11	1	1.01	Ambient	weighed with balance
13-Mar-2024	08:54	09:54	1	1.31	Ambient	weighed with balance
18-Mar-2024	07:59	08:59	1	1.08	Ambient	weighed with balance
20-Mar-2024	08:52	09:52	1	1.23	Ambient	weighed with balance
25-Mar-2024	07:25	08:25	1	1.07	Ambient	weighed with balance
27-Mar-2024	07:26	08:26	1	1.2	Ambient	weighed with balance
4-Apr-2024	08:27	09:27	1	1.49	Heat	weighed with balance
8-Apr-2024	10:21	11:21	1	1.52	Heat	weighed with balance
15-Apr-2024	08:23	09:23	1	1.65	Heat	weighed with balance
17-Apr-2024	08:16	09:16	1	1.37	Heat	weighed with balance
22-Apr-2024	07:38	08:38	1	1.56	Heat	weighed with balance

Date	Start Time	End Time	Flow Rate, L/min	Approximate Volume Collected, mL	Heat or Ambient	Comments
24-Apr-2024	08:16	09:16	1	1.61	Heat	weighed with balance
29-Apr-2024	08:20	09:20	1	1.63	Heat	weighed with balance
1-May-2024	08:45	09:45	1	1.41	Heat	weighed with balance
6-May-2024	07:51	08:51	1	1.06	Ambient	weighed with balance
8-May-2024	07:15	08:15	1	0.78	Ambient	weighed with balance
15-May-2024	07:46	08:46	1	1.07	Ambient	weighed with balance
20-May-2024	08:22	09:22	1	1.05	Ambient	weighed with balance
23-May-2024	07:46	08:46	1	1.34	Ambient	weighed with balance
30-May-2024	08:28	09:28	1	1.19	Ambient	weighed with balance
3-Jun-2024	08:12	09:12	1	1.25	Ambient	weighed with balance
5-Jun-2024	07:40	08:40	1	1.62	Heat	weighed with balance
12-Jun-2024	08:03	09:03	1	2.32	Heat	weighed with balance
18-Jun-2024	08:44	09:44	1	2.73	Heat	weighed with balance
27-Jun-2024	07:49	08:49	1	1.82	Heat	weighed with balance
1-Jul-2024	08:19	09:19	1	1.7	Heat	weighed with balance
3-Jul-2024	08:06	09:06	1	1.61	Heat	weighed with balance
8-Jul-2024	07:36	08:36	1	1.21	Heat	weighed with balance - dry ice ran out and the final cold trap temperature was -37.0 °C
10-Jul-2024	08:04	09:04	1	1.08	Heat	weighed with balance
15-Jul-2024	07:36	08:36	1	0.72	Heat	weighed with balance